applied sciences

MDPI

Review

The Current State of Research of Wire Arc Additive Manufacturing (WAAM): A Review

Kai Treutler * and Volker Wesling

Institute of Welding and Machining, Clausthal University of Technology, 38678 Clausthal-Zellerfeld, Germany; office@isaf.tu-clausthal.de

* Correspondence: treutler@isaf.clausthal.de

Featured Application: Wire Arc Additive Manufacturing (WAAM).

Abstract: Wire arc additive manufacturing is currently rising as the main focus of research groups around the world. This is directly visible in the huge number of new papers published in recent years concerning a lot of different topics. This review is intended to give a proper summary of the international state of research in the area of wire arc additive manufacturing. The addressed topics in this review include but are not limited to materials (e.g., steels, aluminum, copper and titanium), the processes and methods of WAAM, process surveillance and the path planning and modeling of WAAM. The consolidation of the findings of various authors into a unified picture is a core aspect of this review. Furthermore, it intends to identify areas in which work is missing and how different topics can be synergetically combined. A critical evaluation of the presented research with a focus on commonly known mechanisms in welding research and without a focus on additive manufacturing will complete the review.

Keywords: wire arc additive manufacturing; welding; steel; aluminum; titanium; nickel; magnesium; copper; path planning; process surveillance; multi-material; intermetallic

Citation: Treutler, K.; Wesling, V. The Current State of Research of Wire Arc Additive Manufacturing (WAAM): A Review. *Appl. Sci.* **2021**, *11*, 8619. https://doi.org/10.3390/app11188619

Academic Editors: Ana M. Camacho and Richard (Chunhui) Yang

Received: 24 June 2021
Accepted: 13 September 2021
Published: 16 September 2021

1. Introduction and Overview

At present, additive manufacturing is the focus of industry and research due to a large number of new developments in the processes and systems. This is further strengthened by the general trend toward resource efficiency, as additive manufacturing processes offer the possibility of near net shape or net shape production. Particularly for cost-intensive materials like titanium or tungsten, additive manufacturing can be the manufacturing process of choice. The main factors influencing the selection of the additive manufacturing process are the complexity and resolution that can be achieved, as well as the deposition rate and component size, Figure 1 [1]. Furthermore, additive manufacturing grants a lot more degrees of freedom for the product design than conventional manufacturing processes [2] and opens up the possibility of load optimized design [3]. One promising additive manufacturing process area is wire arc additive manufacturing (WAAM), where an electric arc in combination with a wire as deposition material is utilized for manufacturing. This process is part of the direct energy deposition (DED) manufacturing, which includes, for example, laser cladding. In 2020, direct energy deposition technologies represented 16% of the additive manufacturing used in the market [4].

In comparison with other additive manufacturing processes for metals, WAAM has smaller cooling rates and a higher heat input [5]. This is beneficial for most commercially available materials. Furthermore, the deposition rates and the part size can be greater through the reduced complexity and surface quality of the part in comparison with powder bed-based additive manufacturing processes (Figure 1). WAAM is the collective term for all wire-based additive manufacturing processes using arc welding. Due to the long research in arc welding for surfacing and joint welding, the knowledge of the material

and process behavior is widespread, and the known fundamentals can be transferred [6,7]. The difference between normal joint welding with arc welding processes and additive manufacturing was nicely illustrated by Mohebbi et al., Cunningham et al. and others, and it can be summarized as a difference in the thermal conduction of the material [7–9].

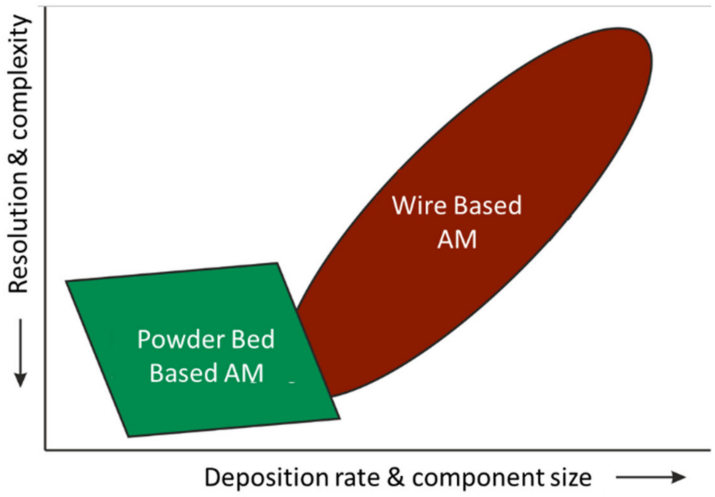

Figure 1. Comparison between wire-based and powder bed-based additive manufacturing [1].

In joint welding, the thermal conductivity takes place in more dimensions (Figure 2a) than in WAAM processes, where the heat has to be deduced, in most cases, in one direction: to bottom of the part (Figure 2b).

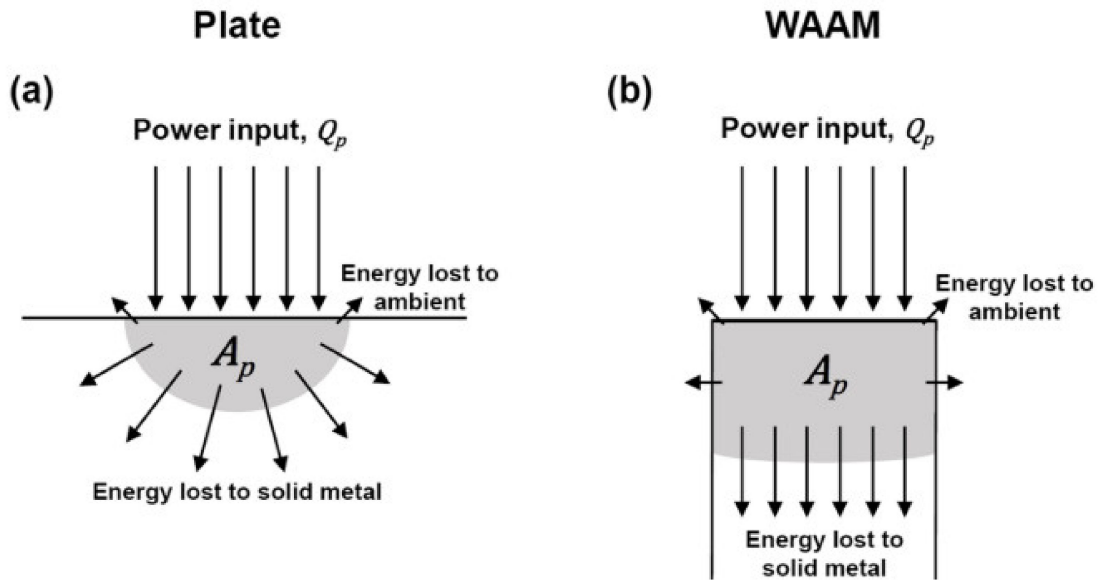

Figure 2. Heat transfer in joint welding and WAAM [8]. (**a**) thermal conductivity takes place in more dimensions; (**b**) thermal conductivity takes place in one direction.

Furthermore, thanks to new developments in the robotics. computer-aided design and manufacturing along with new welding processes and process control possibilities, WAAM is more promising now than it was in the 1970s and 1980s, when WAAM was called "shape welding" (in German: "Formgebendes Schweißen") and was performed for large parts [10].

Figure 3 shows a large piece of equipment for shape welding up to 80 t on the left and a shape welded reservoir on the right side, which showed superior material properties in

comparison with normal manufacturing processes of this time [11]. Furthermore, the first trials of shape welding were carried out in the 1930s [11]. Nevertheless, this manufacturing process has had its niche market throughout the last few decades.

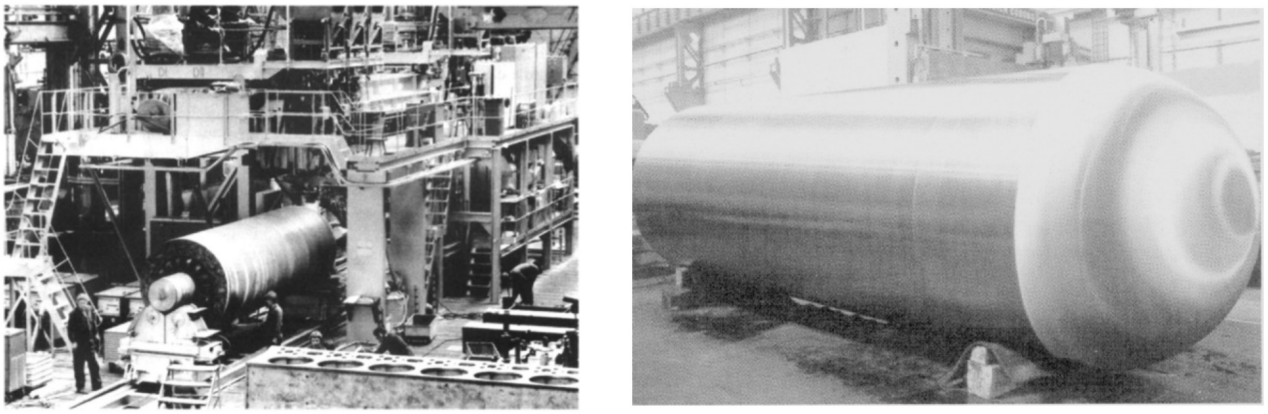

Figure 3. (**Left**) Welding equipment for shape welding up to 80 t (Thyssen factory picture) [11]. (**Right**) Shape welded reservoir of 72 t. Material: 10MnMoNi55 (Thyssen factory picture) [11].

Today, the variety of manufactured and tested parts has increased. Figure 4 shows two different parts which have been tested for use in the industry. On the left is a ship propeller, and on the right are Pelton turbines for waterpower plants shown. The bandwidth of different applications and different used materials is currently being exaggerated by different working groups for uses such as naval applications [12].

Figure 4. (**Left**) WAAM-manufactured propeller (Ramlab) (**Right**) WAAM-manufactured water turbine blades (Hydroworld) [13].

Figure 5 shows the first WAAM-made bridge realized in four parts and combined with non-welded parts [14]. It has a weight of 7.8 t and a welded weight of 4.6 t.

Figure 5. WAAM made bridge [14].

The bridge shows the possibility of organic-looking parts nicely, which usually are not easy to manufacture with conventional manufacturing processes. To utilize this, new design rules are currently being developed [15] and implemented in teaching at universities around the world. Greer et al. showed an example of the utilization of new design rules for a part of a crane arm [15] with less weight than a conventionally manufactured part. Kulikov et al. showed the possibility to manufacture compressor impellers with WAAM and described the whole process chain and the benefit of WAAM in comparison with conventional impeller manufacturing in a decent way [16]. In addition, Bergmann et al. showed this for the manufacturing of a steel knot for construction applications [17].

The advantages of WAAM in comparison with other additive manufacturing processes have been evaluated by Panchenko et al. and are shown in a well-arranged diagram in Figure 6 [18]. Roy et al. stated that the crucial advantages of wire arc additive manufacturing are a shortened lead time, less material waste, improved functionality, customized tooling for lower volume parts and the possibility of multi-material design [19].

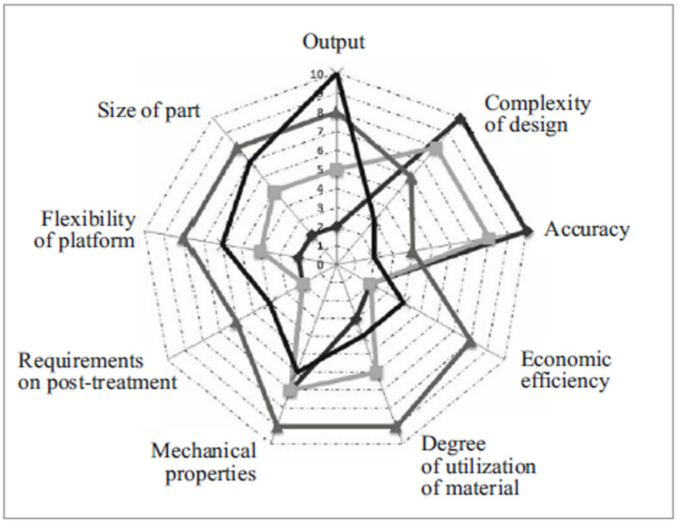

◆) bed deposition; ■) direct deposition; ×) electron beam freeform fabrication; ▲) WAAM.

Figure 6. Advantages of WAAM and other additive manufacturing processes [18].

WAAM is not only used for the manufacturing of new parts; it also can be used for the modification or repurposing of existing parts. One example for modifications is given by Josten and Höfemann for the reinforcement of car parts [20], and one example study on the repurposing of steel parts was conducted by van Le et al. [21]. Furthermore, WAAM can be used for the localized repair of molds and other parts, like Wu et al. showed exemplarily [22] and Li et al. demonstrated with the repair of a sprocket [23].

The previous examples illustrate the variety of possible applications of wire arc additive manufacturing. Nevertheless, the wide range of different applications, processes, materials and used surrounding technologies, such as path planning software and process surveillance methods, are presented in a very specific way, and each focus on an interesting part of the WAAM process, but a general consolidation of the knowledge is missing. Therefore, this review has two objectives. First, it is intended to provide an overview of the international research activities in the field of WAAM, and secondly, it is intended to summarize and evaluate the results achieved and point out where there is a demand for further intensive research. The review is divided into two big parts. The first will focus on the materials, welding process, methods and strategies for welding arc additive manufacturing. The second part will focus on the modeling of welding arc additive manufacturing processes. Modeling is the key to achieve the best possible additive-manufactured parts, aside from a deep understanding of the welding processes and a closed loop process of surveillance and control. This paper will be concluded by the identification of future research interests.

A common method for how additive manufacturing with welding processes is conducted these days is described by Kulikov in [24]. First, the CAD model is drawn. Second, the path planning with the related parameters of the welding process will be performed, and afterward, the welding itself will be performed, in most cases, with a welding robot.

Figure 7 shows a basic process chain for WAAM-made parts, from the product developments and simulation drawn along the information flow to the manufacturing process (e.g., welding), followed by process surveillance and the application along the material flow. Between all steps of the process chain, interactions can be seen. The key for nearly all WAAM-made parts is the parts' properties, especially when the parts are designed for structural applications. In each step, different methods can be used. While welding, the welding process and the cooling or geometry can be observed and controlled in a closed loop. Figure 8 shows the detailed process path of WAAM parts exemplarily. In the presented literature, the tendency towards closed loop control of the weld bead and material property orientated path planning is visible [25,26]. A material property-oriented closed control loop has been achieved for other additive manufacturing [27], which is easier to oversee due to the missing broadband emissions from the metallic/gas arc plasma. Furthermore, active cooling of the part and other methods are focused on influencing the important thermal management of the manufacturing process [28]. Optional post-processing like machining and heat treatment can be conducted accordingly.

The main working groups that focus on wire arc additive manufacturing were given by Jin et al. and can be expandedwith other working groups which published WAAM related research recently (Table 1) [30]. Liu et al. gave a good overview of the working groups working in China for WAAM [31].

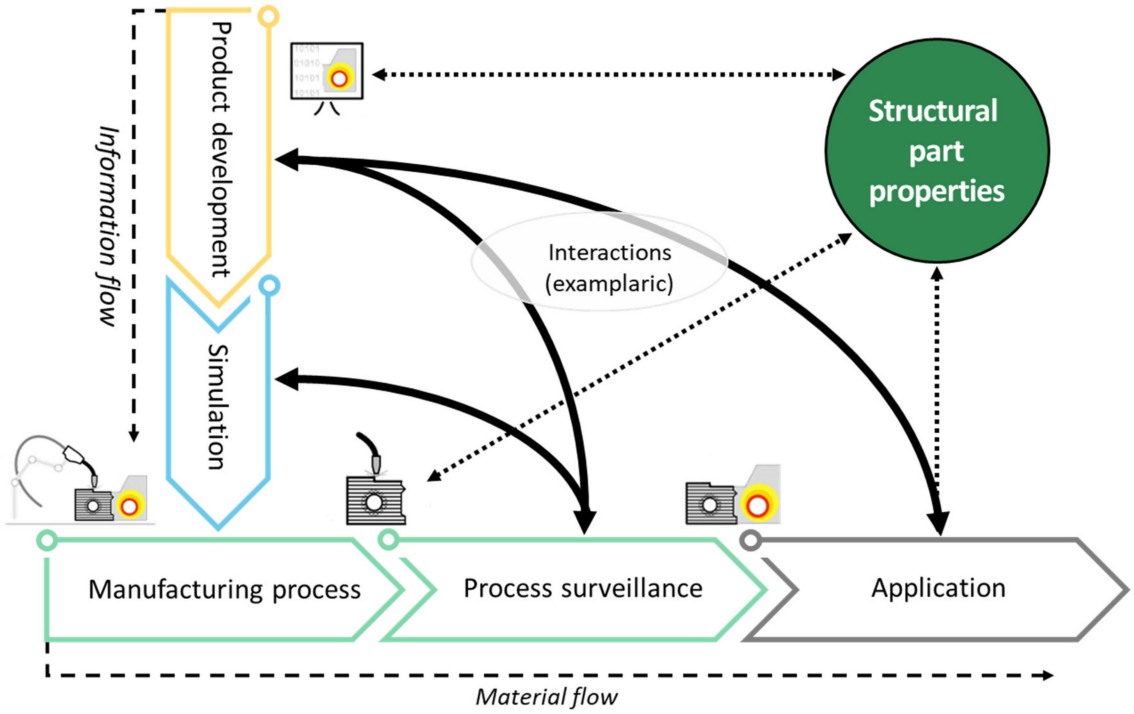

Figure 7. Process chain for WAAM [1].

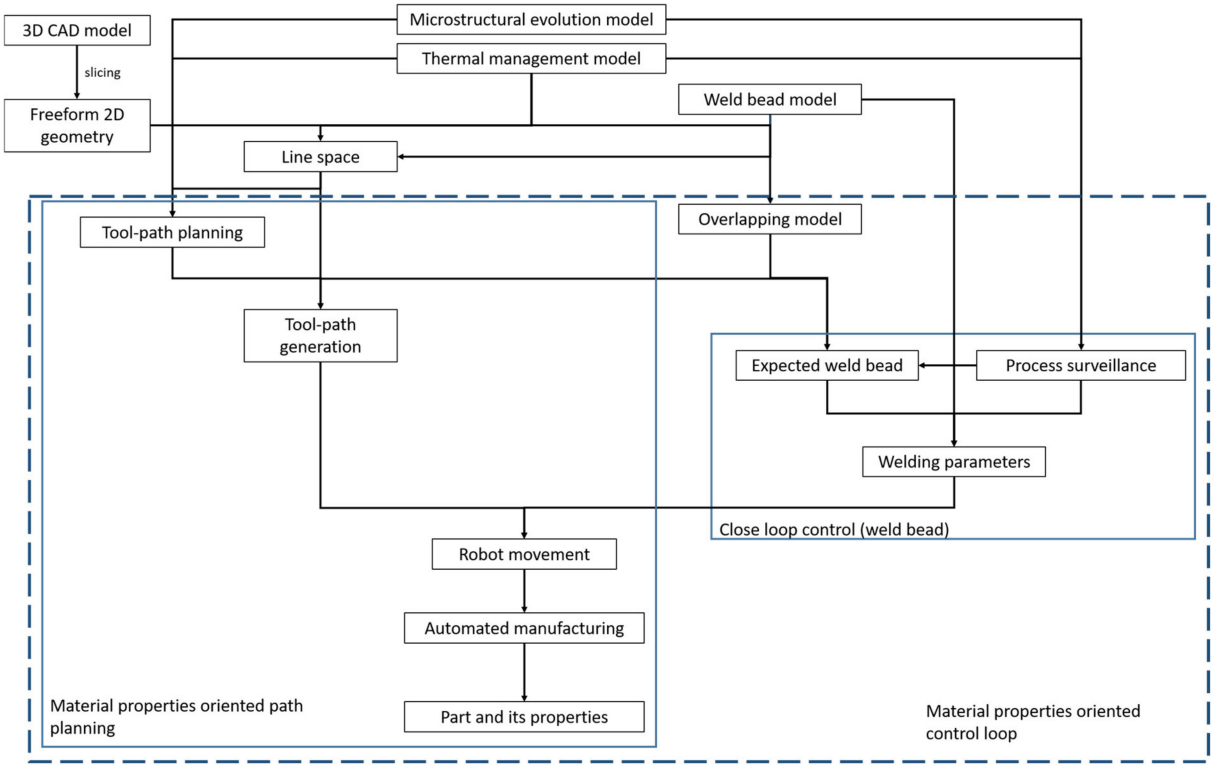

Figure 8. Process path for WAAM (modified, based on [29]).

Table 1. Main research groups working on WAAM (modified) [30].

County	Research Groups	Synonyms of Wire Arc Additive Manufacturing (WAAM)	Reference
United States	Southern Methodist University	Rapid prototyping (RP) based on gas tungsten arc welding (GTAW)	[32]
	Tufts University	Near net shape manufacturing	[33]
South Korea	Korea Institute of Science and Technology	3D welding	[34]
Japan	Osaka University	3D micro welding	[35]
United Kingdom	University of Sheffield	Shaped metal deposition	[36]
	Cranfield University	Wire and arc additive manufacturing (WAAM)	[37,38]
	University of Manchester	Wire and arc additive manufacturing (WAAM)	[39]
	Coventry University	Wire and arc additive manufacturing (WAAM)	[40,41]
	University of Bath	Wire and arc additive manufacturing (WAAM)	[9,42]
	University of Wales Swansea	Shaped metal deposition	[43]
China	Harbin Institute of Technology	GMAW-based rapid manufacturing	[44]
	Xi An Jiao Tong University	MPAW-based rapid prototyping	[45]
	Shanghai Jiao Tong University	Wire arc additive manufacturing (WAAM)	[46]
	Foshan University	Wire arc additive manufacturing (WAAM)	[22]
	School of Mechanical and Vehicular Engineering, Beijing Institute of Technology	Wire and arc additive manufacturing (WAAM)	[47]
India	Indian Institute of Technology	Hybrid layered manufacturing	[48]
	Birla Institute of Technology and Science	GTAW welding-based additive manufacturing	[49]
Australia	University of Wollongong	Wire arc additive manufacturing (WAAM)	[50,51]
Germany	Clausthal University of Technology	Wire arc additive manufacturing (WAAM)	[52,53]
	Ilmenau University of Technology	Wire arc additive manufacturing (WAAM)	[54,55]
	Chemnitz University of Technology and TU Munich University of Technology	Wire arc additive manufacturing (WAAM)	[56,57]
	Braunschweig University of Technology	Wire arc additive manufacturing (WAAM)	[58]
	Brandenburg University of Technology Cottbus-Senftenberg	Wire arc additive manufacturing (WAAM)	[59]
	RWTH Aachen	Wire arc additive manufacturing (WAAM)	[60,61]
Austria	Graz University of Technology	Wire arc additive manufacturing (WAAM)	[62]
Italy	University of Bologna	Wire arc additive manufacturing (WAAM)	[63–65]

2. Materials, Processes and Methods

The key to understanding wire arc additive manufacturing is deep knowledge of the used welding processes. Basically, all welding processes are suitable for additive manufacturing and are scientifically well understood. The differences between additive

manufacturing and joint welding are based on the differences in the thermal conductivity, which is significantly lower for thin-walled structures. This makes thermal management the key factor to achieve the desired part geometry and material properties and influences the choice of the used welding process.

In the following, the used processes for WAAM are described regarding additive manufacturing-related issues. After that process-surveillance and control methods will be summarized, followed by the major process-dependent key factor in wire arc additive manufacturing: the path planning. This is the key factor in thermal management to build a geometrically correct part with the desired material properties. The subsection will be concluded with a summary of the research carried out for various materials.

2.1. Processes

The newly increasing interest in WAAM is based on the advances in robotic control and modern electronic control circuits for welding machines. They made modern controlled short arc welding processes with reduced energy input possible and very stable. The most known modified short arc process, "cold metal transfer" (CMT) [66], has been developed by the company "Fronius" and is the most used process for WAAM based on gas metal arc welding (GMAW) in the literature. Furthermore, for controlled short arcs, the intention to lower the heat input is the focus of some research, increasing the potential applications [67]. Aside from the common gas metal arc welding processes, tungsten inert gas (TIG) welding processes or plasma welding processes have been used due to the separation of energy and mass input. Aside from standard welding processes, the combination of welding processes with others (e.g., laser-assisted welding) or with forming processes have been attempted as well. In the following, each of the most commonly used welding processes and their process behavior in welding arc additive manufacturing will be described. The basic literature about welding (e.g., [11] and Ugla et al. [68]) gives a good overview of the used welding processes.

2.1.1. Tungsten Inert Gas Welding (TIG Welding)

One of the most used manufacturing processes for wire arc additive manufacturing is tungsten inert gas (TIG) welding [49,69,70]. The benefit of the TIG process is the possible separation between the filler and energy input in certain ranges and the possibility to use more than one wire in the same process. Therefore, the separate wire feed leads to difficulties when changing the welding directions, because the wire feeder has to change the working position. Furthermore, while using the TIG welding process, the melt pool's shape can be influenced due to different process values and the use of a pulsed welding process. Benakis et al. showed that a slow and inter-pulsed TIG welding process has a good melt pool shape for additive manufacturing [70]. Dinovitzer et al. showed that the process values have a significant influence on the melt pool shape as well [69].

The effects of the AC-TIG and pulse TIG welding processes are also under investigation [71], and it was shown by Ayarkwa that the percentage of the electropositive time cycle of an ACTIG welding process has a significant influence on the microstructure, oxide removal for welding aluminum and the weld bead shape. The process can be beneficially influenced by using the hot wire technique [72]. Furthermore, the usage of magnetic arc oscillation longitudinal to the welding direction can influence the weld seam's width and reduce the variation in width for thin-walled structures [73,74].

2.1.2. Plasma Arc Welding

Plasma arc welding processes can also be used for additive manufacturing with powder or wire as a filler. One of the variants of the process is plasma transferred arc welding (PTAW). One very simple approach for additive manufacturing—multi-layer surfacing or cladding—has been performed for decades with this process. This process is also able to separate the energy input and the material flow from the filler like TIG welding, and it is applicable for different materials (e.g., steel and co-base alloys) [57,75].

Alaluss and Mayr identified the occurring distortion as a core problem of welding-based additive manufacturing and for additive manufacturing with plasma welding as well, and they implemented mechanical rolling to overcome this issue [57]. Aside from the standard variant of PTAW, µPTAW has been used for additive manufacturing as well [45,75]. This shows the wide range of applications for this process. Like in other welding processes, the droplet transfer mode changes with the welding-related process values and can be divided into three different transition modes regarding the frequency and stability of droplet transfer [76,77].

2.1.3. Gas Metal Arc Welding

Gas metal arc welding is one of the most commonly used welding processes for WAAM and has been used for many decades in surfacing, cladding and additive manufacturing. In recent years, the development of new control systems for arc welding power sources has enabled the development of new welding process variants, such as controlled short arc and controlled spray arc processes. Modern controlled short arc welding processes in particular are used for additive manufacturing due to the reduced energy input they provide in comparison with conventional uncontrolled short arc processes [78,79]. Furthermore, these controlled short arc welding processes can be exaggerated by innovative wire feed control to achieve different droplet detachment [78,79].

Due to the high achievable energy input with current welding machines, high throughput additive manufacturing processes can be achieved and are currently under investigation [80]. Han et al. showed that an additive manufacturing with a modified GMA welding process can have a material deposition rate up to 4.71 kg/h [80]. Another method to increase the mass of the deposited material is to use multi-wire processes [81]. Due to the changed energy input, the material behavior of the finished parts differs between the single-wire and multi-wire processes [44,81]. One critical point for additive manufacturing with the GMA welding process is the movement of the wire tip and the resulting geometrical inaccuracy [82].

On the basis of commonly buyable welding machines, different manufacturing systems have been developed [83] and are sold by various companies. Commonly used welding robots can be easily adopted for additive manufacturing.

2.1.4. Submerged Arc Welding

The submerged arc welding process can be used for additive manufacturing as well [84], but the positioning of the flux limits the flexibility of submerged arc welding for additive manufacturing.

2.1.5. Skeleton Arc Welding

A special variant of wire arc additive manufacturing is skeleton arc additive manufacturing (Figure 9) [85–88]. Here, the part will be built by single dots of material. This method opens the possibility to create skeleton-like structures in nearly every shape. These skeleton structures can be used to push lightweight load path-oriented design into additive manufacturing [89] and are able to create bionic-like structures easily. Laghi et al. realized the creation of diagrid columns with this technique [65]. For skeleton arc welding, designated welding path planning needs to be performed. Yu et al. demonstrated how such a path planning method can be developed and used [90]. The basic limitations for the path planning are the geometrical ones from the manufacturing system that limit the number of possible paths and the geometrical complexity of the parts. Silvestru et al. developed an elastic-plastic material model for skeleton arc-welded low-alloy steels [91].

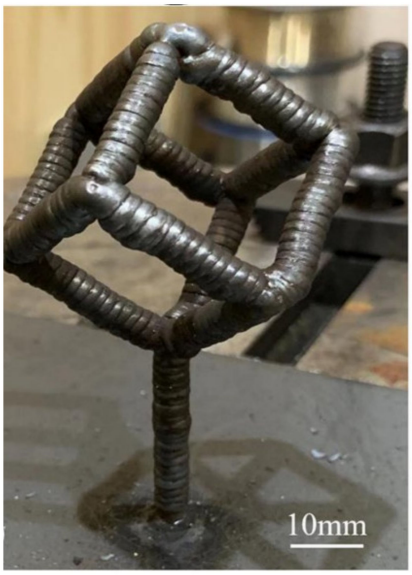

Figure 9. An example of skeleton WAAM [87].

2.1.6. Cross-Process Developments

The influence of a different process environment while welding for joint welding and WAAM is under investigation as well. Most of the found influences on the process, such as the microstructure and mechanical properties, are easily adoptable between both manufacturing variants. A good overview of the current state of hybrid manufacturing processes in combination with additive manufacturing processes is given by Pragana et al. [92], and the occurring physical effects are summarized by Webster et al. [93].

Influence of Shielding Gases

The influence of different shielding gases on welding processes is commonly known. The occurring effects of different shielding gases can be easily adopted to wire arc additive manufacturing, but the purpose might differ. While deep penetration of the weld metal can be beneficial for joint welding and can be supported by a shielding gas, in additive manufacturing, for shallow penetration, a higher build up can be desired, and the shielding gas needs to be chosen for this purpose. Silwal et al., for example, studied the influence of different CO_2 contents on the additive manufacturing of low-alloy steel [94]. They found that an increased CO_2 content led to a lowered layer height and higher meld pool surface temperatures, but it had little influence on the strength and toughness of the used material [94].

Da Silva et al. described the influence of O_2 on arc wandering in WAAM of aluminum alloys. They found that the addition of up to 200 ppm of oxygen had no impact on the arc behavior, and the addition of up to 20.000 ppm of oxygen led to the significant formation of oxides on the weld metal surface [95].

Laser-Assisted Welding

Laser-assisted welding differs from laser hybrid welding and typically uses a laser power less than 1 kW and has some known benefits, like possible geometrical control of the weld seam with the laser's position [96]. Pre-ionization of the laser can be used to direct the arc in a certain direction. For metal inert gas (MIG) welding, stabilization of the arc is also proposed. For additive manufacturing, Zhang et al. showed that an additional laser led to a reduction in the width of an aluminum wall and a higher layer height in certain ranges. Furthermore, the surface quality could be improved [97].

Combined Rolling and Additive Manufacturing Processes

The combination of different additive and forming manufacturing processes can improve the microstructure and mechanical properties of additive-manufactured parts. Basically, two different forming processes are currently being investigated deeply. The first group is a combination of a WAAM process with a rolling process [98–102]. Here, forming-induced recrystallization takes place, and a finer and tougher microstructure with increased strength can be created. Hönnige et al. realized strong recrystallization and mitigated columnar grain growth [103]. Colegrove et al. showed that the application of rolling can lead to significant grain refinement and a reduction in welding-related residual stresses, depending on the rolling direction [101]. These results are supported by the findings of Tangestani et al. [104], who showed that a vertical rolling process can increase the beneficial comprehensive residual stresses in a WAAM part with an FEM model validated with experimental results. Furthermore, Dirisu et al. showed that additional rolling can have a beneficial influence on the fatigue performance of WAAM-made parts [102], and Parvaresh et al. showed that cold working has a beneficial influence on the materials' strength [105].

Figure 10 shows different possible rolling methods. Colegrove et al. stated that rolling processes with the prevention of lateral deformation have the greatest influence on the residual stresses and have been applied for titanium-based alloys and aluminum-based alloys successfully [101]. Basically, ally processes that increase a weld's mechanical properties, like high-frequency impact treatment or shot peening, should improve the properties of WAAM-made parts as well. Shirizly et al. showed for different materials that a combined additive and forming process for tubes can be realized [106].

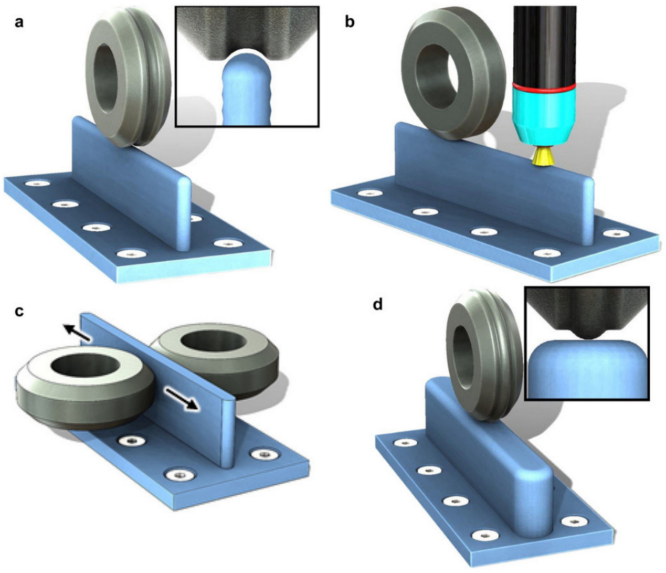

Figure 10. Schematics of possible rolling methods: (**a**) vertical with a profiled roller; (**b**) in situ rolling; (**c**) pinch rolling and (**d**) rolling with an inverted profile roller [101].

A comparable effect to additional rolling can be achieved due to other forming-based processes, like hammer peening and shot peening [107].

For the second process group for a combined process of forming and WAAM [108], Pragana et al. showed that subsequent additive manufacturing, milling and forming is possible and can be realized in one hybrid manufacturing machine [108].

Combined Machining, Heat Treatments and Additive Manufacturing Processes

For the combination of WAAM and machining, optimization of the process control and process values for the milling process is crucial for thin-walled parts as well [109]. Grossi et al. developed a method that allowed for adjusting the machining parameters to avoid resonance in the work piece [109]. An overview of the main challenges of hybrid

additive and subtractive manufacturing is given by Dávila et al. [110]. They summarized the necessary post-processing to overcome the limitations of DED processes in Figure 11. The reduction of pores in WAAM is mostly necessary for aluminum.

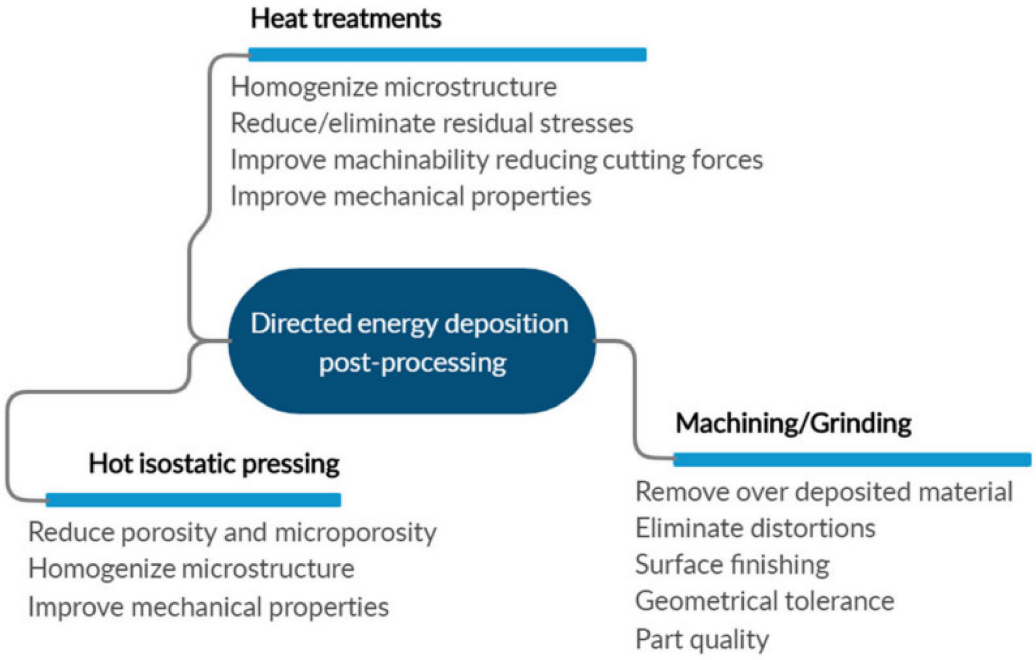

Figure 11. Post-processing techniques used to overcome the limitations of parts fabricated by direct energy deposition (DED) [110].

Furthermore, they derived the gains and challenges of hybrid manufacturing (Figure 12). The challenges and the needed post-processing contend that further research in the field of additive manufacturing needs a holistic approach for a better understanding of the interdependencies between additive manufacturing, post-processing and the built parts' service properties, which need to be addressed through real-time monitoring (process surveillance), process planning (material-oriented path planning) and deep knowledge of the relationships between the deposition process and the deposited material.

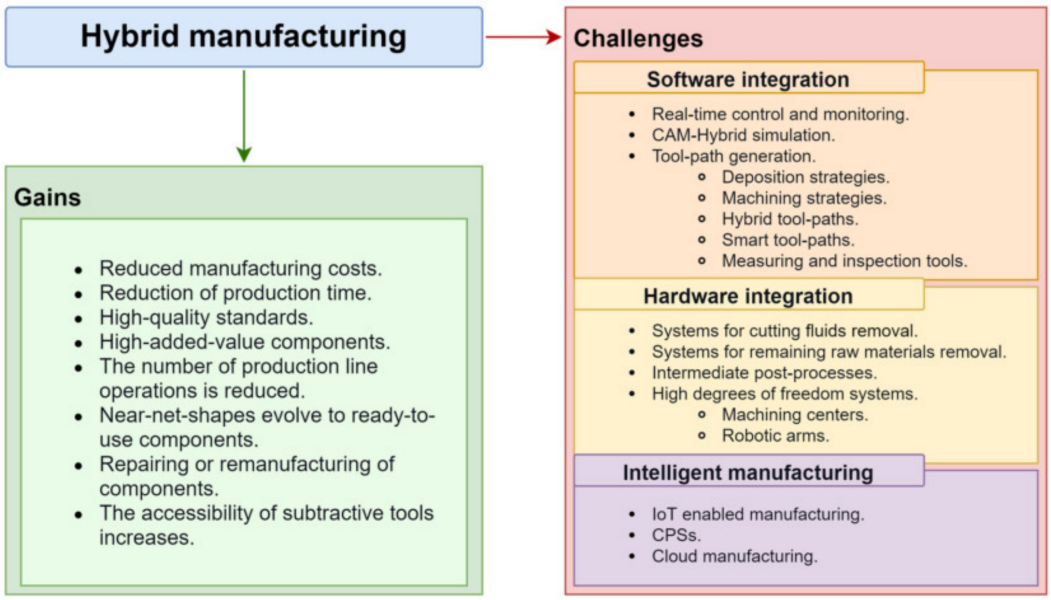

Figure 12. Hybrid manufacturing gains and challenges. IoT = Internet of things; CPSs = cyber-physical systems [110].

Fuchs et al. showed that a basic machinability is given for WAAM-made parts, and they derived a model for acceptable surface waviness [111]. Montevecchi et al. showed that additive-manufactured parts lead to increased cutting forces in a subsequent machining process due to the higher hardness of the material. To reduce the effect of harder machinability, modern machining processes can be used to achieve good machinability and a good surface morphology. For example, Schroepfer et al. showed that the usage of advanced subsequent milling processes for WAAM-made parts can be beneficial [112]. Further information on this topic is given in the nickel-based alloy section of this paper. To reduce the need for subsequent machining, the influence of an unmachined surface especially needs to be considered for fatigue, and Bartsch et al. derived a suggestion for implementing the rough surfaces of WAAM parts into DIE EN 1993-1-9 "Eurocode 3: Design of steel structures-Part 1–9: Fatigue" [113,114].

2.1.7. WAAM Process-Specific Challenges

The WAAM process has very specific challenges which need to be mastered for defect-free and geometrically correct manufacturing of the part. Three of them are the prediction of the layer height in the path planning, the distance between the welding beads and the direction and order of the single beads. Commonly, the choice of welding parameters is made by trial and error, but as the state of the art advances, the prediction of welding parameters becomes more and more model-based (Figure 13) [115].

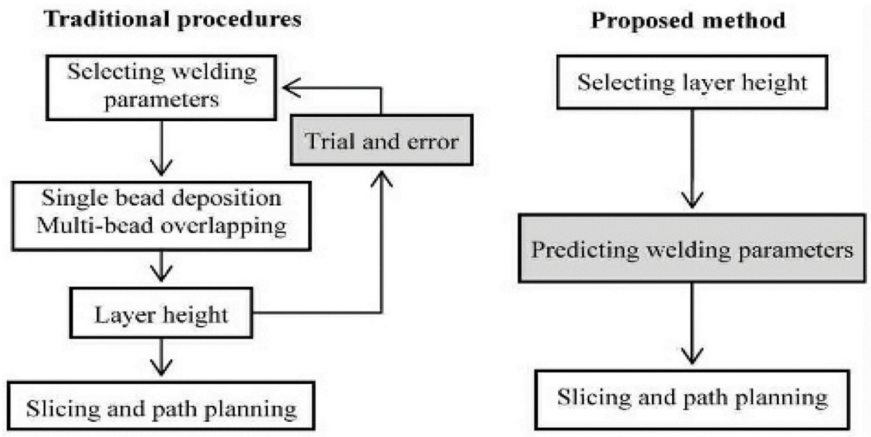

Figure 13. Parameter determination in welding arc additive manufacturing [116].

Hu et al. showed the classical and more knowledge-based way for the determination of the welding parameters, and they derived a model to determine the distance of the weld beads [115,116]. This model shows that an optimal distance between the weld seams lays in the region of 0.63–0.77 times the weld bead's width. This correlates with the commonly known distances of multi-run welds, where the new weld seam is set into the notch between the previous weld seam and the substrate. The proposed models need to be modified for each combination of filler and shielding gas. A similar approach was taken by Plangger et al. [62] and Xia et al. [117] with comparable results. Due to process-imminent surroundings, the order and direction of the welding process has a great influence on the geometrical correctness of the part. An alternating strategy has shown the geometrical best practice [118]. A more detailed description of the challenges regarding adequate path planning can be found in Section 2.2.

The energy input is, like for welding in general, the key point for achieving certain properties and a proper part. In welding, the energy per unit length is considered a sufficient value to describe most phenomena. This has been transferred to WAAM as well from many working groups. However, this approach can be modified to suit the needs of additive manufacturing with a more desired material build. Here, volumetric energy density or volumetric energy was introduced by Lu et al. [119].

Another critical point in wire arc additive manufacturing is a phenomenon called humping [120]. This phenomenon is known from high-speed welding, and Soderstrom and Mendez showed that the effect occurs due to the momentum of the back flow of the melt and that the effect limits the range of usable welding travel speeds [121]. For wire arc additive manufacturing with GMAW, the starting point when humping occurs is determined by the wire feed speed and the travel speed of the torch. For a common CMT process, Adebayo et al. showed that the maximum travel speed without humping is around 60 cm/min [120]. Dinovitzer et al. observed the humping for the TIG welding process [69], as did Jia et al. [77]. To overcome this issue, the travel speed, energy input and filler feed rate need to be balanced with each other in a certain range. Xu et al. developed a shape-driven control of the layer height to overcome uneven substrates or uneven previous welding paths [122]. They chose the deposition rate as the signal and the travel speed as the variable value.

The layer height and layer width are directly related to the welding process conditions [123]. Cui et al. proposed a mixed heat input (MHI) strategy to overcome geometrical and microstructural imperfections [123]. Aside from the heat input, the temperature of the substrate and additional heating or cooling of it will influence the shape of the weld bead as well, as Gudur et al. showed [124].

For automated manufacturing with WAAM, a suitable process of surveillance and control is needed to maintain all relevant parameters in a certain range and overcome any faults.

2.2. Processsurveillance and Control

To maintain the desired process behavior for the building process and keep a desired geometry, surveillance of the welding process can be a crucial part. Some working groups have established a multi-sensor framework for process surveillance [125–127]. Optical observations are one core point in the research [128]. Zhan et al. showed that optical surveillance of the wire tip and the wire tip deviation is possible [82]. The occurring deviation of the wire tip can lead to incorrect geometry of the part and internal faults. This deviation occurs due to the winding of the filler material onto a spool or into a barrel. To achieve the best winding, pre-stress is applied, which is released during the welding process. In addition, the winding causes a deformation of the wire which supports the deviation phenomena. In some automated welding processes, wire straightening showed beneficial effects [82].

Due to the comparison to other additive manufacturing processes with high energy input, one critical point for the manufacturing of large parts is the accumulation of heat. This accumulation leads to a loss of geometrical corrections and to a change in the mechanical properties. One way to overcome this problem is to introduce waiting times in the manufacturing process. Due to, in most cases, limited thermal conductivity of the welded parts, the waiting times increase with the build height. The second option is active cooling of the part due to the manufacturing process. The influence of external cooling on the properties and the surface of WAAM parts is currently under investigation [28,61,129,130]. Hackenhaar et al. integrated an active air cooling in the manufacturing process and showed that this can lead to a significant decrease in thermal accumulation and a decreased substrate temperature [129]. Furthermore, they integrated this into a numerical model [130]. Reisgen et al. showed that, in addition, the usage of a water bath or an aerosol can increase the cooling rate in comparison with active air cooling. However, they stated that in the case of a water bath, handling of the part during manufacturing is more difficult [61].

In welding technology, a basic way to achieve certain weld properties is to maintain the interlayer temperatures in multi-run welds. This method can be adopted in additive manufacturing as well and leads to the development of a WAAM system with interpass temperature control (such as in Kozamernik et al. [131]).

One modern method of process surveillance is automated detection of the weld pool geometry and extending this to monitor the cooling conditions. This can be achieved with

two different approaches. First, the surveillance can be carried out by a couple of cameras, including process and material-dependent filters, as was described by Richter et al. in [26], Halisch in [132] and others in [127,133–135]. In most cases, conventional CCD cameras or similar cameras are used and will be overexposed to light emitted by the welding process. Therefore, suitable filters need to be used.

Richter et al. showed the identification of possible filters for a low-alloy steel and an M21 shielding gas on a partial spectrum of the emitted light (Figure 14) [26]. Furthermore, they showed that two camera differential methods can lead to proper thermal measurements. Figure 15 shows the calculated results for their setup exemplary.

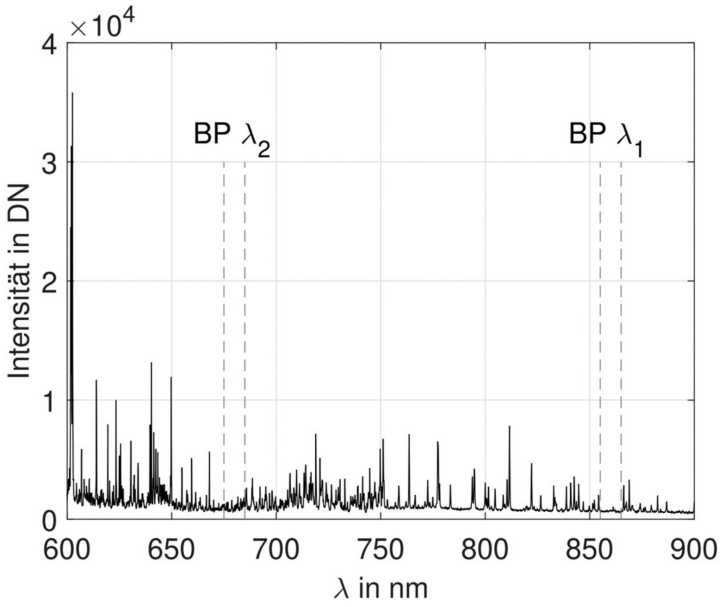

Figure 14. Partial spectrum from 600 nm to 900 nm of arc plasma with the selected band passes plotted [26].

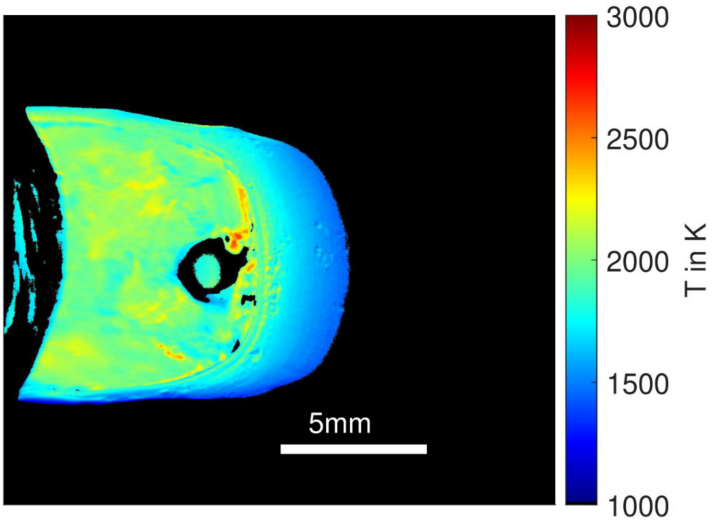

Figure 15. Calculated temperature distribution in the weld seam [26].

Hallish et al. used a high dynamic range two-colored pyrometric camera for the measurement of the melt pool temperature of a titanium alloy during additive manufacturing and used a scanned spectrum of the light emitted from the process to identify a suitable filter [132]. Xia et al. measured the melt pool width using a mask R-CNN-based welding image technique [136]. Wang et al. showed that an optical surveillance system can be used

to predict the weld layer height [137], and Xiong et al. showed that optical surveillance of the layer height of the previous layer and current layer can improve the process stability of the WAAM process [138]. Carter et al. used an IR camera to enhance the quality of a WAAM part [139].

Aside from the identification of a suitable filter for thermal measurement, the spectrum of emitted light can also be used for process surveillance itself. Zhang et al. has shown that process surveillance by optical emission spectroscopy is possible [127,140], as have others [141]. Guo et al. used the emitted spectrum for quality control assessment [127,141]. Zhang et al. showed that there is a correlation between the spectral intensity or electron density with the width of the deposited layers [140]. Reisch et al. developed a multivariate monitoring framework for WAAM using a robotic system. They used current and voltage surveillance alongside a wire feed monitor, gas flow sensor, welding cam, profile scanner, spectrometer, pyrometer, thermal imaging and acoustic surveillance [142]. The usage of artificial intelligence methods, like neural networks, to establish a real-time multi-parameter control has been shown to be beneficial [143].

Process surveillance needs to always be integrated in a certain control loop when its purpose should overcome scientific interest. In Figure 8, a closed loop control and material properties-oriented control loop for wire arc additive manufacturing is proposed. One approach has been created by Xiong et al. for the control of the weld seam width using a controlled travel speed with disturbances in the deposition current and the inter-layer temperature [144]. Another approach was conceived by Li et al. to realize closed loop control of the forming geometry by fuzzy logic [145] and by Xiong et al. for layer flatness [138].

2.3. Path Planning and Building Strategies

Path planning and building strategies have a significant impact on the geometrical correctness and thermal management in wire arc additive manufacturing, as well as reducing residual stresses and distortion [146]. The thermal conditions have a direct impact on the microstructure and mechanical properties of the manufactured part. This has been shown by various working groups. For example, Plangger et al. showed for high-strength steel that the distance between welding paths has a direct influence on the building heights [62]. Therefore, Xia et al. identified the path planning and building strategies as the main challenges in wire arc additive manufacturing [147]. To overcome this issue, different approaches have been created to figure out how process parameters like the wire feed speed, travel speed and others influence the weld bead width and height and make them controllable [51,62,117]. Fang et al. developed a prediction model for the weld seam width and height on the basis of the dynamic response of a WAAM process [148]. These approaches to make the necessary building height for each layer and the path distance predictable are necessary for further path planning. The general adaption of layer heights and layer widths is shown in Figure 13. A common way that the deposition parameter for the different processes could be identified was described by Dahat et al. [149]. Based on these process-related parameters, different path planning strategies for various applications are currently being investigated [50,59,150–171]. Ding et al. proposed path planning based on medial axis transformations, with good results for a fully filled part without a significant amount of defects [150]. Michel et al. showed that division of the part into different zones can be beneficial for path planning [151]. Xiong et al. presented a holistic and data-centric approach through a knowledge base to achieve a welding path plan [152]. Li et al. pointed out that lateral extensions are a critical point and have a significant possibility to generate failures, and they developed a strategy to realize lateral extensions [172].

Aside from the normal geometric aspects of path planning, the thermal history is the second key to reach the proposed material properties, and this in conjunction with adequate process surveillance can lead to material property-oriented path planning, which is supposed in Figure 8. The thermal history, on one hand, has an influence on the welding-related residual stresses and the distortion of the part, and on the other hand, the thermal

history has an influence on the microstructure of the material. Both aspects need to be taken into account for a material property-oriented path planning.

The influence of the path planning strategy on the residual stresses has been studied as well [173]. Zhang et al. showed that the path planning strategy has a direct influence on the residual stress distribution and identified the distance between single welding passes as the key point for accumulation of residual stresses [173]. The occurrence of residual stresses and distortion of welded parts is closely related to the obstruction of thermal expansion and constrictions. If the occurring stresses exceed the yield strength, the material will react and result in geometrical distortion. The distortion of WAAM-generated parts due to welding-related residual stresses has been investigated by Park et al. [174]. They studied the angular distortion of various materials with bead on-plate welds and transferred their results to a finite element model (FEM). Furthermore, they focused on the relationship between characteristic material properties like the yield strength, Young's modulus and thermal expansion coefficient [174]. However, it is important to state that the Young's modulus and yield strength at elevated temperatures need to be taken into account for better correlation. A deeper look at material property-oriented path planning reveals a multi-criteria issue which needs to be solved properly and in an efficient time period. One promising approach is the usage of a state-of-research solver for common (now WAAM-related) path planning problems as shown in [25] by Ehlers et al. Here, a modern Hamiltonian solver-based approach integrates the cooling conditions into material property-orientated path planning. Aside from material property-orientated path planning, different filling and layer-overlapping strategies for larger parts are under investigation as well [50,175].

Additive manufacturing opens the way to honeycomb metal structures for lightweight design in any industrial application [59]. Bähr et al. described a procedure to optimize the inner structure of WAAM honeycomb structures in detail and compared their modeling approach with experimental results for a simplified test piece [59]. Furthermore, they included a thermal conductivity model and path optimization in the path planning process, which led to a reduction in the parts' distortion of around 30%. The geometrical deviations have to be as low as possible, and some effort is being put toward development prediction models. Kumar et al. developed a theoretical model for the prediction of the width and height of multi-layer single-tack additive manufacturing [176]. They used the μ-plasma transferred arc welding process for additive manufacturing. They reached a prediction error of 2.3% for the manufactured height.

Aside from the path planning itself, incorrect movement and speed from the manufacturing equipment, especially for robots, have to be taken into account as well [177]. Bandari et al. found that for robotic-based additive manufacturing, the travel speed is inconsistent with the desired values in corner situations. This results in a greater deposition height and needs to be compensated, and they developed a strategy to do so [177].

Overall, path planning for additive manufacturing is considered a key factor for achieving the desired geometry and the desired material properties. Different approaches have been found to calculate an optimal path for the occurring deposition modes, thin-walled parts or full-body parts. Currently, the research leads to material property-oriented path planning for modern lightweight load-adapted product development.

2.4. Materials

Due to the repeated thermal cycles that an additively manufactured component undergoes, both the microstructure and the material properties differ significantly from those of conventionally manufactured rolled, semi-finished products. Knowledge of the dependencies between the process variables, thermal conditions (number of cycles, cooling conditions, etc.) and the resulting material properties is essential for predicting component properties and realizing material property-oriented path planning. The following is a summary of the current state of research for a wide variety of material groups. In addition, arc-based additive manufacturing enables a multi-material structure. This al-

lows load-dependent material selection and path planning during product development through the targeted utilization of anisotropies within a component. In addition, additive manufacturing enables the targeted control of mixing processes, resulting in advantages in material utilization for corrosion and wear protection. All these aspects are described in the following chapters. One advantage of the commonly used materials for WAAM is the direct transferability of knowledge regarding post-processing from welding-related topics to achieve the desired material properties with only slight changes [178].

2.4.1. Steel

Steel is one of the most used materials in construction and many other sectors of engineering. Therefore, steel is one of the most studied materials for WAAM as well. Due to the intense use in all areas of the industry, the mechanisms regarding welding-related microstructural and property changes are widely understood but still under investigation. For most applications and commonly used steel grades, the knowledge base of welding-related issues is huge. This knowledge includes single- and multi-run welds. These results for multi-run welds can be transferred to additive manufacturing with few changes. For example, the influence of different alloying elements such as titanium niobium and vanadium on the microstructure and properties of low-alloy steels are currently under investigation for joint welding [179–182]. In particular, work regarding nucleation for grain growth and the interaction between the alloying elements can be transferred to WAAM [179,183–185]. Aside from microstructural changes, the building-mechanisms of welding-related residual stresses can be transferred to WAAM as well since they are driven by microstructural phase transformations and restraints [186–188]. However, the restraints between joint welding and WAAM are different. The main difference between WAAM and joint welding is that the heat dissipation and some related microstructural phenomena become more pronounced in WAAM than in joint welding. For example, Wächter et al. has shown that the microstructure of a low-alloy steel can change from a welding-related one into a non-welding-related one due to repeated reheating and the chosen process values [53,189].

Commonly, steels can be divided into two groups: high- and low-alloy steels. In most cases, they differ in the microstructure and the welding-related effects that occur. In both cases, the properties of the deposited material depend on the thermal history of the material and are correlated to the microstructure, toughness, fatigue strength material and the used low-alloy steel [53,62,106,118,189–210] or high-alloy steel [12,19,63,64,105,207,211–227]. The microstructural changes in the dependence of the generation strategy is currently under investigation by many working groups for both low- [62,118,189,192–194,196,198,199,201–203,205,207–210] and high-alloy steels [12,19,105,207,211,212,214–217,223–225,227–230]. The microstructure after manufacturing largely determines the properties of the additively manufactured component, and different steels can be combined in multi-material structures to tailor the material properties to the needs of the application [52,231,232]. The current state of knowledge for the two steel groups is summarized below.

Low-Alloy Steels in Additive Manufacturing

Low-alloy steels are widely used in construction and industry applications (e.g., offshore construction) [233]. Currently, there are different grades of steel under investigation. The most studied grade is ER70S [106,118,178,191–193,198,201–204,206–208,233–235]. This trend in research leads to the usage of more advanced high-strength materials like ER90S [53,189,201], ER110S-G [209,236] or ER120S [62,196,201], but other grades are studied as well, such as ER55-Ni2 [210]. All works regarding the microstructure and the mechanical properties are related to the energy input. This behavior can be anticipated by the common knowledge about steel and its microstructure, and these relationships are known for most welding consumables and obtained for single- or multi-run welds. These differ little in most cases from that one found for additively manufactured materials, although the dilution and the number of heating cycles differ from joint welding. If the energy input into

low-alloy steels is too large, and if they are repeated too often, the microstructure changes from a weld microstructure to a structure of "normal" heat-treated steel. Wächter et al. showed that a ferritic-perlitic microstructure can be achieved due to WAAM. Figure 16 shows this and how the occurring microstructure changes with an increase of the interpass temperature. The beginning of perlite dissolution at a higher interpass temperature can be seen. Normally, however, for their used material, a welding-related microstructure has to be anticipated [53,189].

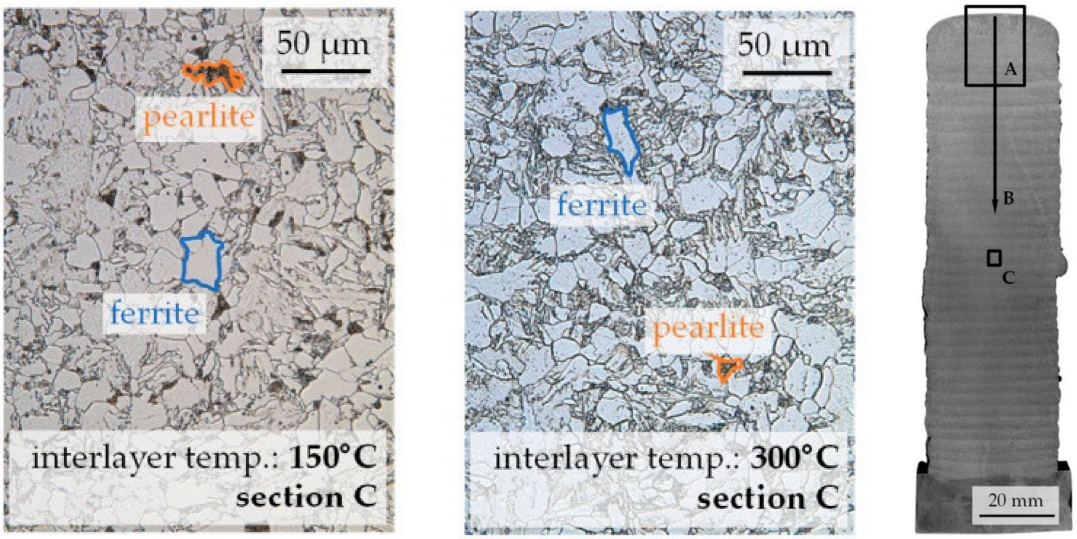

Figure 16. Micrographs of WAAM material for the interlayer [53].

Waqas et al. and Ron et al. showed that an isotropic microstructure is achievable for WAAM parts, and their impact toughness is high enough to have ductile behavior at room temperature [191,192]. Furthermore, Ron et al. showed that the additive-manufactured ER70S has similar corrosion behavior to St37 (S235) [192]. The mechanical properties of WAAM ER70S are highly anisotropic. Figure 17 shows this anisotropy and the found explanations from Ghaffarti et al. [193,198].

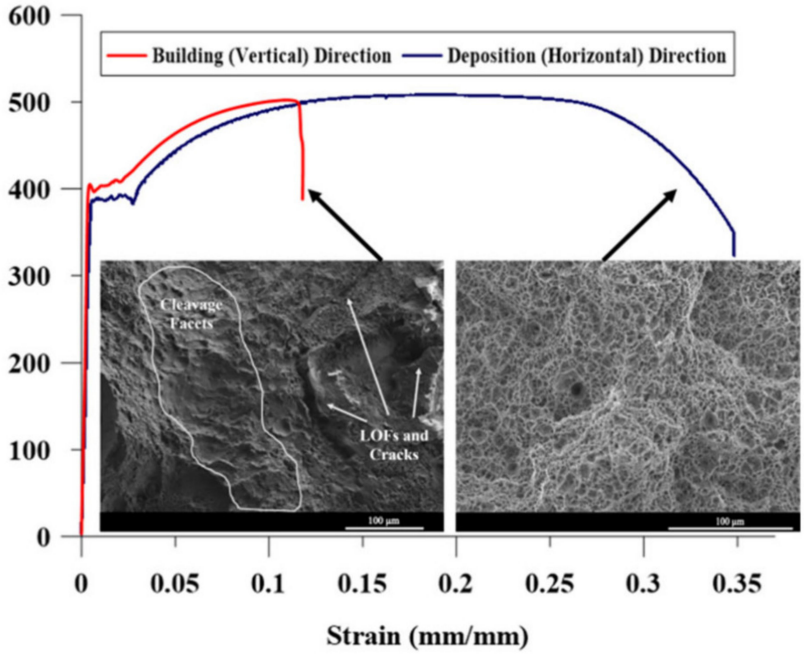

Figure 17. Stress–strain curve for WAAM ER70S [193].

The state of the vertical tensile test specimen across from the building direction has mixed mode fracture behavior of a brittle and ductile fracture, and it was proposed that the found anisotropy is related to welding defects. This anisotropic behavior has also been found in various other studies (e.g., [203]).

For high-strength steels like ER120S, Plangger et al. and Yildiz et al. showed that the mechanical properties are related to the used heat input [62,196]. The heat input is related to the cooling times and the decrease in hardness due to larger cooling times, which is commonly known for high-strength steel welding metal and high-strength low-alloy steels as well. This is also the case for newly developed materials [199]. The dependence of the mechanical properties on the heat input has been shown by Artaza et al. for a cross-process study of GMA welding and plasma arc welding [200]. A detailed model for the cooling times and the geometrical weld seam characteristics has been developed by Schröpfer et al. for a high-strength low-alloy steel (Figure 18) [237]. Furthermore, they showed that the residual stresses within WAAM-made parts increase with increasing heat input [237].

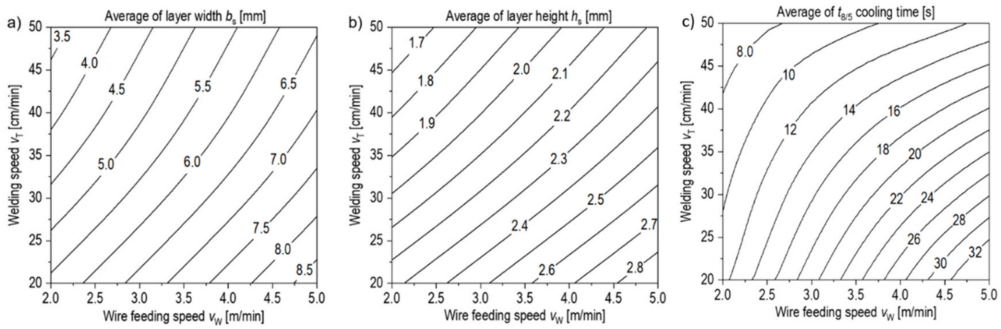

Figure 18. Average layer width (**a**), layer height (**b**) and $t_{8/5}$ cooling times (**c**) as a function of the wire feeding and welding speed in the investigated parameter range (contour plots of the regression models) [237].

For low-alloy steels, toughness is one critical aspect, and the toughness needs to be kept above certain application-dependent ranges. For ER70S, Moore et al. showed the experimental results for Charpy tests (Figure 19) [207]. They showed that the achievable toughness was in the range of the comparable X65 steel and, in some case, above it.

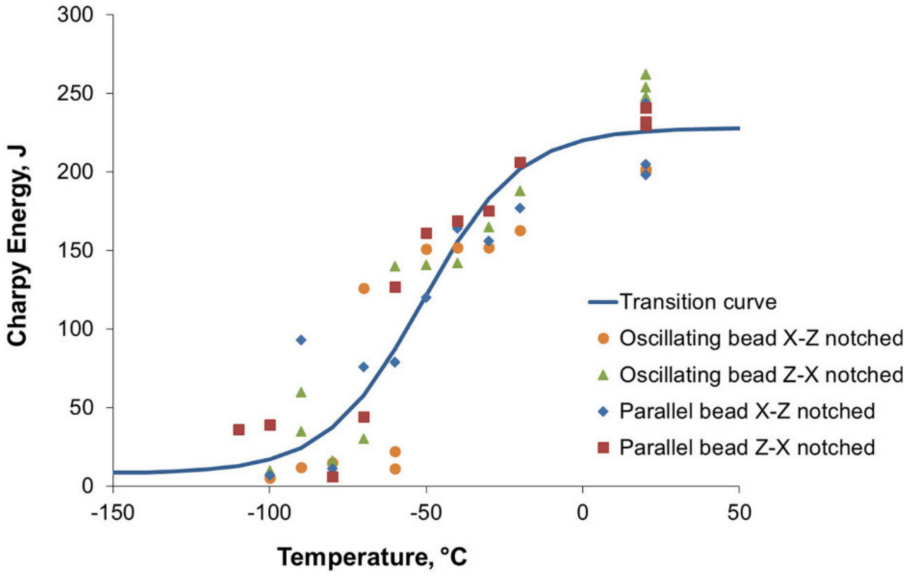

Figure 19. Charpy impact data and ductile-to-brittle transition curve fit for carbon steel arc-AM specimens [207].

The relatively high impact toughness was closely related to the goals for additive manufacturing of pressure vessels in the last century. The toughness of the weld metal can overcome the toughness values for correspondent steels in many cases, especially in the beginning of industrial steel production. Aside from the toughness and strength, the fatigue strength of the additive-manufactured low-alloy steel is one point regarding the usability of the additively manufactured parts. Wächter et al. looked closely at the material behavior under fatigue. They used a tensile specimen cross-wise and lengthwise to the welding direction (Figure 20), welded with two different interlayer temperatures.

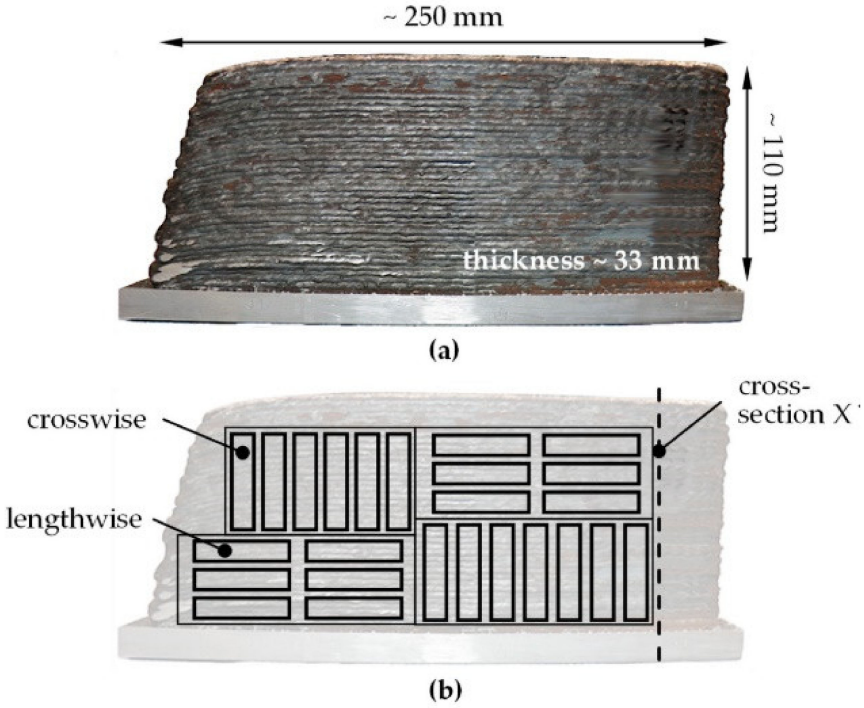

Figure 20. Wire arc additive manufacturing (WAAM) material: (**a**) semi-finished block products, (**b**) sampling plan for tensile specimens with directional designation related to the weld layers [189].

These specimens have undergone different strain-controlled fatigue testing. The stress–strain curves for the four used specimen types are shown in Figure 21. They showed that the Young's modulus from those curves differed between the different states but were more or less in the range of a normal scatter of those values [189].

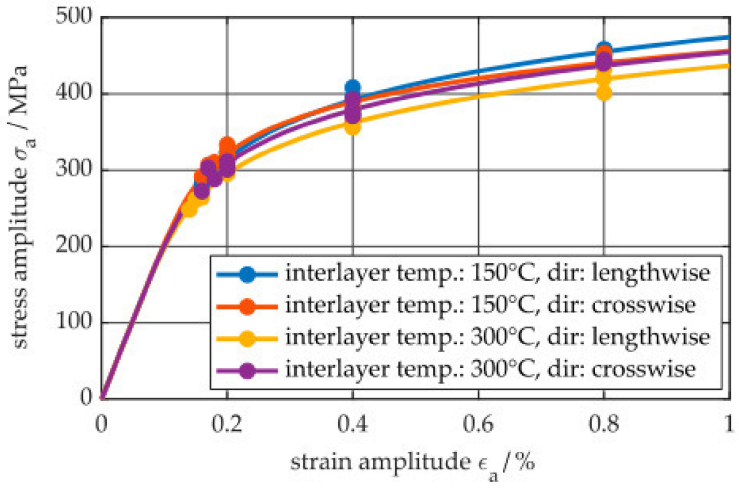

Figure 21. Cyclic stress–strain curves from the strain-controlled tests [189].

Furthermore, they derived stress–strain curves for the four different states and showed that the fatigue strength had no significant anisotropic behavior (Figure 22 and Table 2) [189].

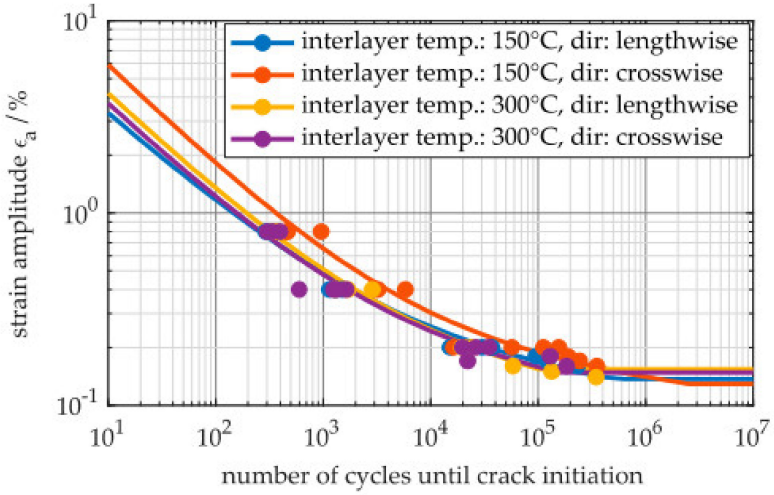

Figure 22. Strain–life curves (logarithmic scale) from the strain-controlled tests, including the fatigue limits from the stress-controlled tests [189].

Table 2. Fatigue limits determined by staircase tests at 5×10^6 cycles with a probability of failure Pf = 50% [189].

Interlayer Temp./°C	Extraction Direction	Fatigue Limit $\sigma_{a,E}$/MPa	Fatigue Limit Converted to Strain $\varepsilon_{a,E}$
150	lengthwise	256	0.137%
150	crosswise	254	0.129%
300	lengthwise	263	0.154%
300	crosswise	267	0.148%

This behavior can be explained by the intense reheating and heat input they chose. This led, as shown in Figure 16, to a non-welding related microstructure which had different mechanical properties and a less pronounced anisotropy.

Aside from the fatigue properties, crack growth rates become more important to avoid brittle instantaneous fractures. Ermakova et al. showed that the crack growth rates did not differ between different specimen orientations in accordance to the welding direction, and they furthermore showed that the commonly used determination methods for fatigue crack growth rates can be applied to WAAM-made parts as well [238].

To conclude, for the subsection regarding the wire arc additive manufacturing of low-alloy steels, it can be stated that low-alloy steels are processable with WAAM and reach a wide range of material properties, which can be in correspondence to known properties from the used welding filler.

High-Alloy Steels in Additive Manufacturing

High-alloy steels are usually grouped with stainless steels and heat-resistant steels, and this group contains other steels as well. Within these classes, high-alloy steels can also be differentiated due to the microstructure (e.g., ferritic stainless steels, austenitic stainless steel, austenitic-ferritic duplex stainless steel, ferritic chrome steels and martensitic chrome steels).

One large group within high-alloy steels is stainless steels. Jin et al. gave a good overview of the work up to January 2020 in the wire arc additive manufacturing of stainless steels [30]. They pointed out that the macroscopic characteristics–the geometry–are closely related to the process values, such as wire feed and travel speed and also the energy input

and cooling times. Furthermore, they stated that understanding of the solidification behavior is crucial for an adequate manufacturing process and the correlates with the common view in joint welding for high-alloy steels, and it is correspondent with the common knowledge of welding processes, where each solidification mode (e.g., ferritic, ferrtic-austenitic or austenitic-ferritic) has its own challenges. Aside from the microstructural implications, the effect of residual stresses and distortion, which occur due to thermal cycles, has to be considered, and thus it will increase with the increasing part size [239]. Furthermore, Jin et al. pointed out that the WAAM techniques, material composition, shielding gas composition, post-heat treatments, microstructure and welding-related defects have a significant influence on the material properties of the stainless steel parts [30].

The main difference of WAAM in comparison with other additive manufacturing processes is the higher energy input (Figure 23) [30].

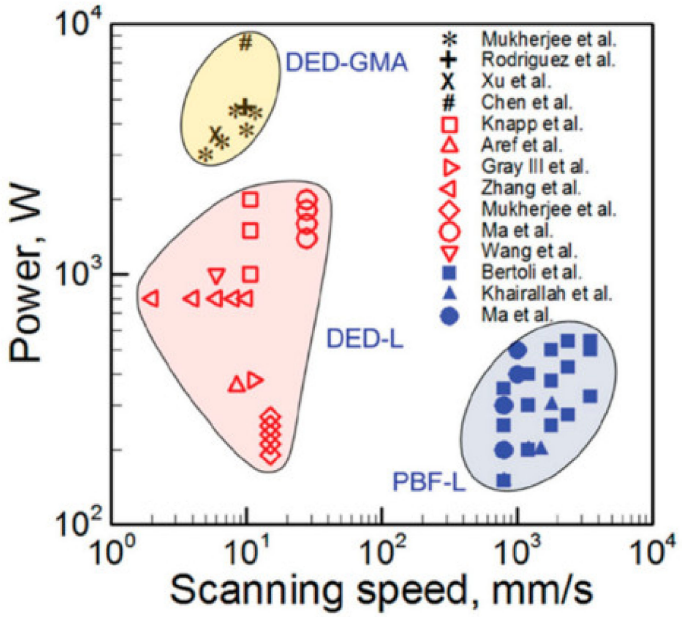

Figure 23. Power and welding speed for different additive manufacturing processes for 316L stainless steel [30] (DED-L = direct energy deposition laser, PBF-L = laser-based powder bed fusion).

This main difference allows the usage of established welding consumables for the welding of high-alloy steels. This leads to known relationships between the heat input, cooling regimes and microstructure and the mechanical properties [30]. In addition, the influence of shielding gasses is mostly known. Furthermore, welding-related microstructural issues like the formation of sigma phase or cracking phenomena [240,241] can be transferred from the knowledge of joint welding.

The geometrical correctness of WAAM-made stainless steel parts has been evaluated by Laghi et al. [242] and others [30]. Jin et al. summarized the different studies and stated that the geometrical correctness is closely related to the welding speed, wire feed speed, welding mode (e.g., impulse or short arc), cooling time and interpass temperature. The welding speed and wire feed can be combined with the energy input. In combination with the part geometry, the energy input and the interpass temperature define the cooling rate. One crucial point for geometrical correctness is the proper assessment of distortion. Manurung et al. presented a model for distortion prediction of 316L steel [243]. They showed that a nonlinear approach shows good results in predicting the distortion of 316L steel. They furthermore showed that current state-of-the-art heat source models can be used to successfully build that prediction model [243].

Aside from geometrical correctness, the mechanical properties of the parts are essential for the use of the parts. Jin et al. stated that the reported mechanical properties of additive-manufactured high-alloy steels match those of machined components [30]. This is

supported by works from Tabernero et al. [211], Ji et al. [212] and others [215,217] as well as work on maraging steels [218] and for other materials due to the highly oriented microstructural growing direction where the anisotropic material properties occur [64,212,221,223]. For quasi-static loads, this behavior is also present for specimens with as-welded surfaces [63]. This anisotropy shows up for the fatigue crack growth behavior as well [214]. Other studies state that additive-manufactured high-alloy steels show a homogeneous distribution of the material properties [216]. This difference can be influenced by the chosen energy input and manufacturing strategy and needs to be addressed in further research. To cover those effects, Laghi et al. developed an orthotropic elastic model for WAAM parts which included the microstructural orientation and calibrated this model with experiments. They stated that this model allowed the prediction of the elastic material behavior [244].

A special group within high-alloy steels are duplex stainless steels, which derive their properties from a defined austenite-to-ferrite ratio. This ratio is highly dependent on the cooling conditions and therefore on the welding parameters, but different welding parameters can also result in acceptable microstructures [222,223,225,228,245]. Furthermore, the repeated reheating during WAAM has an influence on the phase fractions of duplex steels and needs to be considered [246].

Gao et al. showed that the additive manufacturing of heat-resistant martensitic chrome steels is possible as well, and they show proper mechanical properties, aside from the fact that long-term creep results were missing and not expected for the next few years [224]. Furthermore, Ge et al. showed strong texturing of the microstructure [247]. In addition, Vehedi Nemani et al. showed that post-weld heat treatment can have a significant and positive effect on the microstructure and mechanical properties of these types of steels, especially to reduce the amount of retained austenite and generate a fully martensitic microstructure [248].

Aside from the basic mechanical properties, the properties of the materials under wear is in the focus of the research and can be essential for technical applications. For high-alloy steels, those wear resistance properties haven been studied by Parvaresh et al. using the ASTM-G99-05 test on stainless steel 347, and they stated that the direction of the specimen in accordance with the welding direction had no significant influence on the wear resistance of the used steel [216].

Overall, it can be stated that wire and arc additive manufacturing can be realized with a wide range of high-alloy steels. The main challenges for welding high-alloy steels, like the formation of brittle phases or hot cracking, are also present in additive manufacturing with welding processes.

2.4.2. Aluminum

Aluminum is one of the most widely used lightweight construction materials. Therefore, the desire to use aluminum in additive manufacturing to further increase the lightweight potential of additively manufactured structures is even more pronounced. Aluminum also has access to a wide range of additive materials with known properties. In addition, the defects that occur during the welding processing of aluminum have been thoroughly studied. Different working groups are focusing their studies on the usage of aluminum alloys for wire arc additive manufacturing [46,55,58,72,79,97,140,170,249–282]. A wide range of different aluminum alloys is being investigated. It has been shown that the used substrate for additive manufacturing can be preformed [251].

For aluminum alloys, knowledge of the correlations between the welding process variables and the achievable build-up heights and widths is also of decisive importance. Gomez et al. showed this for different welding speeds. In addition, they showed that the layer width also depends on the number of layers [253].

In the case of aluminum, due to the relatively high coefficient of thermal expansion, the consideration of residual stresses and distortion is of decisive interest for geometrically accurate production. It turns out that residual stresses can occur up to the yield point. These residual stresses are distributed anisotropically over the component and with dependence

on the direction of assembly. They can be significantly reduced by mechanical post-treatment to reduce residual stresses, such as rolling or higher-frequency hammering processes. In particular, rolling also leads to a significant reduction in distortion [256].

The surface quality of the manufactured components can be significantly improved for aluminum alloys by adjusting the process edge sizes, particularly the pulse repetition frequency and the polarity [259].

The formation of pores is one critical point in the welding of aluminum and occurs due to the solvability gap of hydrogen in molten and solidified aluminum [283]. Aside from the hydrogen explanation for pore formation, other hypotheses show that a wider range of gases are responsible for pore formation, such as the hydrocarbon hypothesis [284]. Hydrogen-induced pore formation is no new effect for welding aluminum and does not occur only for WAAM [285]. Nevertheless, control of the porosity is crucial for usable WAAM-made aluminum parts [283]. There are different approaches for controlling the porosity in welding and WAAM as well. One new and promising approach is the usage of a hyperbaric process environment. Here, pore formation can be significantly reduced to nearly zero percent porosity when a pressure of more than 10 bar is applied in a manufacturing chamber [285]. Aside from an increased ambient pressure process, side modifications have been studied to reduce the porosity. It has been shown that an increased interlayer temperature leads to decreased porosity [286]. This supports the general assumption that improved outgassing due to delayed solidification of the melt can lead to reduced porosity of the weld but contradicts the general assumption that slower cooling and a hotter melt absorbs more hydrogen, which leads to greater porosity [287]. The influence of the interlayer temperature and the mode of arc welding (e.g., pulsed or controlled short arc) has been studied by Derekar et al. They showed that the effect of the interlayer temperature depends on the welding mode [287]. Therefore, a general assumption on the influence of the interlayer temperature cannot be drawn. Furthermore, they showed that the welding mode itself has an influence on pore formation as well. They stated that an impulse welding mode leads to more pores than controlled short arc processes.

The use of well-studied filler metals avoids the tendency of aluminum to form hot cracks, but in order to be able to use the advantages of age-hardenable aluminum alloys, new filler materials have to be developed. For example, Klein et al. developed and qualified a new TiB2-doped filler metal for additive manufacturing, which can be processed without cracking and shows a significant increase in strength through aging [288]. Morais et al. showed the age-hardening of a novel high-strength Al-Zn-Mg-Cu alloy [252]. This alloy exhibits a light anisotropy in its mechanical properties as well, and Ünsal et al. showed the feasibility of additive manufacturing of EN-AW6016 [254].

The aluminum WAAM-made parts exhibit anisotropy behavior in their mechanical properties [55,58,249,250,258] and meet the mechanical properties given by the wire manufacturers, and post-weld heat treatments are possible [289].

Taken together, it can be concluded that arc-based additive manufacturing is possible and that the mechanical properties are similar to those of standard welded metal. Furthermore, the results show that the typical problems of aluminum welding, such as pore formation or susceptibility to hot cracking, can be overcome.

2.4.3. Copper

The usage of copper alloys like nickel aluminum bronze [290] in different applications in the industry increases the demand for applying WAAM for copper alloys as well [12]. Chen et al. showed that WAAM of a CuAl8Ni2Fe2Mn2 alloy is possible and investigated the effect of the deposition height on the microstructure and mechanical properties of that alloy. They showed that the microstructure is highly oriented with the corresponding anisotropy behavior of the mechanical properties, and furthermore that the mechanical properties decrease with an increasing layer height [291]. In additional work, they showed that the interpass temperature has no significant influence on the microstructure and that ultrasonic stimulation of the molten bath can lead to fining of the microstructure [292].

An altered microstructure can also be achieved by using different welding modes, like impulse welding or short arc welding [293]. Furthermore, due to the usage of in situ alloying, modern Cu-Al alloys can be used for WAAM as well [294] and furthermore be strengthened by the addition of silicon or applying deep cryogenic treatment [295,296].

Overall, copper alloys can be used for WAAM, but there are only a few working groups focusing on copper.

2.4.4. Titanium

The high price of the base material and poor utilization of the material of the semi-finished products in conventional machining production is driving the desire for additive manufacturing of titanium materials in all sectors of industry, like the aviation industry [297]. Due to the high deposition rates, arc-based manufacturing should also be used if possible. Therefore, different working groups are dedicated to this task [39,70,98,107,211,297–319]. There are two key points in the arc-based additive manufacturing of titanium alloy. One is sufficient protection from oxygen to avoid the well-known oxygen-induced embrittlement and the accumulation of heat in the manufacturing process [298,316,320]. For titanium, as a light metal with a density of approximately 4.5 g/cm^3, deposition rates of 2.5 kg could be achieved [211].

As for other materials, a significant anisotropy of the properties and microstructure occurs in titanium alloys [299–301,307]. This is also true for the fatigue crack growth behavior [302,308]. The directional grain growth that occurs in titanium alloys in additive manufacturing can be reduced by an intermediate forming process [39,47,98,107,299,305,312,313], the addition of further elements like boron, silicon or other elements [303,311,317,321,322] or applying post-weld heat treatment [304,314]. Furthermore, like for other materials, the cooling rate or the inter-pass temperature has a significant influence on the mechanical properties of WAAM-made titanium alloy parts [309,310,318]. Furthermore, the machinability of Grade 5 titanium has been investigated, and it has been shown that the manufacturing strategy has a significant influence on the cutting forces [323]. However, overall, wire arc and additive manufacturing is possible for technically relevant titanium alloys, and these alloys can further be modified to suit the needs of additive manufacturing.

2.4.5. Magnesium

Magnesium is, due to its good strength-to-weight ratio, a promising material for lightweight design. As stated above, lightweight design is one possible way to use WAAM, and this makes magnesium a highly interesting material for WAAM. Guo et al. showed that a WAAM TIG-based process with magnesium is possible [324,325]. Gneiger et al. showed the possibility to use a controlled, short arc GMA-based WAAM process for manufacturing AZ61 and AEX11 [289,326]. Figure 24 shows a sample part for the additive manufacturing of an AZ61A magnesium alloy [289].

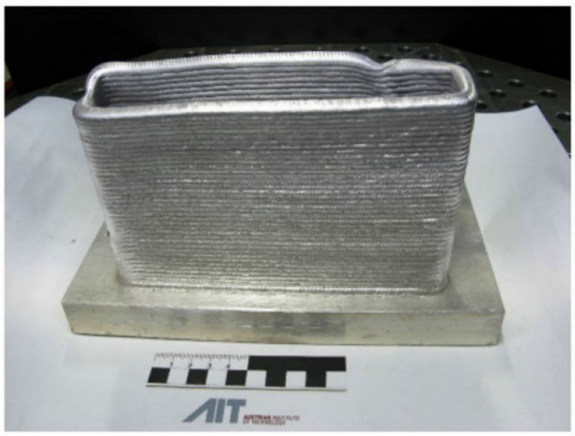

Figure 24. One magnesium (AZ61A) sample fabricated by WAAM [289].

2.4.6. Nickel

Wire arc additive manufacturing is also performed for nickel alloys, and various working groups have realized the WAAM of nickel base alloys successfully [70,81,103,327–341]. Different common nickel base alloys are being used for additive manufacturing like Inconel 625 [327,337,340], Hastelloy C276 [335] or Inconel 718 [328,329,333]. Kindermann et.al. studied the process response of Inconel 718 and CMT-GMA welding and determined correlations between the process parameters and the build-up height and seam width [333].

The mechanical properties of nickel-based alloys are mostly achieved due to post-weld heat treatment. The knowledge of post-weld heat treatment is not only driven by WAAM-related research, especially when new alloys are developed. Tang et al. showed that heat treatment of an additive-manufactured, newly developed alloy changes its material properties through post-weld heat treatment [342]. However, many nickel-based welded alloys undergo additional post-weld heat treatment (PWHT) [112,333]. It has been shown that the post-weld heat treatment parameter can differ from the recommended ones for bulk material [333] and has its most impact on the formed secondary phases [334]. In addition to the properties under quasi-static loading as well as under fatigue, the behavior of materials under increased strain rates (increased loading rates) is becoming more and more interesting for applications. The current focus is on modeling crash behavior. The characteristic values for the modeling of high strain rates have also been determined for WAAM-manufactured nickel-based alloys [329,331].

The milling of a WAAM-made nickel-based alloy has also been investigated [112]. Most nickel base alloys tend to form so-called "white layers" in the process of milling, which will be the most used post-process for WAAM to achieve good surface quality [112].

These surface layers have undesirable properties for technical applications. In addition, milling induces undesirable plastic deformations and residual stresses below the surface (Figure 25). To reduce these effects, ultrasonic assisted milling could be used. Figure 26 shows the occurring residual stresses due to milling of the additively manufactured alloy 725. By using ultrasonic assisted machining, the residual stresses that occur can be significantly reduced, and this is independent of other peripheral variables such as the stepover or the use of cooling lubricants. Figure 26 shows that this effect is also maintained down to the depth of the material. White layers have also been found for additively manufactured alloy 725 (Figure 27).

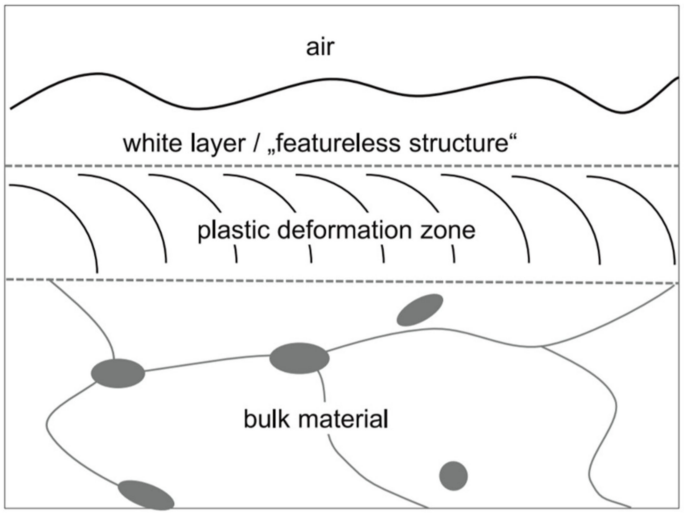

Figure 25. Surface morphology of a white layer [112].

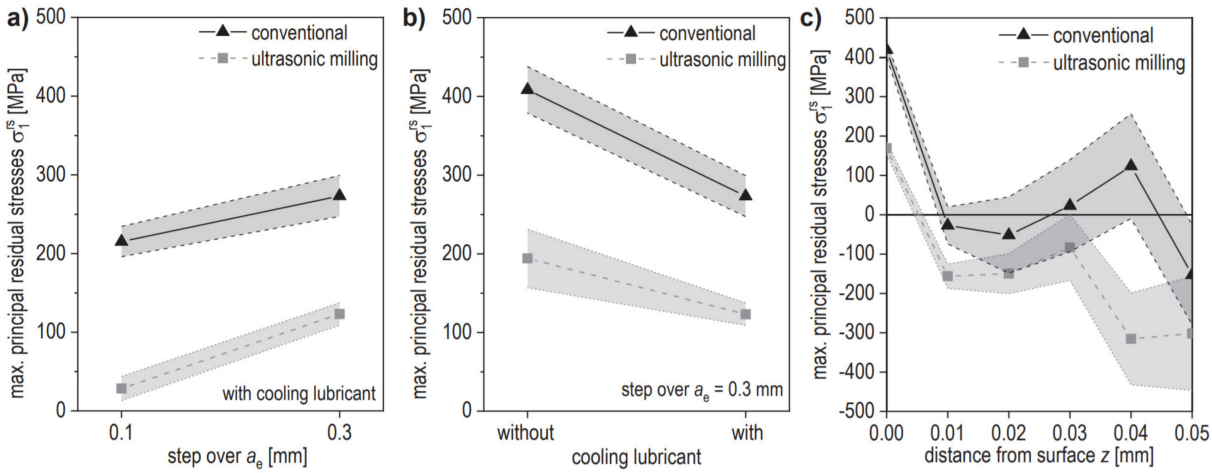

Figure 26. Maximum principal residual stresses vs. step over a_e and the application of ultrasonic assistance (**a**) and vs. the application of cooling lubricant and ultrasonic assistance (**b**), and the maximum principal residual stress profile in the direction of the specimen thickness after finishing milling with and without ultrasonic assistance (**c**) [112].

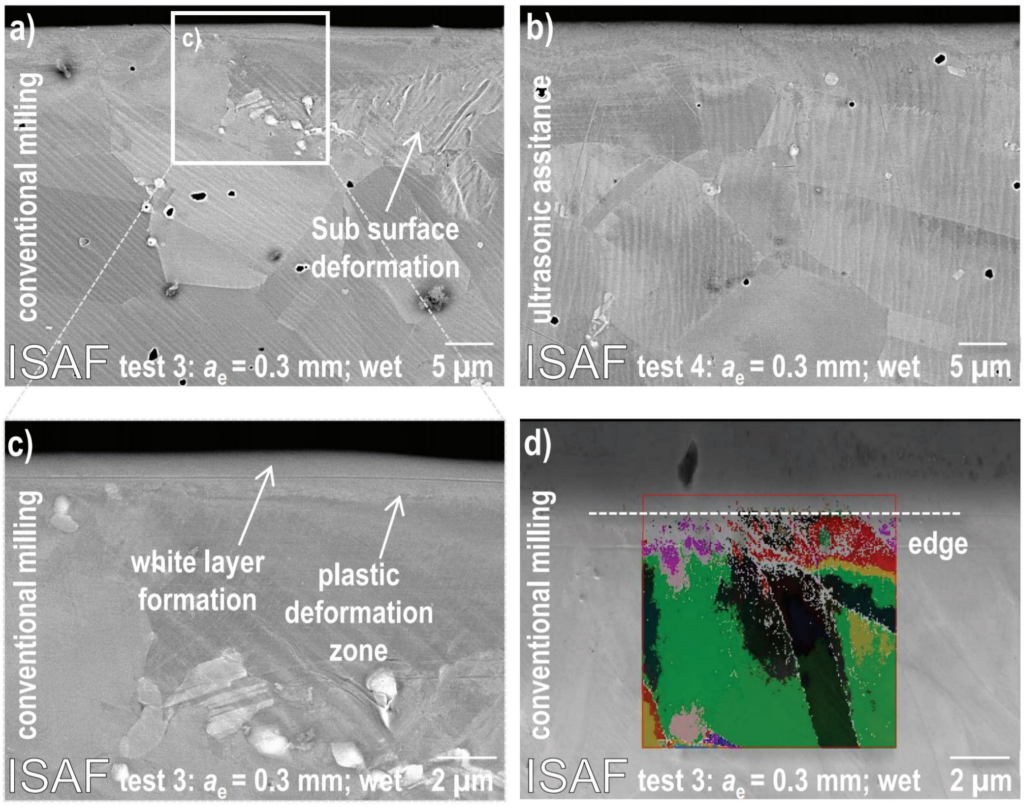

Figure 27. SEM image of cross sections of milled specimens of test 3 (**a**) and test 4 (**b**) and detail of the surface plastic deformation zone and white layer of test 3, showing the SEM analysis (**c**) and EBSD mapping (**d**) [112].

By ultrasonic assisted milling, the occurrence of these can be significantly reduced (Figure 27) for the used WAAM-made alloy 725 [188]. On the left, an REM image of a cross-section of the surface of the additive-manufactured alloy can be seen. In the surface region, a homogeneous phase without any detectable substructure is visible. This brittle white layer can lead to faster damage to the part and needs to be avoided. On the right of Figure 27, this layer is not visible, and no subsurface deformation can be detected. Aside from that, the needed cutting forces could have been reduced by 20%.

Overall, the presented works show that wire arc additive manufacturing of nickel base alloys is possible and gives suitable results.

2.4.7. Tantalum

Wire arc additive manufacturing is also performed for tantalum alloys [343,344]. Two different alloys have been analyzed by Marinelli et al. [344]. They showed that, in general, TIG-based additive manufacturing is possible, but an anisotropic microstructure forms as it has for other elements as well. The tensile properties matched the mechanical properties of the used substrate. Furthermore, they found a notable hardening effect due to multiple cycles of re-heating.

2.4.8. Tungsten

Tungsten can also be used as a material for arc additive manufacturing. Marinelli et al. showed that unalloyed tungsten can be built up into additive structures using the TIG welding process [38,345]. Furthermore, they showed that subsequent heat treatment has no significant effect on the microstructure (Figure 28).

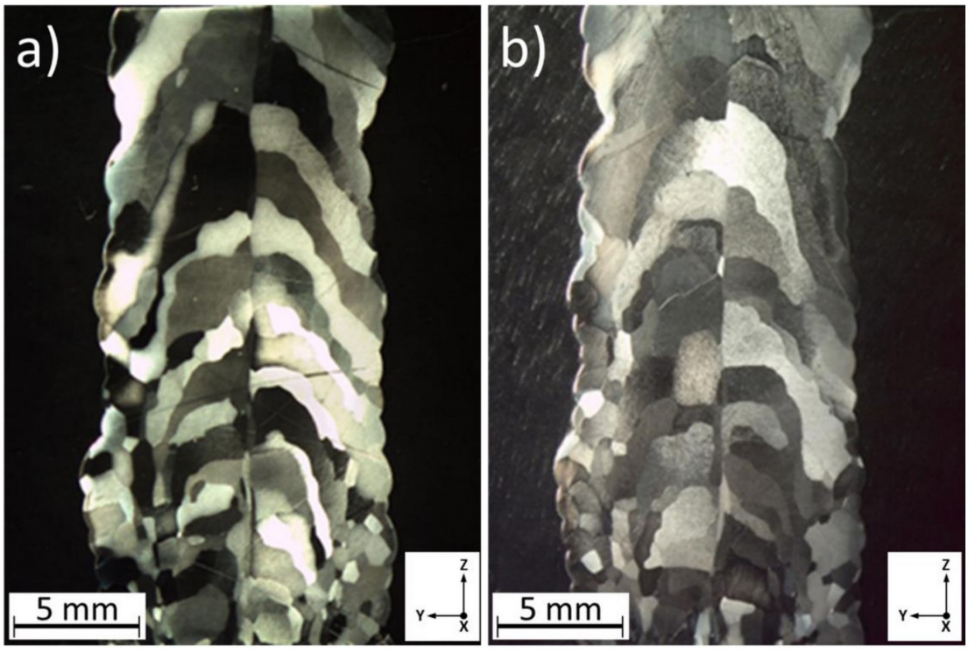

Figure 28. Microstructure of the front view of the as-deposited (**a**) and the heat-treated structure (**b**) [38].

In the given work, they showed how an additive manufacturing system can be used for the production of tungsten parts and also which process variables and process instabilities, such as pores, can occur during the addition of tungsten using the WAAM process.

2.4.9. Intermetallic Materials

Various researchers are using wire arc additive manufacturing for generating intermetallic materials like iron-aluminides [346–351], titanium-aluminides [352–358], iron-nickel [359], iron-titanium [360] or nickel-titanium [361–363]. Most studies on intermetallic materials have shown their interesting mechanical properties for industrial application and how hard they are to machine. In most of the listed studies, dual wire technology was used to achieve intermetallic alloys. This technique is extremely suitable for the targeted investigation of intermetallic materials and also gives rise to hope for industrial implementation.

2.4.10. High-Entropy Alloys

High-entropy alloys are the next upcoming material group with interesting and promising properties that research has focused on. The production and processing of these alloys is still in its infancy, but by applying an extraordinary technique, the arc-based additive manufacturing of a selected high-entropy alloy could also be carried out without having a single wire with the desired alloy composition. For this purpose, a filler metal with a wire-like structure of seven individual strands was produced and successfully processed in an arc welding process. The actual microstructure of the alloy is very similar to that of a cast sample, but it has differences due to the process. Taken together, the procedure presented by Shen et al. suggests further implementation of additive manufacturing of high-entropy alloys [364].

2.4.11. Multi-Material

Different working groups are conducting research on the combination of different materials in one work piece. Two different approaches can be distinguished here. The first one is an in situ alloying approach by different techniques, and the second one is a metallic composite approach with different objectives (e.g., improving material properties for strength, fatigue, corrosion resistance and wear).

In situ alloying can be used for different purposes. Among them is attaining functionally graded structures (e.g., as demonstrated by Marinelli et al. for tantalum, molybdenum and tungsten [365] or Shen et al. for Fe- FeAl material [366] and others for different materials [358,367,368]). One promising approach is the usage of a secondary cold or hot filler material to achieve the desired material properties [296]. Wang et al. used this technique to obtain a $CuAl_{6.6}Si_{3.2}$ alloy [369].

In situ alloying can be performed by various techniques. There are multiple wire processes and modified wires [60,295] as well as the addition of powders [268,370] or the modification of filler by surface coatings [182,371–374], and furthermore, in situ alloying can be used to generate functionally graded structures.

The second approach can be divided into two subsections. First, there is the area of coatings and functionally graded structures, and secondly, there is the area of internal composite-like metallic structures. The basis for these two approaches is the understanding of the metallurgical mechanism to join these different materials. For stainless and mild steel, some occurring challenges have been given by Anirudhan, but the occurring phenomena have been known and studied for mixed material joints for most materials in the past and can be transferred from a metallurgical point of view to additive manufacturing [231].

Functionally Graded Structures

Functionally graded structures are used to generate locally adapted material properties. This is mostly used in the area of wear or corrosion protection. It has been shown that in the area of corrosion-resistant materials, the building strategy can lead to a significant reduction in necessary and cost-intensive cladding material [52,375]. This can be accomplished by a building strategy where the corrosion-resistant material is printed first so the dilution is reduced significantly (see Figure 29).

Here, four different building strategies of alloy 625 on a low-alloy steel with different dilutions were carried out and tested in “green death” to get a correlation between the corrosion resistance and the dilution. It was clearly shown that the building strategies through the dilution had a significant impact on the corrosion resistance [52,375]. Another approach was carried out by Chen et al. They used a double-wire WAAM process to achieve a graded material from titanium to 316L steel with the anticipated brittle intermetallic phases of titanium and iron [376].

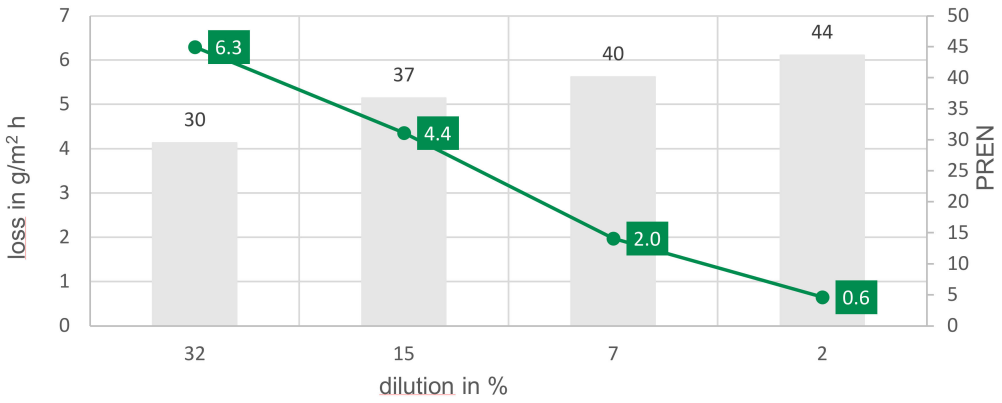

Figure 29. Loss over dilution for different building strategies [52].

Overall, it can be stated that WAAM is suitable for the generation of functionally graded structures and that WAAM can lead to the reduction of cost-intensive materials for corrosion resistance and wear protection due to a dilution-related building strategy.

Metal Matrix Composite-Like Structures

The metal matrix composite-like approach is characterized by generating load-dependent and directed materials for fortification or suiting the integral mechanical properties to the occurring loads. It was shown that layered welding-based manufacturing can realize metal matrix compounds like structures with different fiber types such as carbon fibers (see Figures 30 and 31) [232,377].

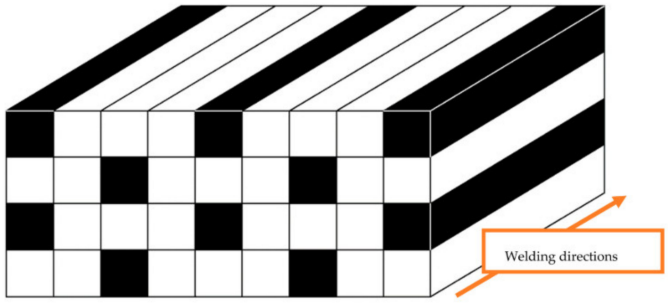

Figure 30. Fiber-like reinforcement of additive-manufactured material (white: soft material; black: strong material) [52,232].

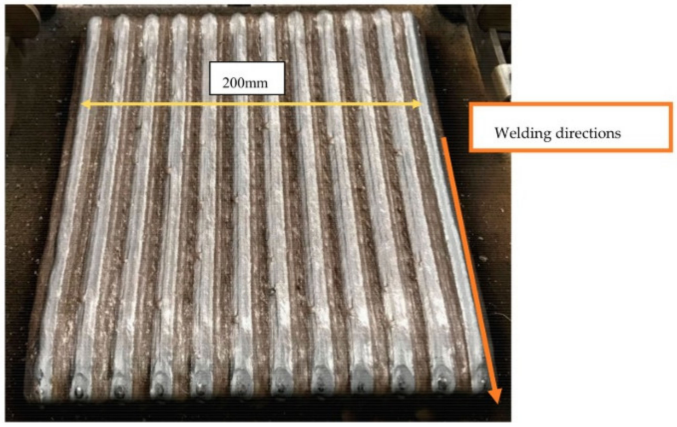

Figure 31. Welded specimen according to [52,232].

Here, as an example, a soft matrix of FeNi36 was reinforced with a high-strength low-alloy steel in accordance with DIN EN ISO 16834-A G 69 6 M21 Mn4Ni1, 5CrMo. Welding-related problems like hot cracks were not observed.

The mechanical properties (see Figure 32) showed that the reinforced material reached far higher values longitudinally then currently used estimation methods predict [52,232].

Direction	$R_{p0,2}$ [MPa]	R_m [MPa]	TEL [%]
Transverse upright	439	591	8
Transverse flat	433	567	7
Longitudinal upright	459	657	15

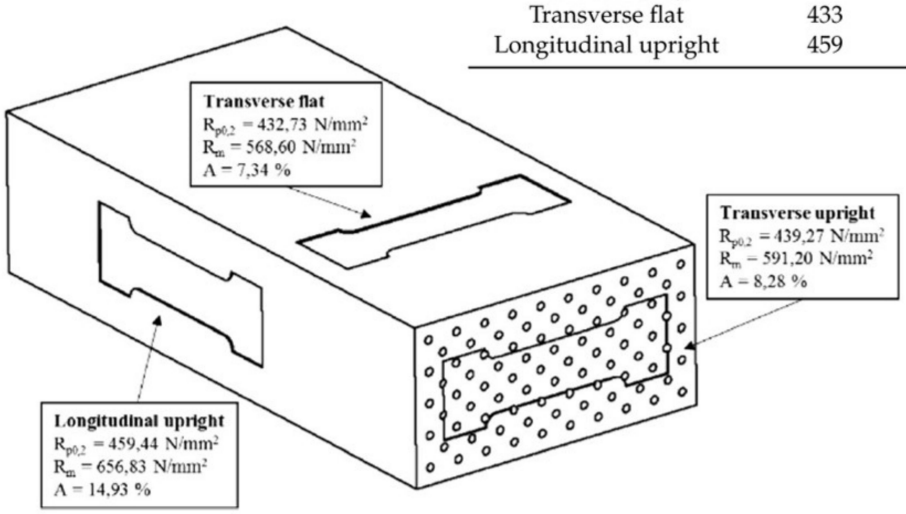

Figure 32. Strength of multi-material system of HSLA steel and FeNi36 [52,232].

This multi-material approach has also been realized by Hauser et al. for different aluminum alloys [378].

The second interesting approach for metal matrix composite-like structures is the application of a different material into notches to achieve the local plastification potential and increase the material's resistance against fatigue [52].

Due to the different material properties in multi-material WAAM, the distortion of the part can increase, but this effect can be countered by an optimized path planning and manufacturing strategy, as He et al. showed for a bi-metallic rocket motor [379]. Overall, the multi-material approach is one of the key features that makes additive manufacturing unique and should be studied further.

3. Modeling

The modeling of WAAM takes a big part in research activities [37,56,59,169,278,329,380–400]. Modeling research can be divided into two main topics: the first one is finite element modeling (FEM) of the manufacturing process, distortion and properties (summarized as material property-oriented modeling), and the second is modeling of the bead shape, overlapping and thermal conduction for path planning reasons, which can be summarized as process-related modeling. In addition, other subtopics in WAAM knowledge from joint welding-related modeling can be transferred to additive manufacturing, like the commonly used Goldak heat source [401] and its further developments [402]. The literature shows that a variety of modern and established simulation methods, such as the use of the Lagrangian method for the modeling of the process behavior (distortion and residual stress) and implicit and explicit solution methods, is used to calculate the thermo-mechanical fully coupled and uncoupled models [398]. Machine learning approaches are also used, for example, to estimate the surface roughness in WAAM [399]. The sub-topography can also be estimated using KI-based methods [403].

3.1. Material Property-Oriented Modeling

A detailed description of a possible modeling FEM path for WAAM was described by Israr et al., and some special problems concerning the solution of FEM models with different solvers was examined as well in [382,398]. Furthermore, Israr et al. showed that the prediction of the distortion occurring in WAAM-made parts is possible and corresponds with comparable experiments.

In arc welding, the resulting part distortion has always been a problem. This also applies to arc-based additive manufacturing. Thus, the prediction of the deformation of the component is of crucial importance for the production of geometrically correct parts. Casuso et al. developed a prediction model for this deformation in thin-walled parts [400]. They showed that their used model and approaches can predict the occurring temperature field with an error of 5% and the distortion with a deviation of 20% [400]. Aside from the deviation, the material's behavior under elastic strain is of interest for various applications and can modeled to predict this behavior [244]. Furthermore, they developed a data-driven surrogate model for the power control in WAAM, which can lead to the reduction of distortion and residual stresses [404]. Manurung et al. worked on a model for distortion prediction in 316L steel [243,405].

Aside from distortion, fatigue assessment is crucial for the usage of WAAM-made parts in industry. Therefore, prediction of the fatigue performance of additive-manufactured parts is necessary. Bercelli et al. developed a probabilistic fatigue model relying on the self-heating behavior and internal imperfections [406]. This model allows theprediction of the fatigue strength with a reduced scatter in comparison with the fatigue test performed on WAAM-made material and should reduce the testing amount. They proposed that only tomography tests need to be conducted to determine the pore population of the material [406]. Based on numerical simulations, Bartsch et al. developed a proposal for the classification of rough, unmachined surfaces in WAAM in the international standard [114].

3.2. Process-Related Modeling

The weld bead geometry has a significant influence on the geometrical correctness of the build part. The prior estimation of the bead's behavior can be beneficial for the path planning and manufacturing process. Therefore, Mohebbi et al. derived a thermo-capillary-gravity model for a WAAM process which includes the material properties of the melt and the process variables of the manufacturing process, which have an influence on the weld bead shape (Figure 33) [8].

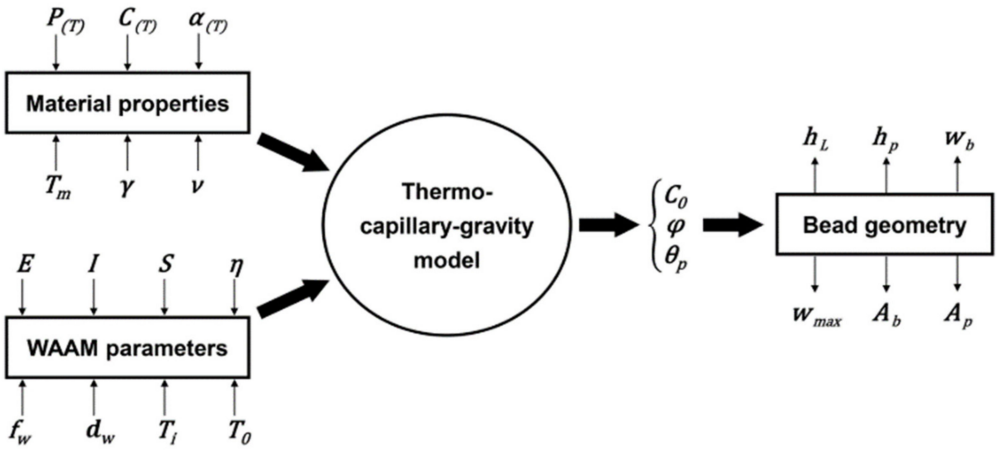

Figure 33. Input and output flowchart of the thermo-capillary-gravity model by Mohebbi [8].

They showed that the developed model had good correlation with the experiments for mild steel. Prajadhiama and Manurung conducted some work on adjustment of the melt pool and the commonly used Goldak's heat source for additive manufacturing [405].

Bähr et al. described a modeling approach with a thermal conductivity model in detail and compared their modeling approach with experimental results for a simplified test piece [59]. Using such models can lead to a reduction of heat accumulation for honeycomb-like structures. The understanding and prediction of material transition is one of the challenging parts in welding-related process simulations and is currently under development not only for WAAM but welding in general [35,380,381,407]. Cadiou et al. developed a model for heat transfer and fluid flow and compared it to experiments with good correlation [381,407]. A similar model has been developed by Zhao et al. for heat transfer, mass transfer, fluid flow and geometry morphology [408].

Due to the distortion occurring in arc-based additive manufacturing, methods for reducing distortion are the subject of modeling. Here, different fixation variants are investigated in terms of their suitability for distortion reduction and the resulting residual stress distribution [409]. Israr et al. found, based on numerical analysis, that less restraints reduced the amount of distortion and residual stresses and that edge fixation was the most suitable fixation strategy for the wall-like structure in their analysis [409]. Furthermore, they developed a model which could be used to avoid heat accumulation, one of the key problems in WAAM of small-to-large parts [404]. This heat accumulation leads to long interlayer waiting times and unwanted inhomogeneous mechanical properties across the part. Aside from the modeling of the WAAM process itself, different post-processes for WAAM-made parts are also subject to modeling activity (e.g., rolling processes [104,410]). The commonly used part of WAAM is the modeling and prediction of the building process regarding layer height and width.

Overall, modeling of WAAM is one of the key points to predict the final part properties and needs to be integrated into the process chain to fully utilize the benefits of WAAM.

4. Quality Control

Aside from proper process surveillance to reduce manufacturing-related imperfections, quality control is the basis for the extensive use of WAAM parts in the industry. Lee et al. gave a good overview of the recent advances in the quality control of additive-manufactured parts [411]. They stated that direct energy deposition (DED) often has quality issues like layer misalignment, dimensional errors and residual stress generation. Furthermore, Lee et al. stated that welding-related quality control can be transferred or directly used for the quality control of additive manufacturing processes [411]. An overview of quality-related topics on WAAM is given by Jafari et al. [412]. Basically, the quality control in WAAM can be divided into two main areas: the process-related side and the quality control of the finished part. Process-related quality control can use the methods described in the process surveillance section in this review to establish quality control criteria. The quality control of the finished parts can use the same methods as for welding (e.g., optical inspection, crack detection, X-ray radiography, ultrasonic inspection [413,414] and computed tomography [415]). Lopez et al. give a good overview of the applicable methods of non-destructive testing [416].

5. Summary

The great economic and scientific interest in arc-based additive manufacturing has resulted in a significant increase in scientific interest in this manufacturing process. This is also shown by the larger number of literature studies conducted so far from all parts of the world [9,10,13,30,31,147,233,417–437]. All the literature sees great potential in this manufacturing process and attributes this potential to new developments in welding processes as well as robotics, sensors and CAX technologies. The current literature presents a wide range of used welding processes for every metal-based material group, including upcoming material groups like intermetallic alloys or high-entropy alloys. For every material group presented in this review, it was stated in the cited research that WAAM is a suitable manufacturing process which gives a lot more degrees of freedom. However, in comparison with some other market-available, direct energy deposition processes, most

scientific experimental set-ups do not utilize the promised degrees of freedom, while for laser powder direct energy deposition, there are existing machines with five axes to weld only in the PA position, and the path planning can be performed in an three-dimensional way. For WAAM, very limited machinery with these state-of-the-art moving and path planning systems are scientifically used. In WAAM, currently, most studies focus on the interdependencies of process-related values, the geometrical correctness (including residual stresses and distortion) and the microstructural behavior of the used materials. These studies already give a good basis to move on to more complex scientific questions, like whether to use a multi-material approach with increased process surveillance.

However, aside from all the presented knowledge and advances in the last few years, wire arc additive manufacturing is not understood completely, and more topics need to be addressed even further. Reisgen et al. identified four main research areas for the next steps on the road to WAAM series production [438]. These steps are as follows: process, materials, modeling and automation. These main topics should be addressed with regard to the residual stresses, geometrical correctness, mechanical properties and cost sensitivity [438]. This is supported by Chaturvedi et al. They identified the residual stresses and distortion as the limiting factors in wire and arc additive manufacturing [436].

Within this this field of issues that needs to be addressed, one crucial point is the control of the heat input due to its direct influence on the microstructure, the building strategy and the geometrical correctness of the manufactured part regarding distortion and residual stresses [435].

Ugla et al. stated that the addition of another wire as a cold wire feed to a gas metal arc welding process and using the doubled filler material for in situ alloying (and the effect in the occurring residual stresses) can widen the field of applications of WAAM [68]. Leicher et al. showed that a multi-material approach can be crucial to tailor the mechanical properties of a WAAM part to the occurring loads [52,232]. Here too, the existing knowledge of mixed joints from the welding technology can be partially transferred and thus facilitates the entry into this new field of research.

Since science aims not only at industrial application but also at a complete understanding of the interrelationships and mechanisms involved in the production of and within the materials, detailed and fully understood correlations between the process, material, environmental variables and occurring process instabilities like humping, among others, are indispensable for a fundamentally oriented and scientifically complete description. For example, the influence of the melt surface tension, melt viscosity, process variables and humping start speed are missing.

Furthermore, the current research often leads to hybrid manufacturing, combining traditional manufacturing processes with additive manufacturing to generate beneficial part properties. The needed integration of additive manufacturing processes in traditional process chains or the development of new combinations of processes is crucial to utilize the full potential of WAAM. Webster et al. gave a good overview on hybrid manufacturing and finally stated that more work on workpiece vibration and the use of magnetic fields to influence the process properties needs to be done. Furthermore, they stated that the combination of laser and arc technologies can lead to improved part properties [93].

In addition to knowledge of the relationships between the process parameters and material reactions, process monitoring is also of decisive importance for process-reliable and defect-free component manufacturing with defined properties. Many advancements are currently being made in this area as well.

The modeling of individual aspects of the WAAM process is also developing in parallel with the manufacturing process-related knowledge gain. Here, the focus is on two areas:

1. The calculation of material reduction (mechanical properties, distortion and residual stresses) as a function of process-relevant variables;
2. The optimal web guiding and determination of the process parameters for the defect-free production of WAAM structures.

Taken together, each aspect of arc-based additive manufacturing shows a significant increase in research activity with the expected gain in knowledge over the last few years.

6. Anticipated Further Research

Additive manufacturing technologies are fundamentally changing the way products are developed and manufactured. The great potential of additive manufacturing technologies has been demonstrated in numerous research studies for various application areas. It has been shown that economic use requires high material deposition rates and an end-to-end process chain from component design to the manufacturing process. Arc-based additive manufacturing processes are also suitable for the production of complex components with homogeneous or locally adapted material properties, as presented in this review. Although this process is widely used, the full potential of targeted heat and material transfer for the locally adapted properties of multi-material systems in components has not yet been tapped. Therefore, this potential should be further explored and complemented by new methods and processes for the development and fabrication of completely new components. The basis for this is the investigation and description of the process-specific interactions between product development, process technology, process control and process simulation. This can lead to material-efficient manufacturing of complex and highly stressed structural components and a new dimension in design freedom and functional integration. For this purpose, on the one hand, process-specific knowledge for wire and arc additive manufacturing (WAAM) is required, and on the other hand, generally applicable methods and processes for the integrated development and flexible process control of additively manufactured, monolithic components are to be researched and tested. In order to research the methods, technological principles and processes required for this, interdisciplinary cooperation is necessary (e.g., between product development, production engineering, materials science and metrology, as well as control engineering and computer science).

The aim of further research should be the development of methods and processes for a continuous and highly automated production process for wire and arc additive-manufactured multi-material components with partially adjusted properties (e.g., strength, toughness and wear resistance) for the occurring operating loads via multi-material approaches. For this purpose, it is necessary to link the sub-areas presented in the review to form a holistic approach. The interactions that occur between the manufacturing process, component development and material and component properties should first be fundamentally investigated in order to be able to tap new potentials. The following questions arise from the current state of research and should be investigated in further research work:

- How can WAAM-compatible components be designed?
- What are the boundary conditions for WAAM-compatible components so that they can be manufactured?
- What are the local system properties to realize multi-material components that are designed for operation under different types of loads (e.g., wear resistance and fatigue strength)?
- Which path planning algorithms allow the use of the full potential of WAAM?
- Which methods and procedures of process monitoring, control and information processing are suitable to enable a local adjustment of material properties in a process-reliable and reproducible way?
- What are the interrelationships between the process setting variables, path planning, other process boundary conditions and the achievable material properties?
- Which multi-material systems and material-dependent manufacturing framework conditions are suitable for WAAM?
- Which modeling methods and procedures enable computer-aided FEM-based computational prediction of the properties for components with locally adjusted properties?
- Which quality control methods are suitable for large WAAM parts, and how do internal defects influence the parts' properties?

In the context of the current state of research, and especially integrating product development into the process chain, manufacturing for WAMM components would enable a new generation of components with load-specific adjusted properties in research and thus may lead to full exploitation of the potential of WAAM. In addition, it can be stated that on the basis of the presented literature, a holistic approach in research for wire arc additive manufacturing, with a focus on localized material property-oriented product design, material property-oriented path planning in combination with a multi-material knowledge base and suitable process surveillance and post-processing, needs to be addressed to take the next big step in wire arc additive manufacturing.

7. Conclusions

The presented literature study allows for drawing some conclusions:

(1) Arc-based additive manufacturing can be used to produce components from a wide range of materials with properties that are at least on a par with conventionally manufactured components.
(2) In addition, the production of multi-material components with graded or specifically functional properties is possible. In this case, the restrictions for mixed joints known from welding technology apply.
(3) Adequate component property-oriented path planning algorithms are currently being developed which will allow additional design degrees of freedom to be implemented through multi-material additive manufacturing.
(4) Process monitoring methods are increasingly being developed to ensure the quality and properties of a component.
(5) Some materials are well studied, like steels, titanium and aluminum, but for some material groups, only limited information can be found (e.g., copper and tungsten). Here, more research effort needs to be made.
(6) There is no holistic approach to the entire process chain from product development through manufacturing to service life assessment, since the specialized working groups are dedicated to individual issues.

Based on the large number of publications in recent years, it is clear that arc-based additive manufacturing, which also includes WAAM, is the focus of scientific attention. However, there is still no comprehensive and complete understanding of the effects and potential of it.

Author Contributions: Conceptualization, K.T. and V.W.; literature survey, K.T.; resources, V.W.; writing—original draft preparation, K.T.; writing—review and editing, K.T. and V.W.; visualization, K.T.; supervision, V.W.; funding acquisition, K.T. and V.W. Both authors have read and agreed to the published version of the manuscript.

Funding: We acknowledge financial support by the Open Access Publishing Fund of the Clausthal University of Technology.

Conflicts of Interest: The authors declare no conflict of interest.

References

1. Wesling, V.; Bohn, C.; Ehlers, R.; Esderts, A.; Hartmann, S.; Lohrengel, A.; Lorenz, S.; Rausch, A.; Rembe, C.; Inkermann, D.; et al. *Werkstofforientierte Prozesskette für Multimaterielle, Lichtbogenadditiv Gefertigte (WAAM) Strukturbauteile*; Collaborative Research Center of the German Research Foundation (DFG): Clausthal-Zellerfeld, Germany, 2021.
2. Galjaard, S.; Hofman, S.; Ren, S. New Opportunities to Optimize Structural Designs in Metal by Using Additive Manufacturing. In *Advances in Architectural Geometry 2014*; Springer: Cham, Switzerland, 2015; pp. 79–93.
3. Reimann, J.; Henckell, P.; Ali, Y.; Hammer, S.; Rauch, A.; Hildebrand, J.; Bergmann, J.P. Production of Topology-optimised Structural Nodes Using Arc-based, Additive Manufacturing with GMAW Welding Process. *J. Civ. Eng. Constr.* **2021**, *10*, 101–107. [CrossRef]
4. Vafadar, A.; Guzzomi, F.; Rassau, A.; Hayward, K. Advances in Metal Additive Manufacturing: A Review of Common Processes, Industrial Applications, and Current Challenges. *Appl. Sci.* **2021**, *11*, 1213. [CrossRef]

5. Wei, H.L.; Bhadeshia, H.K.D.H.; David, S.A.; DebRoy, T. Harnessing the scientific synergy of welding and additive manufacturing. *Sci. Technol. Weld. Join.* **2019**, *24*, 361–366. [CrossRef]
6. Oliveira, J.P.; Santos, T.G.; Miranda, R.M. Revisiting fundamental welding concepts to improve additive manufacturing: From theory to practice. *Prog. Mater. Sci.* **2020**, *107*, 100590. [CrossRef]
7. Klobčar, D.; Baloš, S.; Bašić, M.; Djurić, A.; Lindič, M.; Ščetinec, A. WAAM and Other Unconventional Metal Additive Manufacturing Technologies. *Adv. Technol. Mater.* **2020**, *45*, 1–9. [CrossRef]
8. Mohebbi, M.S.; Kühl, M.; Ploshikhin, V. A thermo-capillary-gravity model for geometrical analysis of single-bead wire and arc additive manufacturing (WAAM). *Int. J. Adv. Manuf. Technol.* **2020**, *109*, 877–891. [CrossRef]
9. Cunningham, C.R.; Flynn, J.M.; Shokrani, A.; Dhokia, V.; Newman, S.T. Invited review article: Strategies and processes for high quality wire arc additive manufacturing. *Addit. Manuf.* **2018**, *22*, 672–686. [CrossRef]
10. Kühne, R.; Feldmann, M.; Citarelli, S.; Reisgen, U.; Sharma, R.; Oster, L. 3D printing in steel construction with the automated Wire Arc Additive Manufacturing. *ce/papers* **2019**, *3*, 577–583. [CrossRef]
11. Dilthey, U. *Schweißtechnische Fertigungsverfahren 1: Schweiß- und Schneidtechnologien, 3., Bearbeitete Auflage*; Springer: Berlin/Heidelberg, Germany, 2006; ISBN 3-540-21673-1.
12. Queguineur, A.; Rückert, G.; Cortial, F.; Hascoët, J.Y. Evaluation of wire arc additive manufacturing for large-sized components in naval applications. *Weld. World* **2018**, *62*, 259–266. [CrossRef]
13. Feldmann, M.; Kühne, R.; Citarelli, S.; Reisgen, U.; Sharma, R.; Oster, L. 3D-Drucken im Stahlbau mit dem automatisierten Wire Arc Additive Manufacturing. *Stahlbau* **2019**, *88*, 203–213. [CrossRef]
14. Gardner, L.; Kyvelou, P.; Herbert, G.; Buchanan, C. Testing and initial verification of the world's first metal 3D printed bridge. *J. Constr. Steel Res.* **2020**, *172*, 106233. [CrossRef]
15. Greer, C.; Nycz, A.; Noakes, M.; Richardson, B.; Post, B.; Kurfess, T.; Love, L. Introduction to the design rules for Metal Big Area Additive Manufacturing. *Addit. Manuf.* **2019**, *27*, 159–166. [CrossRef]
16. Kulikov, A.A.; Sidorova, A.V.; Balanovskiy, A.E. Process Design for the Wire Arc Additive Manufacturing of a Compressor Impeller. *IOP Conf. Ser. Mater. Sci. Eng.* **2020**, *969*, 12098. [CrossRef]
17. Bergmann, J.P.; Lange, J.; Hildebrand, J.; Eiber, M.; Erven, M.; Gaßmann, C.; Chiang, C.-H.; Lenz, C.; Röder, T.; Bashariar, W. Herstellung von 3D-gedruckten Stahlknoten. *Stahlbau* **2020**, *89*, 956–969. [CrossRef]
18. Panchenko, O.V.; Zhabrev, L.A.; Kurushkin, D.V.; Popovich, A.A. Macrostructure and Mechanical Properties of Al – Si, Al – Mg – Si, and Al – Mg – Mn Aluminum Alloys Produced by Electric Arc Additive Growth. *Met. Sci. Heat Treat.* **2019**, *60*, 749–754. [CrossRef]
19. Roy, S.; Shassere, B.; Yoder, J.; Nycz, A.; Noakes, M.; Narayanan, B.K.; Meyer, L.; Paul, J.; Sridharan, N. Mitigating Scatter in Mechanical Properties in AISI 410 Fabricated via Arc-Based Additive Manufacturing Process. *Materials* **2020**, *13*, 4855. [CrossRef]
20. Josten, A.; Höfemann, M. Arc-welding based additive manufacturing for body reinforcement in automotive engineering. *Weld. World* **2020**, *64*, 1449–1458. [CrossRef]
21. van Le, T.; Paris, H. On the use of gas-metal-arc-welding additive manufacturing for repurposing of low-carbon steel components: Microstructures and mechanical properties. *Weld. World* **2020**. [CrossRef]
22. Wu, R.; Yu, Z.; Ding, D.; Lu, Q.; Pan, Z.; Li, H. OICP: An Online Fast Registration Algorithm Based on Rigid Translation Applied to Wire Arc Additive Manufacturing of Mold Repair. *Materials* **2021**, *14*, 1563. [CrossRef]
23. Li, X.; Han, Q.; Zhang, G. Large-size sprocket repairing based on robotic GMAW additive manufacturing. *Weld. World* **2021**. [CrossRef]
24. Kulikov, A.; Nebyshinets, Y.; Sidorova, A.; Balanovskii, A. 3D printing technology for metal products: From an automatic design system to a real part. *Proc. ISTU* **2020**, *24*, 728–739. [CrossRef]
25. Ehlers, R.; Treutler, K.; Wesling, V. SAT Solving with Fragmented Hamiltonian Path Constraints for Wire Arc Additive Manufacturing. In *Theory and Applications of Satisfiability Testing—SAT 2020, Proceedings of the 23rd International Conference, Alghero, Italy, 3–10 July 2020*; Pulina, L., Seidl, M., Eds.; Springer International Publishing: Cham, Switzerland, 2020; pp. 492–500, ISBN 978-3-030-51825-7.
26. Richter, A.; Rembe, C.; Gehling, T.; Treutler, K.; Wesling, V. Echtzeittemperaturmessung bei additivem Lichtbogenschweißen/Real-time temperature measurement at wire arc additive welding. *TM Tech. Mess.* **2019**, *86*, 112–116. [CrossRef]
27. Farshidianfar, M.H.; Khajepour, A.; Gerlich, A. Real-time control of microstructure in laser additive manufacturing. *Int. J. Adv. Manuf. Technol.* **2016**, *82*, 1173–1186. [CrossRef]
28. Wang, B.; Yang, G.; Zhou, S.; Cui, C.; Qin, L. Effects of On-Line Vortex Cooling on the Microstructure and Mechanical Properties of Wire Arc Additively Manufactured Al-Mg Alloy. *Metals* **2020**, *10*, 1004. [CrossRef]
29. Knezović, N.; Topić, A. Wire and Arc Additive Manufacturing (WAAM)—A New Advance in Manufacturing. In *New Technologies, Development and Application*; Karabegović, I., Ed.; Springer International Publishing: Cham, Switzerland, 2019; pp. 65–71, ISBN 9783319908939.
30. Jin, W.; Zhang, C.; Jin, S.; Tian, Y.; Wellmann, D.; Liu, W. Wire Arc Additive Manufacturing of Stainless Steels: A Review. *Appl. Sci.* **2020**, *10*, 1563. [CrossRef]
31. Liu, D.; Lee, B.; Babkin, A.; Chang, Y. Research Progress of Arc Additive Manufacture Technology. *Materials* **2021**, *14*, 1415. [CrossRef] [PubMed]

32. Jandric, Z.; Labudovic, M.; Kovacevic, R. Effect of heat sink on microstructure of three-dimensional parts built by welding-based deposition. *Int. J. Mach. Tools Manuf.* **2004**, *44*, 785–796. [CrossRef]
33. Kwak, Y.-M.; Doumanidis, C.C. Geometry Regulation of Material Deposition in Near-Net Shape Manufacturing by Thermally Scanned Welding. *J. Manuf. Process.* **2002**, *4*, 28–41. [CrossRef]
34. Song, Y.-A.; Park, S.; Choi, D.; Jee, H. 3D welding and milling: Part I–a direct approach for freeform fabrication of metallic prototypes. *Int. J. Mach. Tools Manuf.* **2005**, *45*, 1057–1062. [CrossRef]
35. Ogino, Y.; Asai, S.; Hirata, Y. Numerical simulation of WAAM process by a GMAW weld pool model. *Weld. World* **2018**, *62*, 393–401. [CrossRef]
36. Baufeld, B.; van der Biest, O.; Gault, R. Additive manufacturing of Ti–6Al–4V components by shaped metal deposition: Microstructure and mechanical properties. *Mater. Des.* **2010**, *31*, S106–S111. [CrossRef]
37. Ding, J.; Colegrove, P.; Mehnen, J.; Williams, S.; Wang, F.; Almeida, P.S. A computationally efficient finite element model of wire and arc additive manufacture. *Int. J. Adv. Manuf. Technol.* **2014**, *70*, 227–236. [CrossRef]
38. Marinelli, G.; Martina, F.; Lewtas, H.; Hancock, D.; Mehraban, S.; Lavery, N.; Ganguly, S.; Williams, S. Microstructure and thermal properties of unalloyed tungsten deposited by Wire + Arc Additive Manufacture. *J. Nucl. Mater.* **2019**, *522*, 45–53. [CrossRef]
39. Davis, A.E.; Kennedy, J.R.; Ding, J.; Prangnell, P.B. The effect of processing parameters on rapid-heating β recrystallization in inter-pass deformed Ti-6Al-4V wire-arc additive manufacturing. *Mater. Charact.* **2020**, *163*, 110298. [CrossRef]
40. Biswal, R.; Zhang, X.; Syed, A.K.; Awd, M.; Ding, J.; Walther, F.; Williams, S. Criticality of porosity defects on the fatigue performance of wire + arc additive manufactured titanium alloy. *Int. J. Fatigue* **2019**, *122*, 208–217. [CrossRef]
41. Biswal, R.; Zhang, X.; Shamir, M.; Al Mamun, A.; Awd, M.; Walther, F.; Khadar Syed, A. Interrupted fatigue testing with periodic tomography to monitor porosity defects in wire + arc additive manufactured Ti-6Al-4V. *Addit. Manuf.* **2019**, *28*, 517–527. [CrossRef]
42. Cunningham, C.R.; Wikshåland, S.; Xu, F.; Kemakolam, N.; Shokrani, A.; Dhokia, V.; Newman, S.T. Cost Modelling and Sensitivity Analysis of Wire and Arc Additive Manufacturing. *Proc. Manuf.* **2017**, *11*, 650–657. [CrossRef]
43. Clark, D.; Bache, M.R.; Whittaker, M.T. Shaped metal deposition of a nickel alloy for aero engine applications. *J. Mater. Process. Technol.* **2008**, *203*, 439–448. [CrossRef]
44. Yang, D.; Wang, G.; Zhang, G. A comparative study of GMAW- and DE-GMAW-based additive manufacturing techniques: Thermal behavior of the deposition process for thin-walled parts. *Int. J. Adv. Manuf. Technol.* **2017**, *91*, 2175–2184. [CrossRef]
45. Aiyiti, W.; Zhao, W.H.; Tang, Y.P.; Lu, B.H. Study on the Process Parameters of MPAW-Based Rapid Prototyping. *Key Eng. Mater.* **2007**, *353–358*, 1931–1934. [CrossRef]
46. Yang, Q.; Xia, C.; Deng, Y.; Li, X.; Wang, H. Microstructure and Mechanical Properties of AlSi7Mg0.6 Aluminum Alloy Fabricated by Wire and Arc Additive Manufacturing Based on Cold Metal Transfer (WAAM-CMT). *Materials* **2019**, *12*, 2525. [CrossRef]
47. Yang, Y.; Jin, X.; Liu, C.; Xiao, M.; Lu, J.; Fan, H.; Ma, S. Residual Stress, Mechanical Properties, and Grain Morphology of Ti-6Al-4V Alloy Produced by Ultrasonic Impact Treatment Assisted Wire and Arc Additive Manufacturing. *Metals* **2018**, *8*, 934. [CrossRef]
48. Panchagnula, J.S.; Simhambhatla, S. Manufacture of complex thin-walled metallic objects using weld-deposition based additive manufacturing. *Robot. Comput. Integr. Manuf.* **2018**, *49*, 194–203. [CrossRef]
49. Gokhale, N.P.; Kala, P.; Sharma, V. Thin-walled metal deposition with GTAW welding-based additive manufacturing process. *J. Braz. Soc. Mech. Sci. Eng.* **2019**, *41*. [CrossRef]
50. Ding, D.; Pan, Z.; Cuiuri, D.; Li, H. A tool-path generation strategy for wire and arc additive manufacturing. *Int. J. Adv. Manuf. Technol.* **2014**, *73*, 173–183. [CrossRef]
51. Ding, D.; Pan, Z.; Cuiuri, D.; Li, H. A multi-bead overlapping model for robotic wire and arc additive manufacturing (WAAM). *Robot. Comput. Integr. Manuf.* **2015**, *31*, 101–110. [CrossRef]
52. Treutler, K.; Kamper, S.; Leicher, M.; Bick, T.; Wesling, V. Multi-Material Design in Welding Arc Additive Manufacturing. *Metals* **2019**, *9*, 809. [CrossRef]
53. Wächter, M.; Leicher, M.; Leister, C.; Hupka, M.; Masendorf, L.; Treutler, K.; Kamper, S.; Esderts, A.; Wesling, V.; Hartmann, S. Fatigue Strength Values for Components manufactured in the Wire Arc Additive Manufacturing Process. In *VAL4—Fourth International Conference on Material and Component Performance under Variable Amplitude Loading: Planned from 30 March to 1 April 2020 in Darmstadt, Germany*; Decker, M., Heim, R., Sonsino, C.M., Eds.; German Association for Materials Research and Testing e.V.: Berlin, Germany, 2020; pp. 557–567, ISBN 978-3-9820591-0-5.
54. Ali, Y.; Henckell, P.; Hildebrand, J.; Reimann, J.; Bergmann, J.P.; Barnikol-Oettler, S. Wire arc additive manufacturing of hot work tool steel with CMT process. *J. Mater. Process. Technol.* **2019**, *269*, 109–116. [CrossRef]
55. Gierth, M.; Henckell, P.; Ali, Y.; Scholl, J.; Bergmann, J.P. Wire Arc Additive Manufacturing (WAAM) of Aluminum Alloy AlMg5Mn with Energy-Reduced Gas Metal Arc Welding (GMAW). *Materials* **2020**, *13*, 2671. [CrossRef] [PubMed]
56. Graf, M.; Hälsig, A.; Höfer, K.; Awiszus, B.; Mayr, P. Thermo-Mechanical Modelling of Wire-Arc Additive Manufacturing (WAAM) of Semi-Finished Products. *Metals* **2018**, *8*, 1009. [CrossRef]
57. Alaluss, K.; Mayr, P. Additive Manufacturing of Complex Components through 3D Plasma Metal Deposition—A Simulative Approach. *Metals* **2019**, *9*, 574. [CrossRef]
58. Köhler, M.; Fiebig, S.; Hensel, J.; Dilger, K. Wire and Arc Additive Manufacturing of Aluminum Components. *Metals* **2019**, *9*, 608. [CrossRef]

59. Bähr, M.; Buhl, J.; Radow, G.; Schmidt, J.; Bambach, M.; Breuß, M.; Fügenschuh, A. Stable honeycomb structures and temperature based trajectory optimization for wire-arc additive manufacturing. *Optim. Eng.* **2020**, 1–62. [CrossRef]
60. Reisgen, U.; Sharma, R.; Oster, L. Plasma Multiwire Technology with Alternating Wire Feed for Tailor-Made Material Properties in Wire and Arc Additive Manufacturing. *Metals* **2019**, *9*, 745. [CrossRef]
61. Reisgen, U.; Sharma, R.; Mann, S.; Oster, L. Increasing the manufacturing efficiency of WAAM by advanced cooling strategies. *Weld. World* **2020**, *64*, 1409–1416. [CrossRef]
62. Plangger, J.; Schabhüttl, P.; Vuherer, T.; Enzinger, N. CMT Additive Manufacturing of a High Strength Steel Alloy for Application in Crane Construction. *Metals* **2019**, *9*, 650. [CrossRef]
63. Laghi, V.; Palermo, M.; Gasparini, G.; Girelli, V.A.; Trombetti, T. Experimental results for structural design of Wire-and-Arc Additive Manufactured stainless steel members. *J. Constr. Steel Res.* **2020**, *167*, 105858. [CrossRef]
64. Laghi, V.; Palermo, M.; Tonelli, L.; Gasparini, G.; Ceschini, L.; Trombetti, T. Tensile properties and microstructural features of 304L austenitic stainless steel produced by wire-and-arc additive manufacturing. *Int. J. Adv. Manuf. Technol.* **2020**, *106*, 3693–3705. [CrossRef]
65. Laghi, V.; Palermo, M.; Gasparini, G.; Trombetti, T. Optimization studies on diagrid columns realize with Wire-and-Arc Additive Manufacturing process. In Proceedings of the 2019 IABSE Congress, New York, NY, USA, 4–6 September 2019.
66. Selvi, S.; Vishvaksenan, A.; Rajasekar, E. Cold metal transfer (CMT) technology—An overview. *Def. Technol.* **2018**, *14*, 28–44. [CrossRef]
67. Henckell, P.; Gierth, M.; Ali, Y.; Reimann, J.; Bergmann, J.P. Reduction of Energy Input in Wire Arc Additive Manufacturing (WAAM) with Gas Metal Arc Welding (GMAW). *Materials* **2020**, *13*, 2491. [CrossRef] [PubMed]
68. Ugla, A.A.; Khaudair, H.J.; Almusawi, A.R.J. Metal Inert Gas Welding-Based-Shaped Metal Deposition in Additive Layered Manufacturing: A Review. *Int. J. Mech. Mater. Eng.* **2019**. [CrossRef]
69. Dinovitzer, M.; Chen, X.; Laliberte, J.; Huang, X.; Frei, H. Effect of wire and arc additive manufacturing (WAAM) process parameters on bead geometry and microstructure. *Addit. Manuf.* **2019**, *26*, 138–146. [CrossRef]
70. Benakis, M.; Costanzo, D.; Patran, A. Current mode effects on weld bead geometry and heat affected zone in pulsed wire arc additive manufacturing of Ti-6-4 and Inconel 718. *J. Manuf. Process.* **2020**, *60*, 61–74. [CrossRef]
71. Ayarkwa, K.F.; Williams, S.W.; Ding, J. Assessing the effect of TIG alternating current time cycle on aluminium wire + arc additive manufacture. *Addit. Manuf.* **2017**, *18*, 186–193. [CrossRef]
72. Fu, R.; Tang, S.; Lu, J.; Cui, Y.; Li, Z.; Zhang, H.; Xu, T.; Chen, Z.; Liu, C. Hot-wire arc additive manufacturing of aluminum alloy with reduced porosity and high deposition rate. *Mater. Des.* **2021**, *199*, 109370. [CrossRef]
73. Corradi, D.R.; Coelho, F.G.; Antonello, M.G.; Bracarense, A.Q.; Arias, A.R.; Barbosa, T.P. The Influence of Magnetic Arc Oscillation on the Deposition Width Variation along the Length of Multi-layer Single-Pass Walls Produced by Wire Arc Additive Manufacturing Process. *J. Mater. Eng. Perform.* **2021**. [CrossRef]
74. Corradi, D.R.; Bracarense, A.Q.; Wu, B.; Cuiuri, D.; Pan, Z.; Li, H. Effect of Magnetic Arc Oscillation on the geometry of single-pass multi-layer walls and the process stability in wire and arc additive manufacturing. *J. Mater. Process. Technol.* **2020**, *283*, 116723. [CrossRef]
75. Jhavar, S.; Paul, C.P.; Jain, N.K. Micro-Plasma Transferred Arc Additive Manufacturing for Die and Mold Surface Remanufacturing. *JOM* **2016**, *68*, 1801–1809. [CrossRef]
76. Ríos, S.; Colegrove, P.A.; Williams, S.W. Metal transfer modes in plasma Wire + Arc additive manufacture. *J. Mater. Process. Technol.* **2019**, *264*, 45–54. [CrossRef]
77. Jia, C.; Liu, W.; Chen, M.; Guo, M.; Wu, S.; Wu, C. Investigation on arc plasma, droplet, and molten pool behaviours in compulsively constricted WAAM. *Addit. Manuf.* **2020**, *34*, 101235. [CrossRef]
78. Shukla, P.; Dash, B.; Kiran, D.V.; Bukkapatnam, S. Arc Behavior in Wire Arc Additive Manufacturing Process. *Proc. Manuf.* **2020**, *48*, 725–729. [CrossRef]
79. Gomes, B.F.; Morais, P.J.; Ferreira, V.; Pinto, M.; de Almeida, L.H. Wire-arc additive manufacturing of Al-Mg alloy using CMT and PMC technologies. *MATEC Web Conf.* **2018**, *233*, 31. [CrossRef]
80. Han, Q.; Gao, J.; Han, C.; Zhang, G.; Li, Y. Experimental investigation on improving the deposition rate of gas metal arc-based additive manufacturing by auxiliary wire feeding method. *Weld. World* **2020**. [CrossRef]
81. Queguineur, A.; Marolleau, J.; Lavergne, A.; Rückert, G. Evaluation of tandem controlled short-circuit GMAW for improved deposition in additive manufacture of large Nickel Aluminium Bronze naval components. *Weld. World* **2020**, *64*, 1389–1395. [CrossRef]
82. Zhan, Q.; Liang, Y.; Ding, J.; Williams, S. A wire deflection detection method based on image processing in wire + arc additive manufacturing. *Int. J. Adv. Manuf. Technol.* **2017**, *89*, 755–763. [CrossRef]
83. Chen, X.; Su, C.; Wang, Y.; Siddiquee, A.N.; Sergey, K.; Jayalakshmi, S.; Singh, R.A. Cold Metal Transfer (CMT) Based Wire and Arc Additive Manufacture (WAAM) System. *J. Synch. Investig.* **2018**, *12*, 1278–1284. [CrossRef]
84. Li, Y.; Wu, S.; Li, H.; Cheng, F. Dramatic improvement of impact toughness for the fabricating of low-carbon steel components via submerged arc additive manufacturing. *Mater. Lett.* **2021**, *283*, 128780. [CrossRef]
85. Radel, S.; Diourte, A.; Soulié, F.; Company, O.; Bordreuil, C. Skeleton arc additive manufacturing with closed loop control. *Addit. Manuf.* **2019**, *26*, 106–116. [CrossRef]

86. Radel, S.; Bordreuil, C.; Soulie, F.; Company, O. CAM for On-line Control for Wire Arc Additive Manufacturing. *Comput.-Aided Design Appl.* **2018**, *16*, 558–569. [CrossRef]
87. Yu, Z.; Pan, Z.; Ding, D.; Polden, J.; Yuan, L.; He, F.; Li, H. A practical fabrication strategy for wire arc additive manufacturing of metallic parts with wire structures. *Int. J. Adv. Manuf. Technol.* **2021**, *115*, 3197–3212. [CrossRef]
88. Laghi, V.; Palermo, M.; Silvestri, S.; Gasparini, G.; Trombetti, T. Experimental behaviour of Wire-and-Arc Additively Manufactured stainless steel rods. *ce/papers* **2021**, *4*, 2387–2392. [CrossRef]
89. Wang, Z.; Wu, N.; Wang, Q.; Li, Y.; Yang, Q.; Wu, F. Novel Bionic Design Method for Skeleton Structures Based on Load Path Analysis. *Appl. Sci.* **2020**, *10*, 8251. [CrossRef]
90. Yu, Z.; Ding, D.; Pan, Z.; Li, H.; Lu, Q.; Fang, X. A strut-based process planning method for wire arc additive manufacturing of lattice structures. *J. Manuf. Process.* **2021**, *65*, 283–298. [CrossRef]
91. Silvestru, V.-A.; Ariza, I.; Vienne, J.; Michel, L.; Aguilar Sanchez, A.M.; Angst, U.; Rust, R.; Gramazio, F.; Kohler, M.; Taras, A. Performance under tensile loading of point-by-point wire and arc additively manufactured steel bars for structural components. *Mater. Des.* **2021**, *205*, 109740. [CrossRef]
92. Pragana, J.; Sampaio, R.; Bragança, I.; Silva, C.; Martins, P. Hybrid metal additive manufacturing: A state–of–the-art review. *Adv. Ind. Manuf. Eng.* **2021**, *2*, 100032. [CrossRef]
93. Webster, S.; Lin, H.; Carter, F.M., III; Ehmann, K.; Cao, J. Physical mechanisms in hybrid additive manufacturing: A process design framework. *J. Mater. Process. Technol.* **2021**, *291*, 117048. [CrossRef]
94. Silwal, B.; Nycz, A.; Masuo, C.J.; Noakes, M.W.; Marsh, D.; Vaughan, D. An experimental investigation of the effectiveness of Ar-CO2 shielding gas mixture for the wire arc additive process. *Int. J. Adv. Manuf. Technol.* **2020**, *108*, 1285–1296. [CrossRef]
95. da Silva, L.J.; Scotti, F.M.; Fernandes, D.B.; Reis, R.P.; Scotti, A. Effect of O_2 content in argon-based shielding gas on arc wandering in WAAM of aluminum thin walls. *CIRP J. Manuf. Sci. Technol.* **2021**, *32*, 338–345. [CrossRef]
96. Emde, B.; Huse, M.; Hermsdorf, J.; Kaierle, S.; Wesling, V.; Overmeyer, L.; Kozakov, R.; Uhrlandt, D. Significance of the Resonance Condition for Controlling the Seam Position in Laser-assisted TIG Welding. *Phys. Proc.* **2016**, *83*, 568–576. [CrossRef]
97. Zhang, Z.; Sun, C.; Xu, X.; Liu, L. Surface quality and forming characteristics of thin-wall aluminium alloy parts manufactured by laser assisted MIG arc additive manufacturing. *Int. J. Lightweight Mater. Manuf.* **2018**, *1*, 89–95. [CrossRef]
98. McAndrew, A.R.; Alvarez Rosales, M.; Colegrove, P.A.; Hönnige, J.R.; Ho, A.; Fayolle, R.; Eyitayo, K.; Stan, I.; Sukrongpang, P.; Crochemore, A.; et al. Interpass rolling of Ti-6Al-4V wire + arc additively manufactured features for microstructural refinement. *Addit. Manuf.* **2018**, *21*, 340–349. [CrossRef]
99. Härtel, S.; Adams, T.-E.; Hoefer, K.; Awiszus, B.; Mayr, P. A Novel Method for Improving Weld Seam Properties through Inline Coupling of Welding and Forming. *Materials* **2020**, *13*, 271. [CrossRef]
100. Bauer, A.; Manurung, Y.H.P.; Sprungk, J.; Graf, M.; Awiszus, B.; Prajadhiana, K. Investigation on forming–welding process chain for DC04 tube manufacturing using experiment and FEM simulation. *Int. J. Adv. Manuf. Technol.* **2019**, *102*, 2399–2408. [CrossRef]
101. Colegrove, P.A.; Donoghue, J.; Martina, F.; Gu, J.; Prangnell, P.; Hönnige, J. Application of bulk deformation methods for microstructural and material property improvement and residual stress and distortion control in additively manufactured components. *Scr. Mater.* **2017**, *135*, 111–118. [CrossRef]
102. Dirisu, P.; Supriyo, G.; Martina, F.; Xu, X.; Williams, S. Wire plus arc additive manufactured functional steel surfaces enhanced by rolling. *Int. J. Fatigue* **2020**, *130*, 105237. [CrossRef]
103. Hönnige, J.; Seow, C.E.; Ganguly, S.; Xu, X.; Cabeza, S.; Coules, H.; Williams, S. Study of residual stress and microstructural evolution in as-deposited and inter-pass rolled wire plus arc additively manufactured Inconel 718 alloy after ageing treatment. *Mater. Sci. Eng. A* **2020**, 140368. [CrossRef]
104. Tangestani, R.; Farrahi, G.H.; Shishegar, M.; Aghchehkandi, B.P.; Ganguly, S.; Mehmanparast, A. Effects of Vertical and Pinch Rolling on Residual Stress Distributions in Wire and Arc Additively Manufactured Components. *J. Mater. Eng. Perform.* **2020**, *29*, 2073–2084. [CrossRef]
105. Parvaresh, B.; Miresmaeili, R.; Yazdizadeh, M. Characterization of wire arc additive manufactured products: A comparison between as-deposited and inter-layer cold worked specimens. *J. Manuf. Process.* **2020**, *57*, 61–71. [CrossRef]
106. Shirizly, A.; Dolev, O. From Wire to Seamless Flow-Formed Tube: Leveraging the Combination of Wire Arc Additive Manufacturing and Metal Forming. *JOM* **2019**, *71*, 709–717. [CrossRef]
107. Hönnige, J.R.; Colegrove, P.; Williams, S. Improvement of microstructure and mechanical properties in Wire + Arc Additively Manufactured Ti-6Al-4V with Machine Hammer Peening. *Proc. Eng.* **2017**, *216*, 8–17. [CrossRef]
108. Pragana, J.P.M.; Cristino, V.A.M.; Bragança, I.M.F.; Silva, C.M.A.; Martins, P.A.F. Integration of Forming Operations on Hybrid Additive Manufacturing Systems Based on Fusion Welding. *Int. J. Precis. Eng. Manuf.-Green Tech.* **2020**, *7*, 595–607. [CrossRef]
109. Grossi, N.; Scippa, A.; Venturini, G.; Campatelli, G. Process Parameters Optimization of Thin-Wall Machining for Wire Arc Additive Manufactured Parts. *Appl. Sci.* **2020**, *10*, 7575. [CrossRef]
110. Dávila, J.L.; Neto, P.I.; Noritomi, P.Y.; Coelho, R.T.; da Silva, J.V.L. Hybrid manufacturing: A review of the synergy between directed energy deposition and subtractive processes. *Int. J. Adv. Manuf. Technol.* **2020**, *110*, 3377–3390. [CrossRef]
111. Fuchs, C.; Baier, D.; Semm, T.; Zaeh, M.F. Determining the machining allowance for WAAM parts. *Prod. Eng. Res. Dev.* **2020**, *14*, 629–637. [CrossRef]
112. Schroepfer, D.; Treutler, K.; Boerner, A.; Gustus, R.; Kannengiesser, T.; Wesling, V.; Maus-Friedrichs, W. Surface finishing of hard-to-machine cladding alloys for highly stressed components. *Int. J. Adv. Manuf. Technol.* **2021**. [CrossRef]

113. *DIN EN 1993-1-9:2010-12, Eurocode_3: Bemessung und Konstruktion von Stahlbauten_- Teil_1-9: Ermüdung*; Deutsche Fassung EN_1993-1-9:2005_+ AC:2009; Beuth Verlag GmbH: Berlin, Germany, 2009.
114. Bartsch, H.; Kühne, R.; Citarelli, S.; Schaffrath, S.; Feldmann, M. Fatigue analysis of wire arc additive manufactured (3D printed) components with unmilled surface. *Structures* **2021**, *31*, 576–589. [CrossRef]
115. Hu, Z.; Qin, X.; Li, Y.; Yuan, J.; Wu, Q. Multi-bead overlapping model with varying cross-section profile for robotic GMAW-based additive manufacturing. *J. Intell. Manuf.* **2020**, *31*, 1133–1147. [CrossRef]
116. Hu, Z.; Qin, X.; Li, Y.; Ni, M. Welding parameters prediction for arbitrary layer height in robotic wire and arc additive manufacturing. *J. Mech. Sci. Technol.* **2020**, *34*, 1683–1695. [CrossRef]
117. Xia, C.; Pan, Z.; Zhang, S.; Polden, J.; Wang, L.; Li, H.; Xu, Y.; Chen, S. Model predictive control of layer width in wire arc additive manufacturing. *J. Manuf. Process.* **2020**, *58*, 179–186. [CrossRef]
118. van Le, T.; Mai, D.S.; Hoang, Q.H. A study on wire and arc additive manufacturing of low-carbon steel components: Process stability, microstructural and mechanical properties. *J. Braz. Soc. Mech. Sci. Eng.* **2020**, *42*. [CrossRef]
119. Lu, X.; Li, M.V.; Yang, H. Comparison of wire-arc and powder-laser additive manufacturing for IN718 superalloy: Unified consideration for selecting process parameters based on volumetric energy density. *Int. J. Adv. Manuf. Technol.* **2021**. [CrossRef]
120. Adebayo, A.; Mehnen, J.; Tonnellier, X. Limiting Travel Speed in Additive Layer Manufacturing. In Proceedings of the 9th International Conference on Trends in Welding Research, Hilton Chicago/Indian Lakes Resort, Chicago, IL, USA, 4–8 June 2012; ASM International: Materials Park, OH, USA, 2013, ISBN 9781627089982.
121. Soderstrom, E.; Mendez, P. Humping mechanisms present in high speed welding. *Sci. Technol. Weld. Join.* **2006**, *11*, 572–579. [CrossRef]
122. Xu, B.; Tan, X.; Gu, X.; Ding, D.; Deng, Y.; Chen, Z.; Xu, J. Shape-driven control of layer height in robotic wire and arc additive manufacturing. *Rapid Prototyp. J.* **2019**, *25*, 1637–1646. [CrossRef]
123. Cui, J.; Yuan, L.; Commins, P.; He, F.; Wang, J.; Pan, Z. WAAM process for metal block structure parts based on mixed heat input. *Int. J. Adv. Manuf. Technol.* **2021**. [CrossRef]
124. Gudur, S.; Nagallapati, V.; Pawar, S.; Muvvala, G.; Simhambhatla, S. A study on the effect of substrate heating and cooling on bead geometry in wire arc additive manufacturing and its correlation with cooling rate. *Mater. Today Proc.* **2020**. [CrossRef]
125. Xu, F.; Dhokia, V.; Colegrove, P.; McAndrew, A.; Williams, S.; Henstridge, A.; Newman, S.T. Realisation of a multi-sensor framework for process monitoring of the wire arc additive manufacturing in producing Ti-6Al-4V parts. *Int. J. Comput. Integr. Manuf.* **2018**, *31*, 785–798. [CrossRef]
126. Ma, Y.; Hu, Z.; Tang, Y.; Ma, S.; Chu, Y.; Li, X.; Luo, W.; Guo, L.; Zeng, X.; Lu, Y. Laser opto-ultrasonic dual detection for simultaneous compositional, structural, and stress analyses for wire + arc additive manufacturing. *Addit. Manuf.* **2020**, *31*, 100956. [CrossRef]
127. Zhao, Z.; Guo, Y.; Bai, L.; Wang, K.; Han, J. Quality monitoring in wire-arc additive manufacturing based on cooperative awareness of spectrum and vision. *Optik* **2019**, *181*, 351–360. [CrossRef]
128. Font comas, T.; Diao, C.; Ding, J.; Williams, S.; Zhao, Y. A Passive Imaging System for Geometry Measurement for the Plasma Arc Welding Process. *IEEE Trans. Ind. Electron.* **2017**, *64*, 7201–7209. [CrossRef]
129. Hackenhaar, W.; Montevecchi, F.; Scippa, A.; Campatelli, G. Air-Cooling Influence on Wire Arc Additive Manufactured Surfaces. *Key Eng. Mater.* **2019**, *813*, 241–247. [CrossRef]
130. Hackenhaar, W.; Mazzaferro, J.A.; Montevecchi, F.; Campatelli, G. An experimental-numerical study of active cooling in wire arc additive manufacturing. *J. Manuf. Process.* **2020**, *52*, 58–65. [CrossRef]
131. Kozamernik, N.; Bračun, D.; Klobčar, D. WAAM system with interpass temperature control and forced cooling for near-net-shape printing of small metal components. *Int. J. Adv. Manuf. Technol.* **2020**, *110*, 1955–1968. [CrossRef]
132. Halisch, C.; Radel, T.; Tyralla, D.; Seefeld, T. Measuring the melt pool size in a wire arc additive manufacturing process using a high dynamic range two-colored pyrometric camera. *Weld. World* **2020**, *64*, 1349–1356. [CrossRef]
133. Xiong, J.; Zhang, G. Online measurement of bead geometry in GMAW-based additive manufacturing using passive vision. *Meas. Sci. Technol.* **2013**, *24*, 115103. [CrossRef]
134. Xiong, J.; Liu, Y.; Yin, Z. Passive vision measurement for robust reconstruction of molten pool in wire and arc additive manufacturing. *Measurement* **2020**, *153*, 107407. [CrossRef]
135. Xiong, J.; Shi, M.; Liu, Y.; Yin, Z. Virtual binocular vision sensing and control of molten pool width for gas metal arc additive manufactured thin-walled components. *Addit. Manuf.* **2020**, *33*, 101121. [CrossRef]
136. Xia, C.; Pan, Z.; Zhang, S.; Polden, J.; Li, H.; Xu, Y.; Chen, S. Mask R-CNN-Based Welding Image Object Detection and Dynamic Modelling for WAAM. In *Transactions on Intelligent Welding Manufacturing, 2019*; Chen, S., Zhang, Y., Feng, Z., Eds.; Springer: Berlin/Heidelberg, Germany, 2020; pp. 57–73, ISBN 978-981-15-7214-2.
137. Wang, Y.; Zhang, C.; Lu, J.; Bai, L.; Zhao, Z.; Han, J. Weld Reinforcement Analysis Based on Long-Term Prediction of Molten Pool Image in Additive Manufacturing. *IEEE Access* **2020**, *8*, 69908–69918. [CrossRef]
138. Xiong, J.; Zhang, Y.; Pi, Y. Control of deposition height in WAAM using visual inspection of previous and current layers. *J. Intell. Manuf.* **2020**. [CrossRef]
139. Carter, W.; Masuo, C.; Nycz, A.; Noakes, M.; Vaughan, D. *Thermal Process. Monitoring for Wire—Arc Additive Manufacturing Using IR Cameras*; Oak Ridge National Lab. (ORNL): Oak Ridge, TN, USA, 2019.

140. Zhang, C.; Gao, M.; Chen, C.; Zeng, X. Spectral diagnosis of wire arc additive manufacturing of Al alloys. *Addit. Manuf.* **2019**, *30*, 100869. [CrossRef]
141. Guo, Y.; Zhao, Z.; Han, J.; Bai, L. Quality Monitoring in Wire-Arc Additive Manufacturing Based on Spectrum. In *ICVIP 2018, Proceedings of the 2nd International Conference on Video and Image Processing, Hong Kong, 29–31 December 2018*; Association for Computing Machinery: New York, NY, USA, 2019; pp. 240–244, ISBN 9781450366137.
142. Reisch, R.; Hauser, T.; Kamps, T.; Knoll, A. Robot Based Wire Arc Additive Manufacturing System with Context-Sensitive Multivariate Monitoring Framework. *Proc. Manuf.* **2020**, *51*, 732–739. [CrossRef]
143. Tang, S.; Wang, G.; Song, H.; Li, R.; Zhang, H. A novel method of bead modeling and control for wire and arc additive manufacturing. *Rapid Prototyp. J.* **2021**, *27*, 311–320. [CrossRef]
144. Xiong, J.; Yin, Z.; Zhang, W. Closed-loop control of variable layer width for thin-walled parts in wire and arc additive manufacturing. *J. Mater. Process. Technol.* **2016**, *233*, 100–106. [CrossRef]
145. Li, Y.; Li, X.; Zhang, G.; Horváth, I.; Han, Q. Interlayer closed-loop control of forming geometries for wire and arc additive manufacturing based on fuzzy-logic inference. *J. Manuf. Process.* **2020**. [CrossRef]
146. Paul, A.R.; Manivannan, R.; Mukherjee, M.; Kundu, S.; Chatterjee, A. Development of Y-shape hybrid frame model using wire and arc additive manufacturing process. *Mater. Today Proc.* **2020**. [CrossRef]
147. Xia, C.; Pan, Z.; Polden, J.; Li, H.; Xu, Y.; Chen, S.; Zhang, Y. A review on wire arc additive manufacturing: Monitoring, control and a framework of automated system. *J. Manuf. Syst.* **2020**, *57*, 31–45. [CrossRef]
148. Fang, X.; Ren, C.; Zhang, L.; Wang, C.; Huang, K.; Lu, B. A model of bead size based on the dynamic response of CMT-based wire and arc additive manufacturing process parameters. *Rapid Prototyp. J.* **2021**, *27*, 741–753. [CrossRef]
149. Dahat, S.; Hurtig, K.; Andersson, J.; Scotti, A. A Methodology to Parameterize Wire + Arc Additive Manufacturing: A Case Study for Wall Quality Analysis. *J. Manuf. Mater. Process.* **2020**, *4*, 14. [CrossRef]
150. Ding, D.; Pan, Z.; Cuiuri, D.; Li, H. A practical path planning methodology for wire and arc additive manufacturing of thin-walled structures. *Robot. Comput. Integr. Manuf.* **2015**, *34*, 8–19. [CrossRef]
151. Michel, F.; Lockett, H.; Ding, J.; Martina, F.; Marinelli, G.; Williams, S. A modular path planning solution for Wire + Arc Additive Manufacturing. *Robot. Comput. Integr. Manuf.* **2019**, *60*, 1–11. [CrossRef]
152. Xiong, Y.; Dharmawan, A.G.; Tang, Y.; Foong, S.; Soh, G.S.; Rosen, D.W. A knowledge-based process planning framework for wire arc additive manufacturing. *Adv. Eng. Inform.* **2020**, *45*, 101135. [CrossRef]
153. Sefidi, M.P.; Israr, R.; Buhl, J.; Bambach, M. Rule-Based Path Identification for Direct Energy Deposition. *Proc. Manuf.* **2020**, *47*, 1134–1140. [CrossRef]
154. Ding, D.; Pan, Z.; Cuiuri, D.; Li, H. Process planning for robotic wire and arc additive manufacturing. In Proceedings of the 2015 IEEE 10th Conference on Industrial Electronics and Applications (ICIEA), Auckland, New Zealand, 15—17 June 2015; IEEE: Piscataway, NJ, USA, 2015; pp. 2000–2003, ISBN 978-1-4799-8389-6.
155. Zhang, J.; Zhou, J.; Wang, Q.; Xiao, G.; Quan, G. Process planning of automatic wire arc additive remanufacturing for hot forging die. *Int. J. Adv. Manuf. Technol.* **2020**, *109*, 1613–1623. [CrossRef]
156. Evjemo, L.D.; Langelandsvik, G.; Gravdahl, J.T. Wire Arc Additive Manufacturing by Robot Manipulator: Towards Creating Complex Geometries. *IFAC Pap.* **2019**, *52*, 103–109. [CrossRef]
157. Ding, D.-H.; Pan, Z.-X.; Dominic, C.; Li, H.-J. Process Planning Strategy for Wire and Arc Additive Manufacturing. In *Robotic Welding, Intelligence and Automation: RWIA'2014*; Tarn, T.-J., Chen, S.-B., Chen, X.-Q., Eds.; Springer: Cham, Switzerland, 2016; pp. 437–450, ISBN 978-3-319-18996-3.
158. Nguyen, L.; Buhl, J.; Bambach, M. Multi-bead Overlapping Models for Tool Path Generation in Wire-Arc Additive Manufacturing Processes. *Proc. Manuf.* **2020**, *47*, 1123–1128. [CrossRef]
159. Nguyen, L.; Buhl, J.; Bambach, M. Continuous Eulerian tool path strategies for wire-arc additive manufacturing of rib-web structures with machine-learning-based adaptive void filling. *Addit. Manuf.* **2020**, *35*, 101265. [CrossRef]
160. Lee, S.H. Optimization of Cold Metal Transfer-Based Wire Arc Additive Manufacturing Processes Using Gaussian Process Regression. *Metals* **2020**, *10*, 461. [CrossRef]
161. Diourté, A.; Bugarin, F.; Bordreuil, C.; Segonds, S. Continuous three-dimensional path planning (CTPP) for complex thin parts with wire arc additive manufacturing. *Addit. Manuf.* **2020**, 101622. [CrossRef]
162. Nguyen, L.; Buhl, J.; Bambach, M. Decomposition algorithm for tool path planning for wire-arc additive manufacturing. *J. Mach. Eng.* **2018**, *18*, 96–107. [CrossRef]
163. Liu, H.H.; Zhao, T.; Li, L.Y.; Liu, W.J.; Wang, T.Q.; Yue, J.F. A path planning and sharp corner correction strategy for wire and arc additive manufacturing of solid components with polygonal cross-sections. *Int. J. Adv. Manuf. Technol.* **2020**, *106*, 4879–4889. [CrossRef]
164. Ding, D.; Pan, Z.; Cuiuri, D.; Li, H.; Larkin, N.; van Duin, S. Automatic multi-direction slicing algorithms for wire based additive manufacturing. *Robot. Comput. Integr. Manuf.* **2016**, *37*, 139–150. [CrossRef]
165. Nikam, S.H.; Jain, N.K.; Sawant, M.S. Optimization of parameters of micro-plasma transferred arc additive manufacturing process using real coded genetic algorithm. *Int. J. Adv. Manuf. Technol.* **2020**, *106*, 1239–1252. [CrossRef]
166. Ding, D.; Shen, C.; Pan, Z.; Cuiuri, D.; Li, H.; Larkin, N.; van Duin, S. Towards an automated robotic arc-welding-based additive manufacturing system from CAD to finished part. *Comput. Aided Des.* **2016**, *73*, 66–75. [CrossRef]

167. Ma, G.; Zhao, G.; Li, Z.; Xiao, W. A Path Planning Method for Robotic Wire and Arc Additive Manufacturing of Thin-Walled Structures with Varying Thickness. *IOP Conf. Ser. Mater. Sci. Eng.* **2019**, *470*, 12018. [CrossRef]
168. Wang, R.; Zhang, H.; Wang, G.; Tang, S.; Li, R. Generation of deposition paths and quadrilateral meshes in Additive Manufacturing. In Proceedings of the Solid Freeform Fabrication 2017: Proceedings of the 28th Annual International, Austin, TX, USA, 7–9 August 2017.
169. Tourlomousis, F.; Chang, R.C. Dimensional Metrology of Cell-matrix Interactions in 3D Microscale Fibrous Substrates. *Proc. CIRP* **2017**, *65*, 32–37. [CrossRef]
170. Ma, G.; Zhao, G.; Li, Z.; Yang, M.; Xiao, W. Optimization strategies for robotic additive and subtractive manufacturing of large and high thin-walled aluminum structures. *Int. J. Adv. Manuf. Technol.* **2019**, *101*, 1275–1292. [CrossRef]
171. Dai, F.; Zhang, H.; Li, R. Process planning based on cylindrical or conical surfaces for five-axis wire and arc additive manufacturing. *Rapid Prototyp. J.* **2020**, *26*, 1405–1420. [CrossRef]
172. Li, R.; Zhang, H.; Dai, F.; Huang, C.; Wang, G. End lateral extension path strategy for intersection in wire and arc additive manufactured 2319 aluminum alloy. *Rapid Prototyp. J.* **2019**, *26*, 360–369. [CrossRef]
173. Zhang, C.; Shen, C.; Hua, X.; Li, F.; Zhang, Y.; Zhu, Y. Influence of wire-arc additive manufacturing path planning strategy on the residual stress status in one single buildup layer. *Int. J. Adv. Manuf. Technol.* **2020**, *111*, 797–806. [CrossRef]
174. Park, S.-C.; Bang, H.-S.; Seong, W.-J. Effects of Material Properties on Angular Distortion in Wire Arc Additive Manufacturing: Experimental and Computational Analyses. *Materials* **2020**, *13*, 1399. [CrossRef]
175. Li, Y.; Han, Q.; Zhang, G.; Horváth, I. A layers-overlapping strategy for robotic wire and arc additive manufacturing of multi-layer multi-bead components with homogeneous layers. *Int. J. Adv. Manuf. Technol.* **2018**, *96*, 3331–3344. [CrossRef]
176. Kumar, P.; Jain, N.K.; Sawant, M.S. Modeling of dimensions and investigations on geometrical deviations of metallic components manufactured by μ-plasma transferred arc additive manufacturing process. *Int. J. Adv. Manuf. Technol.* **2020**, *107*, 3155–3168. [CrossRef]
177. Bandari, Y.K.; Charrett, T.O.H.; Michel, F.; Ding, J.; Williams, S.W.; Tatum, R.P. *Compensation Strategies for Robotic Motion Errors for Additive Manufacturing (AM)*; University of Texas: Austin, TX, USA, 2016.
178. Nemani, A.V.; Ghaffari, M.; Nasiri, A. On the Post-Printing Heat Treatment of a Wire Arc Additively Manufactured ER70S Part. *Materials* **2020**, *13*, 2795. [CrossRef]
179. Seo, K.; Kim, Y.; Evans, G.M.; Kim, H.J.; Lee, C. Formation of Mn-depleted zone in Ti-containing weld metals. *Weld. World* **2015**, *59*, 373–380. [CrossRef]
180. Patterson, T.; Lippold, J.C. Effect of niobium on the microstructure and properties of submerged arc welds in HSLA steel. *Weld. World* **2020**, *64*, 1089–1105. [CrossRef]
181. Zhang, L.; Kannengiesser, T. HAZ softening in Nb-, Ti- and Ti + V-bearing quenched and tempered steel welds. *Weld. World* **2016**, *60*, 177–184. [CrossRef]
182. Treutler, K.; Wesling, V. Usage of Ti-surface-modified filler material to increase the joint strength of High-Strength Low Alloyed (HSLA) steels under different load types. *SN Appl. Sci.* **2020**, *2*. [CrossRef]
183. Seo, K.; Kim, K.; Kim, H.J.; Ryoo, H.; Evans, G.M.; Lee, C. Microstructural and Inclusion Characteristics of C–Mn Steel Welds at a Minimal Level of Titanium. *Met. Mater. Int.* **2020**, *26*, 1226–1234. [CrossRef]
184. Seo, J.S.; Seo, K.; Kim, H.J.; Lee, C. Effect of titanium content on weld microstructure and mechanical properties of bainitic GMA welds. *Weld. World* **2014**, *58*, 893–901. [CrossRef]
185. Seo, J.S. Effect of Grain Boundary Ferrite on Susceptibility to Cold Cracking in High-strength Weld Metal. *Met. Mater. Int.* **2008**, *14*, 515–522. [CrossRef]
186. Schaupp, T.; Schroepfer, D.; Kromm, A.; Kannengiesser, T. Welding residual stresses in 960 MPa grade QT and TMCP high-strength steels. *J. Manuf. Process.* **2017**, *27*, 226–232. [CrossRef]
187. Schroepfer, D.; Kannengiesser, T. Stress build-up in HSLA steel welds due to material behaviour. *J. Mater. Process. Technol.* **2016**, *227*, 49–58. [CrossRef]
188. Schroepfer, D.; Kromm, A.; Kannengiesser, T. Engineering approach to assess residual stresses in welded components. *Weld. World* **2017**, *61*, 91–106. [CrossRef]
189. Wächter, M.; Leicher, M.; Hupka, M.; Leistner, C.; Masendorf, L.; Treutler, K.; Kamper, S.; Esderts, A.; Wesling, V.; Hartmann, S. Monotonic and Fatigue Properties of Steel Material Manufactured by Wire Arc Additive Manufacturing. *Appl. Sci.* **2020**, *10*, 5238. [CrossRef]
190. Sridharan, N.; Noakes, M.W.; Nycz, A.; Love, L.J.; Dehoff, R.R.; Babu, S.S. On the toughness scatter in low alloy C-Mn steel samples fabricated using wire arc additive manufacturing. *Mater. Sci. Eng. A* **2018**, *713*, 18–27. [CrossRef]
191. Ali, W.; Qin, X.; Xiong, J.; Yang, C.; Liu, F. Impact toughness of components made by GMAW based additive manufacturing. *Proc. Struct. Integr.* **2018**, *13*, 2065–2070. [CrossRef]
192. Ron, T.; Levy, G.K.; Dolev, O.; Leon, A.; Shirizly, A.; Aghion, E. Environmental Behavior of Low Carbon Steel Produced by a Wire Arc Additive Manufacturing Process. *Metals* **2019**, *9*, 888. [CrossRef]
193. Ghaffari, M.; Vahedi Nemani, A.; Rafieazad, M.; Nasiri, A. Effect of Solidification Defects and HAZ Softening on the Anisotropic Mechanical Properties of a Wire Arc Additive-Manufactured Low-Carbon Low-Alloy Steel Part. *JOM* **2019**, *71*, 4215–4224. [CrossRef]

194. Lu, X.; Zhou, Y.F.; Xing, X.L.; Shao, L.Y.; Yang, Q.X.; Gao, S.Y. Open-source wire and arc additive manufacturing system: Formability, microstructures, and mechanical properties. *Int. J. Adv. Manuf. Technol.* **2017**, *93*, 2145–2154. [CrossRef]
195. Youheng, F.; Guilan, W.; Haiou, Z.; Liye, L. Optimization of surface appearance for wire and arc additive manufacturing of Bainite steel. *Int. J. Adv. Manuf. Technol.* **2017**, *91*, 301–313. [CrossRef]
196. Yildiz, A.S.; Davut, K.; Koc, B.; Yilmaz, O. Wire arc additive manufacturing of high-strength low alloy steels: Study of process parameters and their influence on the bead geometry and mechanical characteristics. *Int. J. Adv. Manuf. Technol.* **2020**, *108*, 3391–3404. [CrossRef]
197. Aldalur, E.; Veiga, F.; Suárez, A.; Bilbao, J.; Lamikiz, A. Analysis of the Wall Geometry with Different Strategies for High Deposition Wire Arc Additive Manufacturing of Mild Steel. *Metals* **2020**, *10*, 892. [CrossRef]
198. Rafieazad, M.; Ghaffari, M.; Vahedi Nemani, A.; Nasiri, A. Microstructural evolution and mechanical properties of a low-carbon low-alloy steel produced by wire arc additive manufacturing. *Int. J. Adv. Manuf. Technol.* **2019**, *105*, 2121–2134. [CrossRef]
199. Sun, L.; Jiang, F.; Huang, R.; Yuan, D.; Guo, C.; Wang, J. Microstructure and Mechanical Properties of Low-Carbon High-Strength Steel Fabricated by Wire and Arc Additive Manufacturing. *Metals* **2020**, *10*, 216. [CrossRef]
200. Artaza, T.; Suárez, A.; Murua, M.; García, J.C.; Tabernero, I.; Lamikiz, A. Wire Arc Additive Manufacturing of Mn4Ni2CrMo Steel: Comparison of Mechanical and Metallographic Properties of PAW and GMAW. *Proc. Manuf.* **2019**, *41*, 1071–1078. [CrossRef]
201. Dirisu, P.; Ganguly, S.; Mehmanparast, A.; Martina, F.; Williams, S. Analysis of fracture toughness properties of wire + arc additive manufactured high strength low alloy structural steel components. *Mater. Sci. Eng. A* **2019**, *765*, 138285. [CrossRef]
202. Müller, J.; Grabowski, M.; Müller, C.; Hensel, J.; Unglaub, J.; Thiele, K.; Kloft, H.; Dilger, K. Design and Parameter Identification of Wire and Arc Additively Manufactured (WAAM) Steel Bars for Use in Construction. *Metals* **2019**, *9*, 725. [CrossRef]
203. Shassere, B.; Nycz, A.; Noakes, M.; Masuo, C.; Sridharan, N. Correlation of Microstructure and Mechanical Properties of Metal Big Area Additive Manufacturing. *Appl. Sci.* **2019**, *9*, 787. [CrossRef]
204. Klobčar, D.; Lindič, M.; Bušić, M. Wire arc additive manufacturing of mild steel. *Mater. Geoenviron.* **2018**, *65*, 179–186. [CrossRef]
205. Dai, Y.; Yu, S.; Huang, A.; Shi, Y. Microstructure and mechanical properties of high-strength low alloy steel by wire and arc additive manufacturing. *Int. J. Miner. Met. Mater.* **2020**, *27*, 933–942. [CrossRef]
206. van Le, T. A preliminary study on gas metal arc welding-based additive manufacturing of metal parts. *Sci. Technol. Dev. J.* **2020**, *23*. [CrossRef]
207. Moore, P.; Addison, A.; Nowak-Coventry, M. Mechanical properties of wire plus arc additive manufactured steel and stainless steel structures. *Weld. World* **2019**, *63*, 1521–1530. [CrossRef]
208. van Le, T.; Hoang, Q.H.; van Tran, C.; Mai, D.S.; Dinh, D.M.; Doan, T.K. Effects of welding current on the shape and microstructure formation of thin-walled low-carbon parts built by wire arc additive manufacturing. *Vietnam J. Sci. Technol.* **2020**, *58*, 461. [CrossRef]
209. Duarte, V.R.; Rodrigues, T.A.; Schell, N.; Santos, T.G.; Oliveira, J.P.; Miranda, R.M. Wire and Arc Additive Manufacturing of High Strength Low Alloy Steel: Microstructure and Mechanical Properties. *Adv. Eng. Mater.* **2021**. [CrossRef]
210. Zhang, W.; Lei, W.; Zhang, Y.; Liu, X. Microstructure and mechanical properties of wire arc additive-manufacturing high-carbon chromium bearing steel. *Mater. Technol.* **2020**, *54*, 359–364. [CrossRef]
211. Tabernero, I.; Paskual, A.; Álvarez, P.; Suárez, A. Study on Arc Welding Processes for High Deposition Rate Additive Manufacturing. *Proc. CIRP* **2018**, *68*, 358–362. [CrossRef]
212. Ji, L.; Lu, J.; Liu, C.; Jing, C.; Fan, H.; Ma, S. Microstructure and mechanical properties of 304L steel fabricated by arc additive manufacturing. *MATEC Web Conf.* **2017**, *128*, 3006. [CrossRef]
213. Rajesh Kannan, A.; Siva Shanmugam, N.; Rajkumar, V.; Vishnukumar, M. Insight into the microstructural features and corrosion properties of wire arc additive manufactured super duplex stainless steel (ER2594). *Mater. Lett.* **2020**, *270*, 127680. [CrossRef]
214. Gordon, J.V.; Haden, C.V.; Nied, H.F.; Vinci, R.P.; Harlow, D.G. Fatigue crack growth anisotropy, texture and residual stress in austenitic steel made by wire and arc additive manufacturing. *Mater. Sci. Eng. A* **2018**, *724*, 431–438. [CrossRef]
215. Chen, X.; Li, J.; Cheng, X.; He, B.; Wang, H.; Huang, Z. Microstructure and mechanical properties of the austenitic stainless steel 316L fabricated by gas metal arc additive manufacturing. *Mater. Sci. Eng. A* **2017**, *703*, 567–577. [CrossRef]
216. Parvaresh, B.; Salehan, R.; Miresmaeili, R. Investigating Isotropy of Mechanical and Wear Properties in As-Deposited and Inter-Layer Cold Worked Specimens Manufactured by Wire Arc Additive Manufacturing. *Met. Mater. Int.* **2020**. [CrossRef]
217. Xie, B.; Xue, J.; Ren, X.; Wu, W.; Lin, Z. A Comparative Study of the CMT + P Process on 316L Stainless Steel Additive Manufacturing. *Appl. Sci.* **2020**, *10*, 3284. [CrossRef]
218. Xu, X.; Ganguly, S.; Ding, J.; Guo, S.; Williams, S.; Martina, F. Microstructural evolution and mechanical properties of maraging steel produced by wire + arc additive manufacture process. *Mater. Charact.* **2018**, *143*, 152–162. [CrossRef]
219. Posch, G.; Chladil, K.; Chladil, H. Material properties of CMT—metal additive manufactured duplex stainless steel blade-like geometries. *Weld. World* **2017**, *61*, 873–882. [CrossRef]
220. Rusteiko, A.C.; Angelo, J.D.; del Conte, E.G.D. Residual stress in metal arc additive manufacturing of mill knives cutting edges. *Int. J. Adv. Manuf. Technol.* **2019**, *104*, 4457–4464. [CrossRef]
221. Wu, W.; Xue, J.; Wang, L.; Zhang, Z.; Hu, Y.; Dong, C. Forming Process, Microstructure, and Mechanical Properties of Thin-Walled 316L Stainless Steel Using Speed-Cold-Welding Additive Manufacturing. *Metals* **2019**, *9*, 109. [CrossRef]
222. Eriksson, M.; Lervåg, M.; Sørensen, C.; Robertstad, A.; Brønstad, B.M.; Nyhus, B.; Aune, R.; Ren, X.; Akselsen, O.M. Additive manufacture of superduplex stainless steel using WAAM. *MATEC Web Conf.* **2018**, *188*, 3014. [CrossRef]

223. Elmer, J.W.; Gibbs, G.; Carpenter, J.S.; Coughlin, D.R.; Hochanadel, P.A.; Vaja, J.A.; Gurung, P.; JOHNSON, A.; Dvornak, M.J. Wire-Based Additive Manufacturing of Stainless Steel Components. *Weld J.* **2020**, *99*, 8–24. [CrossRef]
224. Gao, C.; Chen, X.; Su, C.; Singh, A.R.; Jayalakshmi, S. Microstructure and Mechanical Properties of 9Cr Martensitic Heat-resistant Steel Fabricated by Wire and Arc Additive Manufacture Technology. *Mat. Express* **2019**, *9*, 179–184. [CrossRef]
225. Lervåg, M.; Sørensen, C.; Robertstad, A.; Brønstad, B.M.; Nyhus, B.; Eriksson, M.; Aune, R.; Ren, X.; Akselsen, O.M.; Bunaziv, I. Additive Manufacturing with Superduplex Stainless Steel Wire by CMT Process. *Metals* **2020**, *10*, 272. [CrossRef]
226. Ge, J.; Lin, J.; Fu, H.; Lei, Y.; Xiao, R. A spatial periodicity of microstructural evolution and anti-indentation properties of wire-arc additive manufacturing 2Cr13 thin-wall part. *Mater. Des.* **2018**, *160*, 218–228. [CrossRef]
227. Nikam, P.P.; Arun, D.; Ramkumar, K.D.; Sivashanmugam, N. Microstructure characterization and tensile properties of CMT-based wire plus arc additive manufactured ER2594. *Mater. Charact.* **2020**, *169*, 110671. [CrossRef]
228. A Hosseini, V.; Högström, M.; Hurtig, K.; Valiente Bermejo, M.A.; Stridh, L.-E.; Karlsson, L. Wire-arc additive manufacturing of a duplex stainless steel: Thermal cycle analysis and microstructure characterization. *Weld. World* **2019**, *63*, 975–987. [CrossRef]
229. Ge, J.; Lin, J.; Chen, Y.; Lei, Y.; Fu, H. Characterization of wire arc additive manufacturing 2Cr13 part: Process stability, microstructural evolution, and tensile properties. *J. Alloy. Compd.* **2018**, *748*, 911–921. [CrossRef]
230. Wittig, B.; Zinke, M.; Jüttner, S. Influence of arc energy and filler metal composition on the microstructure in wire arc additive manufacturing of duplex stainless steels. *Weld. World* **2020**. [CrossRef]
231. Anirudhan, B.T.; Devasia, J.; Krishna, T.; Kuruvila, M.T. Manufacturing of a Bimetallic Structure of Stainless Steel and Mild Steel through Wire Arc Additive Manufacturing—A Critical Review. *Int. J. Innov. Sci. Res. Technol.* **2020**, *5*, 679–685. [CrossRef]
232. Leicher, M.; Kamper, S.; Treutler, K.; Wesling, V. Multi-material design in additive manufacturing—feasibility validation. *Weld. World* **2020**, *64*, 1341–1347. [CrossRef]
233. Ermakova, A.; Mehmanparast, A.; Ganguly, S. A review of present status and challenges of using additive manufacturing technology for offshore wind applications. *Proc. Struct. Integr.* **2019**, *17*, 29–36. [CrossRef]
234. Ron, T.; Levy, G.K.; Dolev, O.; Leon, A.; Shirizly, A.; Aghion, E. The Effect of Microstructural Imperfections on Corrosion Fatigue of Additively Manufactured ER70S-6 Alloy Produced by Wire Arc Deposition. *Metals* **2020**, *10*, 98. [CrossRef]
235. Ayan, Y.; Kahraman, N. Wire Arc Additive Manufacturing of Low-Carbon Mild Steel Using Two Different 3D Printers. *Phys. Met. Metallogr.* **2021**. [CrossRef]
236. Rodrigues, T.A.; Duarte, V.; Avila, J.A.; Santos, T.G.; Miranda, R.M.; Oliveira, J.P. Wire and arc additive manufacturing of HSLA steel: Effect of thermal cycles on microstructure and mechanical properties. *Addit. Manuf.* **2019**, *27*, 440–450. [CrossRef]
237. Schroepfer, D.; Scharf-Wildenhain, R.; Haelsig, A.; Wandtke, K.; Kromm, A.; Kannengiesser, T. Process-related influences and correlations in wire arc additive manufacturing of high-strength steels. *IOP Conf. Ser. Mater. Sci. Eng.* **2021**, *1147*, 12002. [CrossRef]
238. Ermakova, A.; Mehmanparast, A.; Ganguly, S.; Razavi, J.; Berto, F. Fatigue crack growth behaviour of wire and arc additively-manufactured ER70S-6 low carbon steel components. *Int. J. Fract.* **2021**. [CrossRef]
239. Gordon, J.V.; Harlow, D.G. Statistical Modeling of Wire and Arc Additive Manufactured Stainless Steel 304: Microstructure and Fatigue. *Int. J. Rel. Qual. Saf. Eng.* **2019**, *26*, 1950016. [CrossRef]
240. Boellinghaus, T.; Lippold, J.C.; Cross, C.E. *Cracking Phenomena in Welds IV*; Springer: Berlin/Heidelberg, Germany, 2016.
241. Böllinghaus, T.; Herold, H.; Cross, C.E.; Lippold, J.C. *Hot Cracking Phenomena in Welds II*, 1st ed.; Springer: Berlin/Heidelberg, Germany, 2008; ISBN 9783540786283.
242. Laghi, V. Geometrical Characterization of Wire-And-Arc Additive Manufactured Steel Element. *Adv. Mater. Lett.* **2019**, *10*, 695–699. [CrossRef]
243. Manurung, Y.H.P.; Prajadhiana, K.P.; Adenan, M.S.; Awiszus, B.; Graf, M.; Haelsig, A. Analysis of material property models on WAAM distortion using nonlinear numerical computation and experimental verification with P-GMAW. *Archiv. Civ. Mech. Eng.* **2021**, *21*. [CrossRef]
244. Laghi, V.; Tonelli, L.; Palermo, M.; Bruggi, M.; Sola, R.; Ceschini, L.; Trombetti, T. Experimentally-validated orthotropic elastic model for Wire-and-Arc Additively Manufactured stainless steel. *Addit. Manuf.* **2021**, *42*, 101999. [CrossRef]
245. Kannan, A.R.; Shanmugam, N.S.; Ramkumar, K.D.; Rajkumar, V. Studies on Super Duplex Stainless Steel Manufactured by Wire Arc Additive Manufacturing. *Trans. Indian Inst. Met.* **2021**. [CrossRef]
246. Binesh, F.; Bahrami, A.; Hebel, M.; Aidun, D.K. Preservation of Natural Phase Balance in Multi-pass and Wire Arc Additive Manufacturing-Made Duplex Stainless Steel Structures. *J. Mater. Eng. Perform.* **2021**, *30*, 2552–2565. [CrossRef]
247. Ge, J.; Lin, J.; Long, Y.; Liu, Q.; Zhang, L.; Chen, W.; Lei, Y. Microstructural evolution and mechanical characterization of wire arc additively manufactured 2Cr13 thin-wall part. *J. Mater. Res. Technol.* **2021**. [CrossRef]
248. Vahedi Nemani, A.; Ghaffari, M.; Salahi, S.; Nasiri, A. Effects of post-printing heat treatment on the microstructure and mechanical properties of a wire arc additive manufactured 420 martensitic stainless steel part. *Mater. Sci. Eng. A* **2021**, *813*, 141167. [CrossRef]
249. Fang, X.; Zhang, L.; Chen, G.; Dang, X.; Huang, K.; Wang, L.; Lu, B. Correlations between Microstructure Characteristics and Mechanical Properties in 5183 Aluminium Alloy Fabricated by Wire-Arc Additive Manufacturing with Different Arc Modes. *Materials* **2018**, *11*, 2075. [CrossRef]
250. Horgar, A.; Fostervoll, H.; Nyhus, B.; Ren, X.; Eriksson, M.; Akselsen, O.M. Additive manufacturing using WAAM with AA5183 wire. *J. Mater. Process. Technol.* **2018**, *259*, 68–74. [CrossRef]

251. Hirtler, M.; Jedynak, A.; Sydow, B.; Sviridov, A.; Bambach, M. Investigation of microstructure and hardness of a rib geometry produced by metal forming and wire-arc additive manufacturing. *MATEC Web Conf.* **2018**, *190*, 2005. [CrossRef]
252. Morais, P.J.; Gomes, B.; Santos, P.; Gomes, M.; Gradinger, R.; Schnall, M.; Bozorgi, S.; Klein, T.; Fleischhacker, D.; Warczok, P.; et al. Characterisation of a High-Performance Al-Zn-Mg-Cu Alloy Designed for Wire Arc Additive Manufacturing. *Materials* **2020**, *13*, 1610. [CrossRef] [PubMed]
253. Gomez Ortega, A.; Corona Galvan, L.; Deschaux-Beaume, F.; Mezrag, B.; Rouquette, S. Effect of process parameters on the quality of aluminium alloy Al5Si deposits in wire and arc additive manufacturing using a cold metal transfer process. *Sci. Technol. Weld. Join.* **2018**, *23*, 316–332. [CrossRef]
254. Ünsal, I.; Hirtler, M.; Sviridov, A.; Bambach, M. Material Properties of Features Produced from EN AW 6016 by Wire-Arc Additive Manufacturing. *Proc. Manuf.* **2020**, *47*, 1129–1133. [CrossRef]
255. Bai, J.Y.; Fan, C.L.; Lin, S.B.; Yang, C.L.; Dong, B.L. Effects of thermal cycles on microstructure evolution of 2219-Al during GTA-additive manufacturing. *Int. J. Adv. Manuf. Technol.* **2016**, *87*, 2615–2623. [CrossRef]
256. Hönnige, J.R.; Colegrove, P.A.; Ganguly, S.; Eimer, E.; Kabra, S.; Williams, S. Control of residual stress and distortion in aluminium wire + arc additive manufacture with rolling. *Addit. Manuf.* **2018**, *22*, 775–783. [CrossRef]
257. Fixter, J.; Gu, J.; Ding, J.; Williams, S.W.; Prangnell, P.B. Preliminary Investigation into the Suitability of 2xxx Alloys for Wire-Arc Additive Manufacturing. *MSF* **2016**, *877*, 611–616. [CrossRef]
258. Geng, H.; Li, J.; Xiong, J.; Lin, X.; Zhang, F. Geometric Limitation and Tensile Properties of Wire and Arc Additive Manufacturing 5A06 Aluminum Alloy Parts. *J. Mater. Eng. Perform.* **2017**, *26*, 621–629. [CrossRef]
259. Klein, T.; Schnall, M. Control of macro-/microstructure and mechanical properties of a wire-arc additive manufactured aluminum alloy. *Int. J. Adv. Manuf. Technol.* **2020**, *108*, 235–244. [CrossRef]
260. Köhler, M.; Hensel, J.; Dilger, K. Effects of Thermal Cycling on Wire and Arc Additive Manufacturing of Al-5356 Components. *Metals* **2020**, *10*, 952. [CrossRef]
261. Ortega, A.G.; Corona Galvan, L.; Salem, M.; Moussaoui, K.; Segonds, S.; Rouquette, S.; Deschaux-Beaume, F. Characterisation of 4043 aluminium alloy deposits obtained by wire and arc additive manufacturing using a Cold Metal Transfer process. *Sci. Technol. Weld. Join.* **2019**, *24*, 538–547. [CrossRef]
262. Qi, Z.; Cong, B.; Qi, B.; Zhao, G.; Ding, J. Properties of wire + arc additively manufactured 2024 aluminum alloy with different solution treatment temperature. *Mater. Lett.* **2018**, *230*, 275–278. [CrossRef]
263. Ren, L.; Gu, H.; Wang, W.; Wang, S.; Li, C.; Wang, Z.; Zhai, Y.; Ma, P. Effect of Sc Content on the Microstructure and Properties of Al–Mg–Sc Alloys Deposited by Wire Arc Additive Manufacturing. *Met. Mater. Int.* **2020**. [CrossRef]
264. Ren, L.; Gu, H.; Wang, W.; Wang, S.; Li, C.; Wang, Z.; Zhai, Y.; Ma, P. The Microstructure and Properties of an Al-Mg-0.3Sc Alloy Deposited by Wire Arc Additive Manufacturing. *Metals* **2020**, *10*, 320. [CrossRef]
265. Wang, S.; Gu, H.; Wang, W.; Li, C.; Ren, L.; Wang, Z.; Zhai, Y.; Ma, P. Study on Microstructural and Mechanical Properties of an Al–Cu–Sn Alloy Wall Deposited by Double-Wire Arc Additive Manufacturing Process. *Materials* **2020**, *13*, 73. [CrossRef] [PubMed]
266. Wang, D.; Lu, J.; Tang, S.; Yu, L.; Fan, H.; Ji, L.; Liu, C. Reducing Porosity and Refining Grains for Arc Additive Manufacturing Aluminum Alloy by Adjusting Arc Pulse Frequency and Current. *Materials* **2018**, *11*, 1344. [CrossRef] [PubMed]
267. Qi, Z.; Qi, B.; Cong, B.; Sun, H.; Zhao, G.; Ding, J. Microstructure and mechanical properties of wire + arc additively manufactured 2024 aluminum alloy components: As-deposited and post heat-treated. *J. Manuf. Process.* **2019**, *40*, 27–36. [CrossRef]
268. Wang, L.; Suo, Y.; Liang, Z.; Wang, D.; Wang, Q. Effect of titanium powder on microstructure and mechanical properties of wire + arc additively manufactured Al-Mg alloy. *Mater. Lett.* **2019**, *241*, 231–234. [CrossRef]
269. Lee, H.; Kim, J.; Pyo, C.; Kim, J. Evaluation of Bead Geometry for Aluminum Parts Fabricated Using Additive Manufacturing-Based Wire-Arc Welding. *Processes* **2020**, *8*, 1211. [CrossRef]
270. Feng, Y.; He, L.; Wang, K.; E, X. The Effects of Low Frequency on the Microstructure and Mechanical Properties of High-Strength Al-Mg Aluminum Alloys by Wire and Double-Pulsed Arc Additive Manufacturing. *J. Mater. Eng. Perform.* **2018**, *27*, 5591–5604. [CrossRef]
271. Li, S.; Zhang, L.-J.; Ning, J.; Wang, X.; Zhang, G.-F.; Zhang, J.-X.; Na, S.-J. Microstructures and mechanical properties of Al–Zn–Mg aluminium alloy samples produced by wire + arc additive manufacturing. *J. Mater. Res. Technol.* **2020**, *9*, 13770–13780. [CrossRef]
272. Eimer, E.; Suder, W.; Williams, S.; Ding, J. Wire Laser Arc Additive Manufacture of aluminium zinc alloys. *Weld. World* **2020**, *64*, 1313–1319. [CrossRef]
273. Hao, Z.; Ao, S.; Cai, Y.; Zhang, W.; Luo, Z. Formation of SUS304/Aluminum Alloys Using Wire and Arc Additive Manufacturing. *Metals* **2018**, *8*, 595. [CrossRef]
274. Wang, S.; Gu, H.; Wang, W.; Li, C.; Ren, L.; Wang, Z.; Zhai, Y.; Ma, P. The Influence of Heat Input on the Microstructure and Properties of Wire-Arc-Additive-Manufactured Al-Cu-Sn Alloy Deposits. *Metals* **2020**, *10*, 79. [CrossRef]
275. Liu, Z.; Zhang, P.; Li, S.; Wu, D.; Yu, Z. Wire and arc additive manufacturing of 4043 Al alloy using a cold metal transfer method. *Int. J. Miner. Met. Mater.* **2020**, *27*, 783–791. [CrossRef]
276. Zhang, Y.; Gao, M.; Zeng, X. Effect of Process Parameters on Mechanical Properties of Wire and Arc Additive-Manufactured AlCu6Mn. *JOM* **2019**, *71*, 886–892. [CrossRef]
277. Zuo, W.; Ma, L.; Lu, Y.; Li, S.; Ji, Z.; Ding, M. Effects of Solution Treatment Temperatures on Microstructure and Mechanical Properties of TIG–MIG Hybrid Arc Additive Manufactured 5356 Aluminum Alloy. *Met. Mater. Int.* **2018**, *24*, 1346–1358. [CrossRef]

278. Pramod, R.; Kumar, S.M.; Girinath, B.; Kannan, A.R.; Kumar, N.P.; Shanmugam, N.S. Fabrication, characterisation, and finite element analysis of cold metal transfer–based wire and arc additive–manufactured aluminium alloy 4043 cylinder. *Weld. World* **2020**, *64*, 1905–1919. [CrossRef]
279. Neto, L. Studying the Application of Additive Manufacturing to Large Parts. 2017. Available online: https://www.semanticscholar.org/paper/Studying-the-Application-of-Additive-Manufacturing-Neto-Leonor/45d01059f90079dcc36be6e4aba8b7989b20cbfa?p2df (accessed on 12 September 2021).
280. Zhong, H.; Qi, B.; Cong, B.; Qi, Z.; Sun, H. Microstructure and Mechanical Properties of Wire + Arc Additively Manufactured 2050 Al–Li Alloy Wall Deposits. *Chin. J. Mech. Eng.* **2019**, *32*. [CrossRef]
281. Teja, K.; Tokala, S.C.; Reddy, Y.P.; Narayana, K.L. Optimization of mechanical properties of wire arc additive manufactured specimens using grey-based taguchi method. *J. Crit. Rev.* **2020**, *7*, 808–817. [CrossRef]
282. Gu, J.; Gao, M.; Yang, S.; Bai, J.; Ding, J.; Fang, X. Pore formation and evolution in wire + arc additively manufactured 2319 Al alloy. *Addit. Manuf.* **2019**, *30*, 100900. [CrossRef]
283. Bai, J.; Ding, H.L.; Gu, J.L.; Wang, X.S.; Qiu, H. Porosity evolution in additively manufactured aluminium alloy during high temperature exposure. *IOP Conf. Ser. Mater. Sci. Eng.* **2017**, *167*, 12045. [CrossRef]
284. Ryazantsev, V.I.; Fedoseev, V.A.; Savostikov, A.N. Hydrocarbon hypothesis of metallurgical porosity when welding aluminium alloys. *Weld. Int.* **1998**, *12*, 907–910. [CrossRef]
285. Treutler, K.; Brechelt, S.; Wiche, H.; Wesling, V. Beneficial use of hyperbaric process conditions for welding of aluminium and copper alloys. *Weld. World* **2021**. [CrossRef]
286. Derekar, K.; Lawrence, J.; Melton, G.; Addison, A.; Zhang, X.; Xu, L. Influence of Interpass Temperature on Wire Arc Additive Manufacturing (WAAM) of Aluminium Alloy Components. *MATEC Web Conf.* **2019**, *269*, 5001. [CrossRef]
287. Derekar, K.S.; Addison, A.; Joshi, S.S.; Zhang, X.; Lawrence, J.; Xu, L.; Melton, G.; Griffiths, D. Effect of pulsed metal inert gas (pulsed-MIG) and cold metal transfer (CMT) techniques on hydrogen dissolution in wire arc additive manufacturing (WAAM) of aluminium. *Int. J. Adv. Manuf. Technol.* **2020**, *107*, 311–331. [CrossRef]
288. Klein, T.; Arnoldt, A.; Lahnsteiner, R.; Schnall, M. *A Structurally Refined Al-Mg-Si Alloy for Wire-Based Additive Manufacturing*; MIGAL.CO GmbH: Landau an der Isar, Germany.
289. Klein, T.; Arnoldt, A.; Schnall, M.; Gneiger, S. Microstructure Formation and Mechanical Properties of a Wire-Arc Additive Manufactured Magnesium Alloy. *JOM* **2021**, *73*, 1126–1134. [CrossRef]
290. Kim, J.; Kim, J.; Pyo, C. Comparison of Mechanical Properties of Ni-Al-Bronze Alloy Fabricated through Wire Arc Additive Manufacturing with Ni-Al-Bronze Alloy Fabricated through Casting. *Metals* **2020**, *10*, 1164. [CrossRef]
291. Chen, W.; Chen, Y.; Zhang, T.; Wen, T.; Feng, X.; Yin, L. Effects of Location on the Microstructure and Mechanical Properties of Cu-8Al-2Ni-2Fe-2Mn Alloy Produced Through Wire Arc Additive Manufacturing. *J. Mater. Eng. Perform.* **2020**, *29*, 4733–4744. [CrossRef]
292. Chen, W.; Chen, Y.; Zhang, T.; Wen, T.; Yin, Z.; Feng, X. Effect of Ultrasonic Vibration and Interpass Temperature on Microstructure and Mechanical Properties of Cu-8Al-2Ni-2Fe-2Mn Alloy Fabricated by Wire Arc Additive Manufacturing. *Metals* **2020**, *10*, 215. [CrossRef]
293. Baby, J.; Amirthalingam, M. Microstructural development during wire arc additive manufacturing of copper-based components. *Weld. World* **2020**, *64*, 395–405. [CrossRef]
294. Dong, B.; Pan, Z.; Shen, C.; Ma, Y.; Li, H. Fabrication of Copper-Rich Cu-Al Alloy Using the Wire-Arc Additive Manufacturing Process. *Met. Mater. Trans. B* **2017**, *48*, 3143–3151. [CrossRef]
295. Wang, Y.; Chen, X.; Konovalov, S.; Su, C.; Siddiquee, A.N.; Gangil, N. In-situ wire-feed additive manufacturing of Cu-Al alloy by addition of silicon. *Appl. Surf. Sci.* **2019**, *487*, 1366–1375. [CrossRef]
296. Liu, K.; Chen, X.; Shen, Q.; Pan, Z.; Singh, R.A.; Jayalakshmi, S.; Konovalov, S. Microstructural evolution and mechanical properties of deep cryogenic treated Cu–Al–Si alloy fabricated by Cold Metal Transfer (CMT) process. *Mater. Charact.* **2020**, *159*, 110011. [CrossRef]
297. Elitzer, D.; Höppel, H.W.; Göken, M.; Baier, D.; Fuchs, C.; Bähr, H.; Meyer, T.; Gallasch, A. Influence of wire arc additive manufacturing of Ti-6Al-4V on microstructure and mechanical properties for potential large-scale aviation parts. *MATEC Web Conf.* **2020**, *321*, 3037. [CrossRef]
298. Wu, B.; Pan, Z.; Ding, D.; Cuiuri, D.; Li, H. Effects of heat accumulation on microstructure and mechanical properties of Ti6Al4V alloy deposited by wire arc additive manufacturing. *Addit. Manuf.* **2018**, *23*, 151–160. [CrossRef]
299. Martina, F.; Colegrove, P.A.; Williams, S.W.; Meyer, J. Microstructure of Interpass Rolled Wire + Arc Additive Manufacturing Ti-6Al-4V Components. *Met. Mat. Trans. A* **2015**, *46*, 6103–6118. [CrossRef]
300. Ho, A.; Zhao, H.; Fellowes, J.W.; Martina, F.; Davis, A.E.; Prangnell, P.B. On the origin of microstructural banding in Ti-6Al4V wire-arc based high deposition rate additive manufacturing. *Acta Mater.* **2019**, *166*, 306–323. [CrossRef]
301. Wang, F.; Williams, S.; Colegrove, P.; Antonysamy, A.A. Microstructure and Mechanical Properties of Wire and Arc Additive Manufactured Ti-6Al-4V. *Met. Mat. Trans. A* **2013**, *44*, 968–977. [CrossRef]
302. Xie, Y.; Gao, M.; Wang, F.; Zhang, C.; Hao, K.; Wang, H.; Zeng, X. Anisotropy of fatigue crack growth in wire arc additive manufactured Ti-6Al-4V. *Mater. Sci. Eng. A* **2018**, *709*, 265–269. [CrossRef]
303. Bermingham, M.J.; Kent, D.; Zhan, H.; StJohn, D.H.; Dargusch, M.S. Controlling the microstructure and properties of wire arc additive manufactured Ti–6Al–4V with trace boron additions. *Acta Mater.* **2015**, *91*, 289–303. [CrossRef]

304. Bermingham, M.J.; Nicastro, L.; Kent, D.; Chen, Y.; Dargusch, M.S. Optimising the mechanical properties of Ti-6Al-4V components produced by wire + arc additive manufacturing with post-process heat treatments. *J. Alloy. Compd.* **2018**, *753*, 247–255. [CrossRef]
305. Martina, F.; Roy, M.J.; Szost, B.A.; Terzi, S.; Colegrove, P.A.; Williams, S.W.; Withers, P.J.; Meyer, J.; Hofmann, M. Residual stress of as-deposited and rolled wire + arc additive manufacturing Ti–6Al–4V components. *Mater. Sci. Technol.* **2016**, *32*, 1439–1448. [CrossRef]
306. Lin, J.J.; Lv, Y.H.; Liu, Y.X.; Xu, B.S.; Sun, Z.; Li, Z.G.; Wu, Y.X. Microstructural evolution and mechanical properties of Ti-6Al-4V wall deposited by pulsed plasma arc additive manufacturing. *Mater. Des.* **2016**, *102*, 30–40. [CrossRef]
307. Wang, J.; Lin, X.; Wang, J.; Yang, H.; Zhou, Y.; Wang, C.; Li, Q.; Huang, W. Grain morphology evolution and texture characterization of wire and arc additive manufactured Ti-6Al-4V. *J. Alloy. Compd.* **2018**, *768*, 97–113. [CrossRef]
308. Zhang, X.; Martina, F.; Ding, J.; Wang, X.; Williams, S.W. Fracture toughness and fatigue crack growth rate properties in wire + arc additive manufactured Ti-6Al-4V. *Fatigue Fract. Eng. Mater. Struct.* **2017**, *40*, 790–803. [CrossRef]
309. Yi, H.-J.; Kim, J.-W.; Kim, Y.-L.; Shin, S. Effects of Cooling Rate on the Microstructure and Tensile Properties of Wire-Arc Additive Manufactured Ti–6Al–4V Alloy. *Met. Mater. Int.* **2020**, *26*, 1235–1246. [CrossRef]
310. Lu, Y. The Effects of Inter-Pass Temperature on the Microstructure and Mechanical Properties of Ti-6Al-4V Alloy Deposited by Wire Arc Additive Manufacturing (WAAM). Master's Thesis, School of Mechanical, Materials, Mechatronic and Biomedical Engineering, University of Wollongong, Wollongong, Australia, 2018. Available online: https://ro.uow.edu.au/theses1/330 (accessed on 12 September 2021).
311. Mereddy, S.; Bermingham, M.J.; StJohn, D.H.; Dargusch, M.S. Grain refinement of wire arc additively manufactured titanium by the addition of silicon. *J. Alloy. Compd.* **2017**, *695*, 2097–2103. [CrossRef]
312. Martina, F.; Williams, S.W.; Colegrove, P.A. *Improved Microstructure and Increased Mechanical Properties of Additive Manufacture Produced TI-6AL-4V by Interpass Cold Rolling*; University of Texas: Austin, TX, USA, 2013.
313. Hönnige, J.R.; Davis, A.E.; Ho, A.; Kennedy, J.R.; Neto, L.; Prangnell, P.; Williams, S. The Effectiveness of Grain Refinement by Machine Hammer Peening in High Deposition Rate Wire-Arc AM Ti-6Al-4V. *Met. Mat. Trans. A* **2020**, *51*, 3692–3703. [CrossRef]
314. Li, Y.Y.; Ma, S.Y.; Liu, C.M.; Zhang, M. Microstructure and Mechanical Properties of Ti-6.5Al-3.5Mo-1.5Zr-0.3Si Alloy Fabricated by Arc Additive Manufacturing with Post Heat Treatment. *Key Eng. Mater.* **2018**, *789*, 161–169. [CrossRef]
315. Fu, J.; Qiu, K.; Gong, L.; Liu, C.; Wu, Q.; Lu, J.; Fan, H. Effect of Tool-Path on Morphology and Mechanical Properties of Ti-6Al-4V Fabricated by Wire and Arc Additive Manufacturing. *MATEC Web Conf.* **2017**, *128*, 5009. [CrossRef]
316. Wu, B. Quality improvement in wire arc additive manufacturing. Ph.D. Thesis, University of Wollongong, Wollongong, Australia, 2018.
317. Mereddy, S.; Bermingham, M.J.; Kent, D.; Dehghan-Manshadi, A.; StJohn, D.H.; Dargusch, M.S. Trace Carbon Addition to Refine Microstructure and Enhance Properties of Additive-Manufactured Ti-6Al-4V. *JOM* **2018**, *70*, 1670–1676. [CrossRef]
318. Vázquez, L.; Rodríguez, N.; Rodríguez, I.; Alberdi, E.; Álvarez, P. Influence of interpass cooling conditions on microstructure and tensile properties of Ti-6Al-4V parts manufactured by WAAM. *Weld. World* **2020**, *64*, 1377–1388. [CrossRef]
319. Raguvarun, K.; Balasubramaniam, K.; Rajagopal, P.; Palanisamy, S.; Nagarajah, R.; Hoye, N.; Curiri, D.; Kapoor, A. A study of internal structure in components made by additive manufacturing process using 3 D X-ray tomography. In Proceedings of the AIP Conference Proceedings 1650, 41st Annual Review of Progress in Quantitative Nondestructive Evaluation: Volume 34, Boise, ID, USA, 20–25 July 2014; AIP Publishing LLC: Melville, NY, USA, 2015; pp. 146–155.
320. Bermingham, M.J.; Thomson-Larkins, J.; St John, D.H.; Dargusch, M.S. Sensitivity of Ti-6Al-4V components to oxidation during out of chamber Wire + Arc Additive Manufacturing. *J. Mater. Process. Technol.* **2018**, *258*, 29–37. [CrossRef]
321. Bermingham, M.J.; StJohn, D.H.; Krynen, J.; Tedman-Jones, S.; Dargusch, M.S. Promoting the columnar to equiaxed transition and grain refinement of titanium alloys during additive manufacturing. *Acta Mater.* **2019**, *168*, 261–274. [CrossRef]
322. Yin, B.; Ma, H.; Wang, J.; Fang, K.; Zhao, H.; Liu, Y. Effect of CaF_2 addition on macro/microstructures and mechanical properties of wire and arc additive manufactured Ti-6Al-4V components. *Mater. Lett.* **2017**, *190*, 64–66. [CrossRef]
323. Alonso, U.; Veiga, F.; Suárez, A.; Artaza, T. Experimental Investigation of the Influence of Wire Arc Additive Manufacturing on the Machinability of Titanium Parts. *Metals* **2020**, *10*, 24. [CrossRef]
324. Guo, Y.; Pan, H.; Ren, L.; Quan, G. Microstructure and mechanical properties of wire arc additively manufactured AZ80M magnesium alloy. *Mater. Lett.* **2019**, *247*, 4–6. [CrossRef]
325. Guo, Y.; Quan, G.; Jiang, Y.; Ren, L.; Fan, L.; Pan, H. Formability, microstructure evolution and mechanical properties of wire arc additively manufactured AZ80M magnesium alloy using gas tungsten arc welding. *J. Magnes. Alloy.* **2020**. [CrossRef]
326. Gneiger, S.; Österreicher, J.A.; Arnoldt, A.R.; Birgmann, A.; Fehlbier, M. Development of a High Strength Magnesium Alloy for Wire Arc Additive Manufacturing. *Metals* **2020**, *10*, 778. [CrossRef]
327. Cheepu, M.; Lee, C.I.; Cho, S.M. Microstructural Characteristics of Wire Arc Additive Manufacturing with Inconel 625 by Super-TIG Welding. *Trans. Indian Inst. Met.* **2020**, *73*, 1475–1479. [CrossRef]
328. Xu, X.; Ding, J.; Ganguly, S.; Williams, S. Investigation of process factors affecting mechanical properties of INCONEL 718 superalloy in wire + arc additive manufacture process. *J. Mater. Process. Technol.* **2019**, *265*, 201–209. [CrossRef]
329. Asala, G.; Andersson, J.; Ojo, O.A. Analysis and constitutive modelling of high strain rate deformation behaviour of wire–arc additive-manufactured ATI 718Plus superalloy. *Int. J. Adv. Manuf. Technol.* **2019**, *103*, 1419–1431. [CrossRef]
330. Asala, G.; Andersson, J.; Ojo, O.A. Hot corrosion behaviour of wire-arc additive manufactured Ni-based superalloy ATI 718Plus®. *Corros. Sci.* **2019**, *158*, 108086. [CrossRef]

331. Asala, G.; Andersson, J.; Ojo, O.A. Improved dynamic impact behaviour of wire-arc additive manufactured ATI 718Plus®. *Mater. Sci. Eng. A* **2018**, *738*, 111–124. [CrossRef]
332. Asala, G.; Khan, A.K.; Andersson, J.; Ojo, O.A. Microstructural Analyses of ATI 718Plus® Produced by Wire-ARC Additive Manufacturing Process. *Met. Mat. Trans. A* **2017**, *48*, 4211–4228. [CrossRef]
333. Kindermann, R.M.; Roy, M.J.; Morana, R.; Prangnell, P.B. Process response of Inconel 718 to wire + arc additive manufacturing with cold metal transfer. *Mater. Des.* **2020**, *195*, 109031. [CrossRef]
334. Tanvir, A.N.M.; Ahsan, M.R.U.; Ji, C.; Hawkins, W.; Bates, B.; Kim, D.B. Heat treatment effects on Inconel 625 components fabricated by wire + arc additive manufacturing (WAAM)—Part 1: Microstructural characterization. *Int. J. Adv. Manuf. Technol.* **2019**, *103*, 3785–3798. [CrossRef]
335. Qiu, Z.; Wu, B.; Zhu, H.; Wang, Z.; Hellier, A.; Ma, Y.; Li, H.; Muransky, O.; Wexler, D. Microstructure and mechanical properties of wire arc additively manufactured Hastelloy C276 alloy. *Mater. Des.* **2020**, *195*, 109007. [CrossRef]
336. Hassel, T.; Carstensen, T. Properties and anisotropy behaviour of a nickel base alloy material produced by robot-based wire and arc additive manufacturing. *Weld. World* **2020**, *64*, 1921–1931. [CrossRef]
337. Jurić, I.; Garašić, I.; Bušić, M.; Kožuh, Z. Influence of Shielding Gas Composition on Structure and Mechanical Properties of Wire and Arc Additive Manufactured Inconel 625. *JOM* **2019**, *71*, 703–708. [CrossRef]
338. Marenych, O.O.; Ding, D.; Pan, Z.; Kostryzhev, A.G.; Li, H.; van Duin, S. Effect of chemical composition on microstructure, strength and wear resistance of wire deposited Ni-Cu alloys. *Addit. Manuf.* **2018**, *24*, 30–36. [CrossRef]
339. Wang, Y.; Chen, X.; Su, C. Microstructure and mechanical properties of Inconel 625 fabricated by wire-arc additive manufacturing. *Surf. Coat. Technol.* **2019**, *374*, 116–123. [CrossRef]
340. Chintala, A.; Tejaswi Kumar, M.; Sathishkumar, M.; Arivazhagan, N.; Manikandan, M. Technology Development for Producing Inconel 625 in Aerospace Application Using Wire Arc Additive Manufacturing Process. *J. Mater. Eng. Perform.* **2021**. [CrossRef]
341. Zinke, M.; Burger, S.; Arnhold, J.; Jüttner, S. Effect of different variants of filler metal S Ni 6625 on properties and microstructure by additive layer manufactured using CMT process. *Weld. World* **2021**. [CrossRef]
342. Tang, Y.T.; Ghoussoub, J.N.; Panwisawas, C.; Collins, D.M.; Amirkhanlou, S.; Clark, J.W.G.; Németh, A.A.N.; Graham McCartney, D.; Reed, R.C. The Effect of Heat Treatment on Tensile Yielding Response of the New Superalloy ABD-900AM for Additive Manufacturing. In *Superalloys 2020: Proceedings of the 14th International Symposium on Superalloys*; Tin, S., Hardy, M., Clews, J., Cormier, J., Feng, Q., Marcin, J., O'Brien, C., Suzuki, A., Eds.; Springer Nature: Cham, Switzerland, 2020; pp. 1055–1065, ISBN 978-3-030-51833-2.
343. Marinelli, G.; Martina, F.; Ganguly, S.; Williams, S. Grain refinement in an unalloyed tantalum structure by combining Wire + Arc additive manufacturing and vertical cold rolling. *Addit. Manuf.* **2020**, *32*, 101009. [CrossRef]
344. Marinelli, G.; Martina, F.; Ganguly, S.; Williams, S. Microstructure, hardness and mechanical properties of two different unalloyed tantalum wires deposited via wire + arc additive manufacture. *Int. J. Refract. Met. Hard Mater.* **2019**, *83*, 104974. [CrossRef]
345. Marinelli, G.; Martina, F.; Ganguly, S.; Williams, S. Development of Wire + Arc additive manufacture for the production of large-scale unalloyed tungsten components. *Int. J. Refract. Met. Hard Mater.* **2019**, *82*, 329–335. [CrossRef]
346. Shen, C.; Pan, Z.; Cuiuri, D.; Ding, D.; Li, H. Influences of deposition current and interpass temperature to the Fe_3Al-based iron aluminide fabricated using wire-arc additive manufacturing process. *Int. J. Adv. Manuf. Technol.* **2017**, *88*, 2009–2018. [CrossRef]
347. Shen, C.; Pan, Z.; Cuiuri, D.; Dong, B.; Li, H. In-depth study of the mechanical properties for Fe_3Al based iron aluminide fabricated using the wire-arc additive manufacturing process. *Mater. Sci. Eng. A* **2016**, *669*, 118–126. [CrossRef]
348. Shen, C.; Pan, Z.; Ma, Y.; Cuiuri, D.; Li, H. Fabrication of iron-rich Fe–Al intermetallics using the wire-arc additive manufacturing process. *Addit. Manuf.* **2015**, *7*, 20–26. [CrossRef]
349. Shen, C.; Reid, M.; Liss, K.-D.; Pan, Z.; Ma, Y.; Cuiuri, D.; van Duin, S.; Li, H. Neutron diffraction residual stress determinations in Fe3Al based iron aluminide components fabricated using wire-arc additive manufacturing (WAAM). *Addit. Manuf.* **2019**, *29*, 100774. [CrossRef]
350. Shen, C.; Pan, Z.; Cuiuri, D.; van Duin, S.; Luo, D.; Dong, B.; Li, H. Influences of postproduction heat treatment on Fe_3Al-based iron aluminide fabricated using the wire-arc additive manufacturing process. *Int. J. Adv. Manuf. Technol.* **2018**, *97*, 335–344. [CrossRef]
351. Shen, C. Application of Wire-Arc Additive Manufacturing (WAAM) Process in In-Situ Fabrication of Iron Aluminide Structures. Ph.D. Thesis, School of Mechanical, Materials, and Mechatronic Engineering, University of Wollongong, Wollongong, Australia, 2016. Available online: https://ro.uow.edu.au/theses/4844 (accessed on 12 September 2021).
352. Wang, J.; Pan, Z.; Wei, L.; He, S.; Cuiuri, D.; Li, H. Introduction of ternary alloying element in wire arc additive manufacturing of titanium aluminide intermetallic. *Addit. Manuf.* **2019**, *27*, 236–245. [CrossRef]
353. Wang, J.; Pan, Z.; Cuiuri, D.; Li, H. Phase constituent control and correlated properties of titanium aluminide intermetallic alloys through dual-wire arc additive manufacturing. *Mater. Lett.* **2019**, *242*, 111–114. [CrossRef]
354. Cai, X.; Dong, B.; Yin, X.; Lin, S.; Fan, C.; Yang, C. Wire arc additive manufacturing of titanium aluminide alloys using two-wire TOP-TIG welding: Processing, microstructures, and mechanical properties. *Addit. Manuf.* **2020**, *35*, 101344. [CrossRef]
355. Henckell, P.; Ali, Y.; Metz, A.; Bergmann, J.P.; Reimann, J. In Situ Production of Titanium Aluminides during Wire Arc Additive Manufacturing with Hot-Wire Assisted GMAW Process. *Metals* **2019**, *9*, 578. [CrossRef]
356. Guo, C.; Hu, R.; Chen, F. Microstructure and performances for 15-5 PH stainless steel fabricated through the wire-arc additive manufacturing technology. *Mater. Technol.* **2020**, 1–12. [CrossRef]

357. Wang, J.; Pan, Z.; Ma, Y.; Lu, Y.; Shen, C.; Cuiuri, D.; Li, H. Characterization of wire arc additively manufactured titanium aluminide functionally graded material: Microstructure, mechanical properties and oxidation behaviour. *Mater. Sci. Eng. A* **2018**, *734*, 110–119. [CrossRef]
358. Ma, Y.; Cuiuri, D.; Shen, C.; Li, H.; Pan, Z. Effect of interpass temperature on in-situ alloying and additive manufacturing of titanium aluminides using gas tungsten arc welding. *Addit. Manuf.* **2015**, *8*, 71–77. [CrossRef]
359. Shen, C.; Liss, K.-D.; Reid, M.; Pan, Z.; Hua, X.; Li, F.; Mou, G.; Huang, Y.; Zhu, Y.; Li, H. Fabrication of FeNi intermetallic using the wire-arc additive manufacturing process: A feasibility and neutron diffraction phase characterization study. *J. Manuf. Process.* **2020**, *57*, 691–699. [CrossRef]
360. Sujan, G.K.; Wu, B.; Pan, Z.; Li, H. In-Situ Fabrication of Titanium Iron Intermetallic Compound by the Wire Arc Additive Manufacturing Process. *Met. Mat. Trans. A* **2020**, *51*, 552–557. [CrossRef]
361. Wang, J.; Pan, Z.; Yang, G.; Han, J.; Chen, X.; Li, H. Location dependence of microstructure, phase transformation temperature and mechanical properties on Ni-rich NiTi alloy fabricated by wire arc additive manufacturing. *Mater. Sci. Eng. A* **2019**, *749*, 218–222. [CrossRef]
362. Wang, J.; Pan, Z.; Wang, L.; Su, L.; Carpenter, K.; Wang, J.; Wang, R.; Li, H. In-situ dual wire arc additive manufacturing of NiTi-coating on Ti_6Al_4V alloys: Microstructure characterization and mechanical properties. *Surf. Coat. Technol.* **2020**, *386*, 125439. [CrossRef]
363. Zeng, Z.; Cong, B.; Oliveira, J.P.; Ke, W.; Schell, N.; Peng, B.; Qi, Z.W.; Ge, F.; Zhang, W.; Ao, S.S. Wire and arc additive manufacturing of a Ni-rich NiTi shape memory alloy: Microstructure and mechanical properties. *Addit. Manuf.* **2020**, *32*, 101051. [CrossRef]
364. Shen, Q.; Kong, X.; Chen, X. Fabrication of bulk Al-Co-Cr-Fe-Ni high-entropy alloy using combined cable wire arc additive manufacturing (CCW-AAM): Microstructure and mechanical properties. *J. Mater. Sci. Technol.* **2021**, *74*, 136–142. [CrossRef]
365. Marinelli, G.; Martina, F.; Lewtas, H.; Hancock, D.; Ganguly, S.; Williams, S. Functionally graded structures of refractory metals by wire arc additive manufacturing. *Sci. Technol. Weld. Join.* **2019**, *24*, 495–503. [CrossRef]
366. Shen, C.; Pan, Z.; Cuiuri, D.; Roberts, J.; Li, H. Fabrication of Fe-FeAl Functionally Graded Material Using the Wire-Arc Additive Manufacturing Process. *Met. Mater. Trans. B* **2016**, *47*, 763–772. [CrossRef]
367. Chandrasekaran, S.; Hari, S.; Amirthalingam, M. Wire arc additive manufacturing of functionally graded material for marine risers. *Mater. Sci. Eng. A* **2020**, *792*, 139530. [CrossRef]
368. Yang, Z.; Liu, Q.; Wang, Y.; Ma, Z.; Liu, Y. Fabrication of multi-element alloys by twin wire arc additive manufacturing combined with in-situ alloying. *Mater. Res. Lett.* **2020**, *8*, 477–482. [CrossRef]
369. Wang, Y.; Konovalov, S.; Chen, X.; Ivanov, Y.; Jayalakshmi, S.; Singh, R.A. Research on Cu-6.6%Al-3.2%Si Alloy by Dual Wire Arc Additive Manufacturing. *J. Mater. Eng. Perform.* **2021**, *30*, 1694–1702. [CrossRef]
370. Rodrigues, T.A.; Duarte, V.R.; Tomás, D.; Avila, J.A.; Escobar, J.D.; Rossinyol, E.; Schell, N.; Santos, T.G.; Oliveira, J.P. In-situ strengthening of a high strength low alloy steel during Wire and Arc Additive Manufacturing (WAAM). *Addit. Manuf.* **2020**, *34*, 101200. [CrossRef]
371. Wesling, V.; Schram, A.; Müller, T.; Treutler, K. Influencing the arc and the mechanical properties of the weld metal in GMA-welding processes by additive elements on the wire electrode surface. *IOP Conf. Ser. Mater. Sci. Eng.* **2016**, *118*, 12006. [CrossRef]
372. Gehling, T.; Treutler, K.; Wesling, V. Targeted influence on the weld strength of high-strength fine-grain structural steels in the GMA welding process through functionalized weld material surfaces. *Weld. World* **2019**, *63*, 783–792. [CrossRef]
373. Treutler, K. Schweißen von Leichtbaurahmenkonstruktionen: Funktionale Werkstoffauswahl und Schweißzusatzwerkstoffmodifikation. Ph.D. Thesis, Clausthal University of Technology, Clausthal-Zellerfeld, Germany, 2019. [CrossRef]
374. Gehling, T.; Treutler, K.; Wesling, V. Development of surface coatings for high-strength low alloy steel filler wires and their effect on the weld metal microstructure and properties. *Weld. World* **2021**. [CrossRef]
375. Bick, T.; Treutler, K.; Wesling, V. Additive Fertigung korrosionsbeständiger Strukturen. In Proceedings of the 40. Assistentenseminar Füge- und Schweißtechnik: Vorträge der gleichnamigen Veranstaltung, Braunlage, Germany, 25–27 September 2019; DVS Berichte, Band: 357, ISBN 9783961440719.
376. Chen, X.; Han, J.; Wang, J.; Cai, Y.; Zhang, G.; Lu, L.; Xin, Y.; Tian, Y. A functionally graded material from TC4 to 316L stainless steel fabricated by double-wire + arc additive manufacturing. *Mater. Lett.* **2021**, 130141. [CrossRef]
377. Wagner, L.; Riehemann, W.; Arlic, U.; Hebing, J.; Wesling, V.; Schram, A.; Hamje, J.; Treutler, K. Additives Fertigen von faserverstärkten Aluminiumbauteilen—Composite Weld Modeling. In *Tagungsband 2. Niedersächsisches Symposium Materialtechnik: 23. bis 24. Februar 2017*; Shaker: Herzogenrath, Germany, 2017; ISBN 3844050698.
378. Hauser, T.; Reisch, R.T.; Seebauer, S.; Parasar, A.; Kamps, T.; Casati, R.; Volpp, J.; Kaplan, A.F. Multi-Material Wire Arc Additive Manufacturing of low and high alloyed aluminium alloys with in-situ material analysis. *J. Manuf. Process.* **2021**, *69*, 378–390. [CrossRef]
379. He, T.; Yu, S.; Yu, R.; Zheng, B. Oscillating Wire Arc Additive Manufacture of Rocket Motor Bimetallic Conical Shell. *Res. Sq.* **2021**. [CrossRef]
380. Bai, X.; Colegrove, P.; Ding, J.; Zhou, X.; Diao, C.; Bridgeman, P.; Roman Hönnige, J.; Zhang, H.; Williams, S. Numerical analysis of heat transfer and fluid flow in multilayer deposition of PAW-based wire and arc additive manufacturing. *Int. J. Heat Mass Transf.* **2018**, *124*, 504–516. [CrossRef]

381. Cadiou, S.; Courtois, M.; Carin, M.; Berckmans, W.; Le masson, P. 3D heat transfer, fluid flow and electromagnetic model for cold metal transfer wire arc additive manufacturing (Cmt-Waam). *Addit. Manuf.* **2020**, *36*, 101541. [CrossRef]
382. Israr, R.; Buhl, J.; Elze, L.; Bambach, M. Simulation of different path strategies for wire-arc additive manufacturing with Lagrangian finite element methods. 15.LS-DYna Forum 2018, Bamberg. 2018. Available online: https://www.dynamore.de/de/fortbildung/konferenzen/vergangene/2018-ls-dyna-forum/agenda/c-21-additive-manufacturing-buhl-btucottbus-senftenberg.pdf (accessed on 12 September 2021).
383. Graf, M.; Pradjadhiana, K.P.; Hälsig, A.; Manurung, Y.H.P.; Awiszus, B. Numerical simulation of metallic wire arc additive manufacturing (WAAM). *AIP Conf. Proc.* **2018**, *1960*, 140010. [CrossRef]
384. Huang, H.; Ma, N.; Chen, J.; Feng, Z.; Murakawa, H. Toward large-scale simulation of residual stress and distortion in wire and arc additive manufacturing. *Addit. Manuf.* **2020**, *34*, 101248. [CrossRef]
385. Cambon, C.; Rouquette, S.; Bendaoud, I.; Bordreuil, C.; Wimpory, R.; Soulie, F. Thermo-mechanical simulation of overlaid layers made with wire + arc additive manufacturing and GMAW-cold metal transfer. *Weld. World* **2020**, *64*, 1427–1435. [CrossRef]
386. Ahmad, S.N.; Manurung, Y.H.P.; Mat, M.F.; Minggu, Z.; Jaffar, A.; Pruller, S.; Leitner, M. FEM Simulation Procedure for Distortion and Residual Stress Analysis of Wire Arc Additive Manufacturing. *IOP Conf. Ser. Mater. Sci. Eng.* **2020**, *834*, 12083. [CrossRef]
387. Bonifaz, E.A.; Palomeque, J.S. A mechanical model in wire + Arc additive manufacturing process. *Prog. Addit. Manuf.* **2020**, *5*, 163–169. [CrossRef]
388. Geng, H.; Luo, J.; Li, J.; Gao, J.; Lin, X. Thermal Boundary Evolution of Molten Pool During Wire and Arc Additive Manufacturing of Single Walls of 5A06 Aluminum Alloy. *Metals* **2020**, *10*, 848. [CrossRef]
389. Geng, H.; Li, J.; Gao, J.; Lin, X. Theoretical Model of Residual Stress and Warpage for Wire and Arc Additive Manufacturing Stiffened Panels. *Metals* **2020**, *10*, 666. [CrossRef]
390. Bonifaz, E.A. Modelling of Thermal Transport in Wire + Arc Additive Manufacturing Process. In Proceedings of the Computational Science—ICCS 2019: 19th International Conference, Faro, Portugal, 12–14 June 2019; Dongarra, J., Rodrigues, J., Sloot, P., Eds.; Springer International Publishing: Cham, Switzerland, 2019; pp. 647–659, ISBN 978-3-030-22746-3.
391. Abbaszadeh, M.; Hönnige, J.R.; Martina, F.; Neto, L.; Kashaev, N.; Colegrove, P.; Williams, S.; Klusemann, B. Numerical Investigation of the Effect of Rolling on the Localized Stress and Strain Induction for Wire + Arc Additive Manufactured Structures. *J. Mater. Eng. Perform.* **2019**, *28*, 4931–4942. [CrossRef]
392. Sawant, M.S.; Jain, N.K.; Nikam, S.H. Theoretical modeling and finite element simulation of dilution in micro-plasma transferred arc additive manufacturing of metallic materials. *Int. J. Mech. Sci.* **2019**, *164*, 105166. [CrossRef]
393. Lange, J.; Feucht, T.; Erven, M. 3D printing with steel. *Steel Constr.* **2020**, *13*, 144–153. [CrossRef]
394. Saadatmand, M.; Talemi, R. Study on the thermal cycle of Wire Arc Additive Manufactured (WAAM) carbon steel wall using numerical simulation. *Frat. Integrità Strutt.* **2020**, *14*, 98–104. [CrossRef]
395. Kumar, A.; Maji, K. Bead Modelling and Deposition Path Planning in Wire Arc Additive Manufacturing of Three Dimensional Parts. *Mater. Sci. Forum* **2019**, *969*, 582–588. [CrossRef]
396. Geng, H.; Xiong, J.; Huang, D.; Lin, X.; Li, J. A prediction model of layer geometrical size in wire and arc additive manufacture using response surface methodology. *Int. J. Adv. Manuf. Technol.* **2017**, *93*, 175–186. [CrossRef]
397. Reddy, S.; Kumar, M.; Panchagnula, J.S.; Parchuri, P.K.; Kumar, S.S.; Ito, K.; Sharma, A. A new approach for attaining uniform properties in build direction in additive manufactured components through coupled thermal-hardness model. *J. Manuf. Process.* **2019**, *40*, 46–58. [CrossRef]
398. Buhl, J.; Israr, R.; Bambach, M. Modeling and convergence analysis of directed energy deposition simulations with hybrid implicit/explicit and implicit solutions. *J. Mach. Eng.* **2019**, *19*, 95–108. [CrossRef]
399. Xia, C.; Pan, Z.; Polden, J.; Li, H.; Xu, Y.; Chen, S. Modelling and prediction of surface roughness in wire arc additive manufacturing using machine learning. *J. Intell. Manuf.* **2021**. [CrossRef]
400. Casuso, M.; Veiga, F.; Suárez, A.; Bhujangrao, T.; Aldalur, E.; Artaza, T.; Amondarain, J.; Lamikiz, A. Model for the Prediction of Deformations in the Manufacture of Thin-Walled Parts by Wire Arc Additive Manufacturing Technology. *Metals* **2021**, *11*, 678. [CrossRef]
401. Goldak, J.; Chakravarti, A.; Bibby, M. A new finite element model for welding heat sources. *Metall. Mater. Trans. B* **1984**, *15*, 299–305. [CrossRef]
402. Montevecchi, F.; Venturini, G.; Scippa, A.; Campatelli, G. Finite Element Modelling of Wire-arc-additive-manufacturing Process. *Proc. CIRP* **2016**, *55*, 109–114. [CrossRef]
403. Wittek, S.; Treutler, K. Nutzung von KI-Methoden zur Geometriedetektion beim MSG-SChweißen. In *Tagungsband 4. Symposium Materialtechnik: 25–26 Februar 2021*, 1st ed.; Materialtechnik, C.Z.F., Ed.; Shaker: Düren, Germany, 2021; ISBN 9783844080216.
404. Israr, R.; Buhl, J.; Bambach, M. A Study on Power-Controlled Wire-Arc Additive Manufacturing using a Data-driven Surrogate Model. *Int. J. Adv. Manuf. Technol.* **2021**. [CrossRef]
405. Prajadhiama, K.P.; Manurung, Y.H.P.; Minggu, Z.; Pengadau, F.H.S.; Graf, M.; Haelsig, A.; Adams, T.-E.; Choo, H.L. Development of Bead Modelling for Distortion Analysis Induced by Wire Arc Additive Manufacturing using FEM and Experiment. *MATEC Web Conf.* **2019**, *269*, 5003. [CrossRef]
406. Bercelli, L.; Moyne, S.; Dhondt, M.; Doudard, C.; Calloch, S.; Beaudet, J. A probabilistic approach for high cycle fatigue of Wire and Arc Additive Manufactured parts taking into account process-induced pores. *Addit. Manuf.* **2021**, 101989. [CrossRef]

407. Cadiou, S.; Courtois, M.; Carin, M.; Berckmans, W.; Le Masson, P. Heat transfer, fluid flow and electromagnetic model of droplets generation and melt pool behaviour for wire arc additive manufacturing. *Int. J. Heat Mass Transf.* **2020**, *148*, 119102. [CrossRef]
408. Zhao, W.; Wei, Y.; Long, J.; Chen, J.; Liu, R.; Ou, W. Modeling and simulation of heat transfer, fluid flow and geometry morphology in GMAW-based wire arc additive manufacturing. *Weld. World* **2021**. [CrossRef]
409. Israr, R.; Buhl, J.; Bambach, M. Numerical Analysis of Different Fixation Strategies in Direct Energy Deposition Processes. *Proc. Manuf.* **2020**, *47*, 1184–1189. [CrossRef]
410. Gornyakov, V.; Sun, Y.; Ding, J.; Williams, S. Computationally Efficient Models of High Pressure Rolling for Wire Arc Additively Manufactured Components. *Appl. Sci.* **2021**, *11*, 402. [CrossRef]
411. Lee, J.; Park, H.J.; Chai, S.; Kim, G.R.; Yong, H.; Bae, S.J.; Kwon, D. Review on Quality Control Methods in Metal Additive Manufacturing. *Appl. Sci.* **2021**, *11*, 1966. [CrossRef]
412. Jafari, D.; Vaneker, T.H.; Gibson, I. Wire and arc additive manufacturing: Opportunities and challenges to control the quality and accuracy of manufactured parts. *Mater. Des.* **2021**, 109471. [CrossRef]
413. Javadi, Y.; Macleod, C.N.; Pierce, S.G.; Gachagan, A.; Kerr, W.; Ding, J.; Williams, S.; Vasilev, M.; Su, R.; Mineo, C.; et al. Ultrasonic Phased Array Inspection of Wire + Arc Additive Manufacture Samples Using Conventional and Total Focusing Method Imaging Approaches. *Insight* **2019**, *61*, 144–148. [CrossRef]
414. Javadi, Y.; MacLeod, C.N.; Pierce, S.G.; Gachagan, A.; Lines, D.; Mineo, C.; Ding, J.; Williams, S.; Vasilev, M.; Mohseni, E.; et al. Ultrasonic phased array inspection of a Wire + Arc Additive Manufactured (WAAM) sample with intentionally embedded defects. *Addit. Manuf.* **2019**, *29*, 100806. [CrossRef]
415. Al-Nabulsi, Z.; Mottram, J.T.; Gillie, M.; Kourra, N.; Williams, M.A. Mechanical and X ray computed tomography characterisation of a WAAM 3D printed steel plate for structural engineering applications. *Constr. Build. Mater.* **2021**, *274*, 121700. [CrossRef]
416. Lopez, A.; Bacelar, R.; Pires, I.; Santos, T.; Quintino, L. Mapping of non-destructive techniques for inspection of wire and arc additive manufacturing. In Proceedings of the 7th International Conference on Mechanics and Materials in Design, Albufeira, Portugal, 11–15 June 2017; Silva Gomes, J.F., Meguid, S.A., Eds.; INEGI/FEUP: Porto, Portugal, 2017; pp. 1829–1844.
417. Wu, B.; Pan, Z.; Ding, D.; Cuiuri, D.; Li, H.; Xu, J.; Norrish, J. A review of the wire arc additive manufacturing of metals: Properties, defects and quality improvement. *J. Manuf. Process.* **2018**, *35*, 127–139. [CrossRef]
418. Rodrigues, T.A.; Duarte, V.; Miranda, R.M.; Santos, T.G.; Oliveira, J.P. Current Status and Perspectives on Wire and Arc Additive Manufacturing (WAAM). *Materials* **2019**, *12*, 1121. [CrossRef]
419. Savyasachi, N.; Richard, S.; James, J.T.; Thomas, D.; Ashok, A. A Review on Wire and Arc Additive Manufacturing (WAAM). *Int. Res. J. Eng. Technol.* **2020**, 4981–4989.
420. Busachi, A.; Erkoyuncu, J.; Colegrove, P.; Martina, F.; Ding, J. Designing a WAAM Based Manufacturing System for Defence Applications. *Proc. CIRP* **2015**, *37*, 48–53. [CrossRef]
421. Frazier, W.E. Metal Additive Manufacturing: A Review. *J. Mater. Eng. Perform.* **2014**, *23*, 1917–1928. [CrossRef]
422. Pan, Z.; Ding, D.; Wu, B.; Cuiuri, D.; Li, H.; Norrish, J. Arc Welding Processes for Additive Manufacturing: A Review. In *Transactions on Intelligent Welding Manufacturing*; Chen, S., Zhang, Y., Feng, Z., Eds.; Springer: Singapore, 2018; pp. 3–24, ISBN 978-981-10-5354-2.
423. Uriondo, A.; Esperon-Miguez, M.; Perinpanayagam, S. The present and future of additive manufacturing in the aerospace sector: A review of important aspects. *Proc. Inst. Mech. Eng. Part. G J. Aerosp. Eng.* **2015**, *229*, 2132–2147. [CrossRef]
424. Busachi, A.; Erkoyuncu, J.; Colegrove, P.; Martina, F.; Watts, C.; Drake, R. A review of Additive Manufacturing technology and Cost Estimation techniques for the defence sector. *CIRP J. Manuf. Sci. Technol.* **2017**, *19*, 117–128. [CrossRef]
425. Rumman, R.; Lewis, D.A.; Hascoet, J.Y.; Quinton, J.S. Laser Metal Deposition and Wire Arc Additive Manufacturing of Materials: An Overview. *Arch. Metall. Mater.* **2019**, *64*, 467–473.
426. Karayel, E.; Bozkurt, Y. Additive manufacturing method and different welding applications. *J. Mater. Res. Technol.* **2020**, *9*, 11424–11438. [CrossRef]
427. Singh, S.R.; Khanna, P. Wire arc additive manufacturing (WAAM): A new process to shape engineering materials. *Mater. Today Proc.* **2020**. [CrossRef]
428. Ding, D.; Pan, Z.; Cuiuri, D.; Li, H. Wire-feed additive manufacturing of metal components: Technologies, developments and future interests. *Int. J. Adv. Manuf. Technol.* **2015**, *81*, 465–481. [CrossRef]
429. Liu, J.; Xu, Y.; Ge, Y.; Hou, Z.; Chen, S. Wire and arc additive manufacturing of metal components: A review of recent research developments. *Int. J. Adv. Manuf. Technol.* **2020**, *111*, 149–198. [CrossRef]
430. Zhukov, V.V.; Grigorenko, G.M.; Shapovalov, V.A. Additive manufacturing of metal products (Review). *Paton Weld. J.* **2016**, *2016*, 137–142. [CrossRef]
431. DebRoy, T.; Wei, H.L.; Zuback, J.S.; Mukherjee, T.; Elmer, J.W.; Milewski, J.O.; Beese, A.M.; Wilson-Heid, A.; De, A.; Zhang, W. Additive manufacturing of metallic components—Process, structure and properties. *Prog. Mater. Sci.* **2018**, *92*, 112–224. [CrossRef]
432. Yilmaz, O.; Ugla, A.A. Shaped metal deposition technique in additive manufacturing: A review. *Proc. Inst. Mech. Eng. Part B J. Eng. Manuf.* **2016**, *230*, 1781–1798. [CrossRef]
433. Dhinakaran, V.; Stalin, B.; Ravichandran, M.; Balasubramanian, M.; Anand Chairman, C.; Pritima, D. Wire Arc Additive Manufacturing Perspectives and Recent Developments. *IOP Conf. Ser. Mater. Sci. Eng.* **2020**, *988*, 12102. [CrossRef]

434. Li, J.Z.; Alkahari, M.R.; Rosli, N.A.B.; Hasan, R.; Sudin, M.N.; Ramli, F.R. Review of Wire Arc Additive Manufacturing for 3D Metal Printing. *Int. J. Autom. Technol.* **2019**, *13*, 346–353. [CrossRef]
435. Rosli, N.A.; Alkahari, M.R.; Abdollah, M.F.B.; Maidin, S.; Ramli, F.R.; Herawan, S.G. Review on effect of heat input for wire arc additive manufacturing process. *J. Mater. Res. Technol.* **2021**, *11*, 2127–2145. [CrossRef]
436. Chaturvedi, M.; Scutelnicu, E.; Rusu, C.C.; Mistodie, L.R.; Mihailescu, D.; Subbiah, A.V. Wire Arc Additive Manufacturing: Review on Recent Findings and Challenges in Industrial Applications and Materials Characterization. *Metals* **2021**, *11*, 939. [CrossRef]
437. Norrish, J.; Polden, J.; Richardson, I. A review of wire arc additive manufacturing: Development, principles, process physics, implementation and current status. *J. Phys. D Appl. Phys.* **2021**, *54*, 473001. [CrossRef]
438. Reisgen, U.; Willms, K.; Oster, L. Lichtbogenbasierte additive Fertigung—Forschungsfelder und industrielle Anwendungen. In *Additive Serienfertigung: Erfolgsfaktoren und Handlungsfelder für Die*; Lachmayer, R., Lippert, R.B., Kaierle, S., Eds.; Springer: Berlin, Germany, 2018; pp. 89–106, ISBN 978-3-662-56462-2.